U.PORTO

PROGRAMA DOUTORAL EM METABOLISMO - CLÍNICA E EXPERIMENTAÇÃO

Obesity and Melanoma: Unravelling the Molecular and Cellular Mechanisms

Pedro Miguel Vieira Coelho

D

2017

OBESITY

— AND —

MELANOMA

•

Unravelling the Molecular and Cellular Mechanisms

•

Pedro Miguel Vieira Coelho

PORTO • 2017

Dissertação de candidatura ao Grau de Doutor
em Metabolismo - Clínica e Experimentação
apresentada à Faculdade de Medicina da Universidade do Porto

ORIENTADORA

Doutora Raquel Ângela Silva Soares Lino
Professora Catedrática da Faculdade de Medicina da Universidade do Porto

CO-ORIENTADORES

Doutora Maria Cristina Prudêncio Pereira Soares
Professora Coordenadora com Agregação da Escola Superior de Saúde do Instituto Politécnico do Porto

Doutor Rúben Miguel Pereira Fernandes
Professor Adjunto da Escola Superior de Saúde do Instituto Politécnico do Porto

Constituição dos Membros do Júri

PRESIDENTE

Doutor José Manuel Pereira Dias de Castro Lopes
Professor Catedrático da Faculdade de Medicina da Universidade do Porto

VOGAIS

Doutora Susana Constantino Rosa Santos
Professora Auxiliar da Faculdade de Medicina da Universidade de Lisboa

Doutora Maria de Fátima Monginho Baltazar
Professora Associada da Escola de Ciências da Saúde da Universidade do Minho

Doutora Maria de Fátima Rodrigues Moutinho Gartner
Professora Catedrática do Instituto de Ciências Biomédicas Abel Salazar da Universidade do Porto

Doutor Filipe Gil Ramada Faria
Professor Auxiliar Convidado do Instituto de Ciências Biomédicas Abel Salazar da Universidade do Porto

Doutora Raquel Ângela Silva Soares Lino
Professora Catedrática da Faculdade de Medicina da Universidade do Porto

Artigo 48º, Parágrafo 3º:
"A Faculdade não responde pelas doutrinas expendidas na dissertação"

Regulamento da Faculdade de Medicina da Universidade do Porto
Decreto-Lei nº 19337 de 29 de Janeiro de 1931

O trabalho experimental presente nesta dissertação foi executado no Departamento de Bioquímica da Faculdade de Medicina da Universidade do Porto.

Os trabalhos desenvolvidos foram subsidiados pela Fundação para a Ciência e Tecnologia, pelo FEDER-COMPETE - PEst-OE/SAU/UI0038/2011, UID/BIM/04293/2013 e NORTE2020 - Programa Operacional Regional do Norte (NORTE-01-0145-FEDER-000012).

O candidato realizou o trabalho experimental com o apoio de uma bolsa de Doutoramento atribuída pela Fundação para a Ciência e a Tecnologia (SFRH/BD/80434/2011).

Corpo Catedrático da Faculdade de Medicina da Universidade do Porto

PROFESSORES CATEDRÁTICOS EFETIVOS

Doutor Manuel Alberto Coimbra Sobrinho Simões
Doutora Maria Amélia Duarte Ferreira
Doutor José Agostinho Marques Lopes
Doutor Patrício Manuel Vieira Araújo Soares-da-Silva
Doutor Alberto Manuel Barros da Silva
Doutor José Manuel Lopes Teixeira Amarante
Doutor José Henrique Dias Pinto de Barros
Doutora Maria de Fátima Machado Henriques Carneiro
Doutora Isabel Maria Amorim Pereira Ramos
Doutora Deolinda Maria Valente Alves Lima Teixeira
Doutora Maria Dulce Cordeiro Madeira
Doutor Altamiro Manuel Rodrigues da Costa Pereira
Doutor José Carlos Neves da Cunha Areias
Doutor Manuel Jesus Falcão Pestana Vasconcelos
Doutor João Francisco Montenegro Andrade Lima Bernardes
Doutora Maria Leonor Martins Soares David
Doutor Rui Manuel Lopes Nunes
Doutor José Eduardo Torres Eckenroth Guimarães
Doutor Francisco Fernando Rocha Gonçalves
Doutor José Manuel Pereira Dias de Castro Lopes
Doutor António Albino Coelho Marques Abrantes Teixeira
Doutor Joaquim Adelino Correia Ferreira Leite Moreira
Doutora Raquel Ângela Silva Soares Lino

PROFESSORES JUBILADOS OU APOSENTADOS

Doutor Alexandre Alberto Guerra de Sousa Pinto
Doutor Álvaro Jerónimo Leal Machado de Aguiar
Doutor António Augusto Lopes Vaz
Doutor António Carlos Freitas Ribeiro Saraiva
Doutor António Carvalho Almeida Coimbra
Doutor António Fernandes Oliveira Barbosa Ribeiro Braga
Doutor António José Pacheco Palha
Doutor António Manuel Sampaio de Araújo Teixeira
Doutor Belmiro dos Santos Patrício
Doutor Cândido Alves Hipólito Reis
Doutor Carlos Rodrigo Magalhães Ramalhão
Doutor Cassiano Pena de Abreu e Lima
Doutor Daniel Filipe de Lima Moura
Doutor Eduardo Jorge Cunha Rodrigues Pereira
Doutor Fernando Tavarela Veloso
Doutor Henrique José Ferreira Gonçalves Lecour de Menezes
Doutor Jorge Manuel Mergulhão Castro Tavares
Doutor José Carvalho de Oliveira
Doutor José Fernando Barros Castro Correia
Doutor José Luís Medina Vieira
Doutor José Manuel Costa Mesquita Guimarães
Doutor Levi Eugénio Ribeiro Guerra
Doutor Luís Alberto Martins Gomes de Almeida
Doutor Manuel António Caldeira Pais Clemente
Doutor Manuel Augusto Cardoso de Oliveira
Doutor Manuel Machado Rodrigues Gomes
Doutor Manuel Maria Paula Barbosa
Doutora Maria da Conceição Fernandes Marques Magalhães
Doutora Maria Isabel Amorim de Azevedo
Doutor Rui Manuel Almeida Mota Cardoso
Doutor Serafim Correia Pinto Guimarães
Doutor Valdemar Miguel Botelho dos Santos Cardoso
Doutor Walter Friedrich Alfred Osswald

Contribuição Pessoal & Lista de Autores

O candidato declara que teve uma contribuição determinante quer na realização do trabalho experimental (programação, preparação e execução prática das experiências), bem como na análise, interpretação e discussão dos resultados apresentados em todos os capítulos desta dissertação. O candidato declara ainda que contribuiu ativamente para a redação dos manuscritos e artigos apresentados. Para além do candidato, os autores infracitados contribuíram para os respectivos capítulos:

Capítulo 2
Os seguintes autores contribuíram para o Capítulo 2: Joana Almeida, Cristina Prudêncio, Rúben Fernandes e Raquel Soares. PC, RF, CP e RS desenharam o estudo. CP, RF e RS supervisionaram o projeto. PC executou as experiências e analisou os dados. As colorações citoquímicas foram realizadas com a ajuda da JA. Todos os autores participaram ativamente na escrita do artigo.

Capítulo 3
Os seguintes autores contribuíram para o Capítulo 3: Liliana Silva, Isabel Faria, Mónica Vieira, Armanda Monteiro, Gabriela Pinto, Cristina Prudêncio, Rúben Fernandes e Raquel Soares. PC, LS, RF e RS desenharam o estudo. CP, RF e RS orientaram a execução do projeto. PC e LS realizaram as experiências e processaram os dados obtidos. MV supervisionou as técnicas cromatográficas. O planeamento dosimétrico de radioterapia foi executado por IF, AM e GP. Todos os autores participaram ativamente na escrita do manuscrito.

Capítulo 4
Os seguintes autores contribuíram para o Capítulo 4: Joana Almeida, Cristina Prudêncio, Rúben Fernandes e Raquel Soares. PC, CP, RF e RS desenharam o estudo. CP, RF e RS monitorizaram o desenrolar do projeto. PC e JA estiveram envolvidos na manutenção dos animais. JA executou o processamento histológico dos tecidos. PC realizou as colorações histoquímicas e imunohistoquímicas, analisou e interpretou os resultados. Todos os autores participaram ativamente na escrita do documento final.

> “We can only see a short distance ahead, but we can see plenty there that needs to be done”
>
> *Alan Turing*

Agradecimentos

Gostaria de deixar o meu profundo agradecimento a todos os que estiveram envolvidos ou contribuíram, de uma forma direta ou indiretamente para a realização deste projeto. Em especial...

... à minha orientadora Doutora Raquel Soares, co-orientadora Doutora Cristina Prudêncio e co-orientador Doutor Rúben Fernandes pelo exemplo de dedicação à vida académica e científica. Obrigado por me demonstrarem sistematicamente que é sempre possível fazer mais e melhor.

... aos elementos do Departamento de Bioquímica da Faculdade de Medicina da Universidade do Porto pelo apoio, companheirismo e disponibilidade constantes.

... aos meus colegas da Área Técnico-Científica das Ciências Químicas e das Biomoléculas da Escola Superior de Saúde do Instituto Politécnico do Porto pelo ânimo e força essenciais à conclusão de mais esta etapa.

... aos elementos do Serviço de Radioterapia do Centro Hospitalar de São João. Obrigado pela colaboração científica e total disponibilidade demonstradas.

... à minha família e aos meus amigos. Mãe, Pai, Tia e Mana: obrigado pelo apoio incondicional. Meras palavras não bastam para expressar o meu agradecimento!

A todos, um grande bem hajam!

Resumo

O aumento da prevalência mundial da obesidade é um grave problema de saúde pública. Entre as muitas complicações associadas à obesidade, estão algumas patologias malignas. O melanoma é um dos cancros cuja incidência apresenta mais rápido crescimento e a obesidade tem sido apontada como um possível fator subjacente à maior prevalência de melanoma. No presente trabalho, abordou-se esta relação e investigaram-se os mecanismos biológicos que relacionam a elevada adiposidade com a progressão do melanoma. Recorrendo a culturas celulares de melanócitos malignos de murganho (B16-F10) e humanos (MeWo) tratados com meio condicionado (MC) de adipócitos 3T3-L1 e de fragmentos *ex vivo* de tecido adiposo subcutâneo (TAS) e visceral (TAV), demonstrou-se que a gordura liberta fatores potenciadores da proliferação, atividade metabólica e simultaneamente inibidores da apoptose das células de melanoma. A migração e adesão celulares foram distintamente moduladas pelos MC do TAS e TAV. Além disso, o MC dos adipócitos 3T3-L1 promoveu a sobrevivência e homeostasia redox das células B16-F10 após tratamentos de radioterapia. O aumento da viabilidade, motilidade e defesas antioxidantes dos melanócitos, com uma ativação concomitante da via de sinalização da AKT, reverteu os danos induzidos pela radiação ionizante contribuindo para a radiorresistência dos melanócitos. Subsequentemente, murganhos C57Bl/6J alimentados com uma dieta rica em gordura foram inoculados com células de melanoma B16-F10 por via subcutânea ou intravenosa. *In vivo*, a adiposidade potenciou a progressão e a vascularização do melanoma primário mas, por outro lado, diminuiu o potencial metastizante das células B16-F10 em circulação. Curiosamente, em culturas 3D *in vitro*, os fatores libertados pelos adipócitos induziram a reorganização das células B16-F10 e MeWo em estruturas tipo-capilar caraterísticas de mimetização vascular (MV). Observou-se também um aumento *in vivo* da MV nos animais HFD, apesar de estatisticamente não significativo. A caraterização molecular do soro dos animais, bem como do MC das células 3T3-L1 e do TAS e TAV, permitiu destacar possíveis mediadores moleculares e mecanismos biológicos pelos quais o tecido adiposo promove a vascularização e a progressão do melanoma. Em suma, estes resultados reforçam os efeitos nefastos que um microambiente rico em fatores derivados do tecido adiposo induz na progressão, agressividade, stresse oxidativo, angiogénese e MV tumoral, com possíveis implicações diretas no prognóstico, resposta ao tratamento e, em última análise, sobrevida dos pacientes com melanoma.

Abstract

Obesity is now a major health problem due to its rapidly increasing incidence worldwide. Among many conditions associated with obesity are some malignancies. The incidence of melanoma has been increasing steadily over the past decades and obesity has been pointed out as a potential underlying morbidity subsidising melanoma development. In the present work, we address the above relationship and inquire into the biological mechanisms linking high-adiposity and melanoma progression. Employing murine B16-F10 and human MeWo melanoma cell cultures exposed to 3T3-L1 adipocytes secretome, and *ex vivo* subcutaneous (SAT) and visceral (VAT) adipose tissue conditioned medium (CM), we were able to demonstrate that fat-released factors heighten melanoma cell proliferation, metabolic activity, and simultaneously decrease apoptosis. B16-F10 cell migration and adhesive properties were distinctively modulated by SAT and VAT released factors. Furthermore, 3T3-L1 adipocytes CM upheld B16-F10 cell survival and redox homeostasis following radiotherapy treatments. Remarkably, 3T3-L1 secretome increased melanocytes viability, motility, catalase activity and total antioxidant status, with a concomitant activation of the AKT signalling pathway, reversing ionizing radiation damages and enhancing the radioresistant phenotype of melanocytes. Subsequently, we employed a high-fat diet (HFD)-induced obese mice melanoma allograft model, where C57Bl/6J mice were subcutaneously or intravenously) inoculated with B16-F10 melanoma cells. *In vivo* fat-released circulating factors led to subcutaneous melanoma growth and vascularization but, on the other hand weakened the metastasizing capacity of circulating malignant B16-F10 cells. Surprisingly, exposure to 3T3-L1 CM induced B16-F10 and MeWo cells to rearrange, on 3D *in vitro* cultures, into characteristic vasculogenic mimicry (VM) vessel-like structures. An *in vivo* increase in VM was also observed in tumour-bearing HFD animals, though not reaching statistical significance. Our findings are corroborated by molecular characterization of animals serum, as well as 3T3-L1, SAT, and VAT CM, and led us to highlight possible molecular candidates and mechanisms by which adipose tissue promotes melanoma progression and enhances vascularization. Altogether, our results reinforce the deleterious effects that an adipose-derived factor-rich environment partakes in melanoma progression, aggressiveness, oxidative stress, angiogenesis and VM with direct implications in disease prognosis, treatment outcomes and ultimately overall survival.

Table of Contents

Resumo **xv**

Abstract **xvii**

List of Figures **xxi**

List of Tables **xxiii**

List of Abbreviations **xxv**

1 Introduction **1**

1.1 Melanoma . . . 1

1.1.1 Histologic Changes in Melanoma Progression . . . 2

1.1.2 Molecular Basis of Melanoma Pathogenesis . . . 3

1.1.3 Management of Melanoma . . . 5

1.1.3.1 Chemotherapy, Targeted Therapy and Immunotherapy . . . 6

1.1.3.2 Radiation Therapy . . . 6

1.1.4 Final Remarks . . . 7

1.2 Obesity and Melanoma . . . 7

1.2.1 Mechanisms Linking Obesity and Melanoma . . . 8

1.2.1.1 Adipokines and Growth Factors . . . 9

1.2.1.2 Angiogenesis . . . 11

1.2.1.3 Hypoxia . . . 12

1.2.1.4 Inflammation . . . 13

1.2.1.5 Oxidative Stress . . . 14

1.2.1.6 Energy Metabolism . . . 15

1.2.2 Final Remarks . . . 16

1.3 Rationale . . . 17

2 Effect of Adipocyte Secretome in Melanoma Progression and Vasculogenic Mimicry **19**
2.1 Background . . . 20
2.2 Materials & Methods . . . 20
2.2.1 Cell Culture and *In Vitro* Treatments . . . 20
2.2.2 Adipocyte Differentiation and Conditioned Medium Collection . . . 21
2.2.3 Adipose Tissue Organ Culture . . . 21
2.2.4 Mouse Adipokine Array Analysis . . . 21
2.2.5 Cell Viability Assay . . . 21
2.2.6 Apoptosis Assay . . . 22
2.2.7 BrdU Proliferation Assay . . . 22
2.2.8 Cell Spreading and Adhesion Determination . . . 22
2.2.9 Adhesion to Endothelium Evaluation . . . 22
2.2.10 Melanin Content Determination . . . 23
2.2.11 Transwell Migration . . . 23
2.2.12 Injury Assay . . . 23
2.2.13 Matrigel Cultures . . . 23
2.2.14 Soft-Agar Colony Formation . . . 24
2.2.15 Hanging-Drop Cell Cultures . . . 24
2.2.16 Statistical Analysis . . . 24
2.3 Results . . . 24
2.3.1 3T3-L1 Secretome Increases Melanocytes Survival, Proliferation and Melanin Content, and Decreases Apoptosis . . . 24
2.3.2 Adipocyte Secretome Profile Characterization . . . 25
2.3.3 Subcutaneous and Visceral Adipose Tissue Distinctively Modulate Melanocyte Migration and Cell Spreading . . . 27
2.3.4 Adipose Tissue Secretome Modulates Melanoma Cells Adhesion and Tumourigenesis . . . 27
2.3.5 Adipocytes Secreted Factors Induce Malignant Melanocytes Vasculogenic Mimicry . . . 29
2.4 Discussion . . . 29
2.5 Acknowledgments . . . 34
2.6 Supporting Information . . . 35

3 Adipocyte Secretome Increases Radioresistance of Malignant Melanocytes by Improving Cell Survival and Decreasing Oxidative Status **39**
3.1 Background . . . 40
3.2 Material & Methods . . . 41

3.2.1 Cell Cultures . . . 41
3.2.2 Adipocytes Differentiation and Conditioned Medium Collection . . . 41
3.2.3 Irradiation of Cells . . . 41
3.2.4 Metabolic Activity Assay . . . 42
3.2.5 Total Antioxidant Status Determination . . . 42
3.2.6 Catalase Activity . . . 42
3.2.7 TBARS Determination . . . 42
3.2.8 Nitrotyrosine Quantification . . . 43
3.2.9 *In Vitro* Scratch Assay . . . 43
3.2.10 Western Blotting Analysis . . . 43
3.2.11 Statistical Analysis . . . 43
3.3 Results . . . 44
3.3.1 3T3-L1 Conditioned Medium Protects B16-F10 Cells from Radiation Damage . . . 44
3.3.2 Adipocyte Secretome Contributes to Melanoma Radioresistance . . . 46
3.4 Discussion . . . 47
3.5 Acknowledgments . . . 49
3.6 Supplementary Data . . . 50

4 Adipose-Derived Factors Increase B16-F10 Tumour Vascularization but Decrease Metastatic Potential **53**
4.1 Background . . . 54
4.2 Materials & Methods . . . 54
4.2.1 Cell Culture . . . 54
4.2.2 Animals and Diets . . . 55
4.2.3 B16-F10 Cell Inoculation . . . 55
4.2.4 Histologic Analysis . . . 55
4.2.5 CD31 Immunohistochemistry . . . 56
4.2.6 Periodic Acid–Schiff Reaction . . . 56
4.2.7 Melanin Staining and Quantification . . . 56
4.2.8 Metastasis Assessment . . . 56
4.2.9 Microvessel and Vasculogenic Mimicry Density Determination . . . 56
4.2.10 Adipokine and Angiogenesis Antibody Arrays . . . 57
4.2.11 Statistical Analysis . . . 57
4.3 Results . . . 57
4.3.1 High-Fat Diet Causes Significant Weight Gain and Increases Serum Levels of Growth and Angiogenic Factors in C57Bl/6J Mice . . . 57
4.3.2 Fat-Rich Diet Promotes Melanoma Progression and Vascularization . . . 59

4.3.3 High-Fat Diet Decreases B16-F10 Lung Metastasis 60
4.4 Discussion 63
4.5 Acknowledgments 65
4.6 Supplemental Data 67

5 General Discussion **71**

References **77**

Appendix A Reproduction Licences **95**

List of Figures

1 Introduction

1.1 The MAPK and PI3K-AKT signalling pathways in melanoma. 4

1.2 Mechanisms linking obesity and melanoma 9

2 Effect of Adipocyte Secretome in Melanoma Progression and Vasculogenic Mimicry

2.1 3T3-L1 secretome increases melanoma cell survival 25

2.2 Secretion profiles of 3T3-L1 cells and subcutaneous and visceral adipose tissue organ cultures 26

2.3 *In vitro* motility, migration and spreading analysis of B16-F10 melanocytes 28

2.4 Melanoma cells adhesion and achorage-independent growth were increased after incubation with adipose tissue conditioned medium 30

2.5 Vasculogenic mimicry by melanoma cells was stimulated by adipose tissue conditioned medium 31

3 Adipocyte Secretome Increases Radioresistance of Malignant Melanocytes by Improving Cell Survival and Decreasing Oxidative Status

3.1 B16-F10 survival and antioxidant status upon single 2 Gy irradiation 45

3.2 Migration of B16-F10 melanocytes exposed to 3T3-L1 conditioned medium and/or radiation 46

3.3 Adipocyte released factors protect B16-F10 melanocytes from fractionated radiation damage 47

3.S1 Conformal radiotherapy planning CT for the multi-well cell culture plates 50

3.S2 Conformal radiotherapy simulation for the multi-well cell culture plates 51

3.S3 Representative chromatograms of 3-nitrotyrosine determination 51

4 Adipose-Derived Factors Increase B16-F10 Tumour Vascularization but Decrease Metastastatic Potential

4.1 Weight gain and serum profiles of C57Bl/6J mice 58
4.2 Subcutaneous melanoma progression in high-fat diet-feeded animals 60
4.3 Microvessel and vasculogenic mimicry density in melanoma tumours 61
4.4 Melanoma lung metastases in high-fat diet-feeded animals 62

5 General Discussion

5.1 Possible new molecular players and mechanisms linking obesity and melanoma . . 73

List of Tables

2 Effect of Adipocyte Secretome in Melanoma Progression and Vasculogenic Mimicry

2.S1 Gene expression profile of secretomes from 3T3-L1, SAT and VAT by microarray . 35
2.S1 Gene expression profile of secretomes from 3T3-L1, SAT and VAT by microarray . 36
2.S1 Gene expression profile of secretomes from 3T3-L1, SAT and VAT by microarray . 37

3 Adipocyte Secretome Increases Radioresistance of Malignant Melanocytes by Improving Cell Survival and Decreasing Oxidative Status

3.S1 Detailed chromatographic conditions for 3-nitrotyrosine detection 50

4 Adipose-Derived Factors Increase B16-F10 Tumour Vascularization but Decrease Metastastatic Potential

4.S1 Serum Profile by Microarray 67
4.S1 Serum Profile by Microarray 68
4.S1 Serum Profile by Microarray 69
4.S1 Serum Profile by Microarray 70

List of Abbreviations

3-NT 3-nitrotyrosine.

ADAMTS angiogenesis stimulators A disintegrin and metalloproteinase with thrombospondin motifs.

AgRP Agouti-related protein.

ASC adipose stromal cells.

AT adipose tissue.

ATM adipose tissue macrophages.

BrdU bromodeoxyuridine.

CM conditioned medium.

CT control.

CTLA cytotoxic T lymphocyte-associated antigen.

DMEM Dulbeco's modified Eagle's medium.

EGF epidermal growth factor.

FBS fetal bovine serum.

FGF fibroblast growth factor.

H&E hematoxylin and eosin.

HFD high-fat diet.

HGF hepatocyte growth factor.

HIF hypoxia inducible factor.

HMEC human dermal microvascular endothelial cells.

IGF insulin-like growth factor.

IGFBP insulin-like growth factor-binding protein.

IL interleukin.

IV intravenous.

LIF leukaemia inhibitory factor.

MAPK mitogen activated protein kinase.

MCP monocyte chemotactic protein.

MDA malondialdehyde.

MMP matrix metalloproteinase.

NF-κB nuclear factor-κB.

PAI plasminogen activator inhibitor.

PAS periodic acid-Schiff.

PBS phosphate buffered saline.

PD programmed death.

PDGF platelet-derived growth factor.

PlGF placental growth factor.

RBP retinol binding protein.

RNS reactive nitrogen species.

ROS reactive oxygen species.

RT radiation therapy.

SAT subcutaneous adipose tissue.

SC subcutaneous.

SD standard diet.

SEM standard error of the mean.

TAM tumour-associated macrophages.

TAS total antioxidant status.

TBARS thiobarbituric acid-reactive substances.

TGF transforming growth factor.

TIMP tissue inhibitor of metalloproteinases.

TNF tumour necrosis factor.

TUNEL terminal deoxynucleotidyl transferase-mediated deoxyuridine triphosphate nick-end labelling.

VAT visceral adipose tissue.

VEGF vascular endothelial growth factor.

VM vasculogenic mimicry.

1 Introduction

Cancer is a worldwide phenomenon. Its relation with obesity has become a reality in our days. The common features of the two most deadly and chronic diseases of the modern world overlap in many characteristics along their pathogenesis. In this review the current scientific and medical state of the art of both diseases are explored, enlightening their cross-talk and putative overlapping role in melanoma.

1.1 Melanoma

Melanoma, also known as malignant melanoma, is a cancer that develops in melanocytes. Melanoma predominantly occurs in the skin, but may in rare instances occur at other sites, and possesses an high metastasis potential and poor survival rates once metastasised. Melanoma is one of the world's most rapidly increasing malignancies.[1] Cutaneous melanoma prevalence has been increasing year by year in the last decades,[2] with an estimate doubling of incidence rates every 10 to 20 years,[3,4] raising melanoma to the most rapidly increasing cancer in Caucasians.[4] Annually more than 176000 new cases of melanoma are found solely in Europe and the US.[5,6] Although malignant melanoma comprises less than 10% of diagnosed dermatologic cancers, it is responsible for almost 80% of skin cancer deaths. Globally, in 2012, melanoma occurred in more than 200000 people and resulted in 55000 deaths.[7]

The causes of melanoma development are multifactorial and not fully elucidated. However, several risk factors are known to contribute to melanoma development: intermittent sun and UV-radiation exposure, a previous episode or family history of melanoma, high number of nevi present in the skin, the degree of skin pigmentation, a weakened or suppressed immune system, among others.[2,8]

Standard approaches in melanoma treatment involve surgical resection when diagnosed at early stage, chemotherapy and radiation therapy (RT) together with immunotherapy in the later stages of the disease. However, these approaches are less effective in terms of advanced and metastatic melanoma.

1.1.1 Histologic Changes in Melanoma Progression

In the skin, maintenance of tissue homeostasis determines whether a cell remains quiescent, proliferates, differentiates, or undergoes programmed death. Melanocytes are found in the deepest layer (the *stratum basale*) of the skin's epidermis and, upon proliferation, migrate along the basal layer extending their dendrites to establish contacts with adjacent keratinocytes and Langerhans cells.[9] Under normal conditions, surrounding keratinocytes control the growth and behaviour of melanocytes by means of a complex system of mechanic cell-to-cell adhesive interactions and the secretion of paracrine growth factors.[10,11] Once this delicate homeostatic balance is disrupted, melanocyte proliferation and migration becomes unrestrained, which can result in the formation of nevi or even malignant melanoma development.[10]

The great majority of melanomas begin as intraepidermal proliferations, which may have some relationship to a melanocytic nevus. The histological diagnosis of melanocytic lesions requires assessment of architectural and cytological features that are more often present in melanoma than benign nevi, such as higher lesional diameter, asymmetry and architectural disorder, pagetoid melanocytosis, poorly circumscribed lesions, nesting and sheetlike arrangements of melanocytes, high degree of cytological atypia, nuclear atypia and enlarged nuclei with irregular contours, effacement of the epidermis, absence of maturation, dermal mitoses, ulceration, and host immune response.[12] Histological interpretation discloses three clinically and histomorphologically distinct steps along melanoma progression. In an early stage, the tumour may be confined to the epidermis and displays only radial/lateral growth (melanoma *in situ*). When melanoma progresses, it can develop into microinvasive melanoma, in which microscopic extensions invade the uppermost layers of the dermis. As melanomas further advance, they progress to the vertical growth phase, which is characterized by invasive growth with discernable involvement deep into the dermis and subcutaneous fat layer. In this stage of growth, the melanoma has entered the tumourigenic and/or mitogenic phase and gained the potential to metastasise.[13]

Along melanocytes progression to malignancy, alterations in gene expression patterns include genes that are usually expressed by several other cell types such as precursors of endothelial, pericyte, fibroblast, haematopoietic, kidney, neuronal and muscle cells.[14,15] Aggressive melanoma cells can "mask" as other cell types while reverting to a more embryonic-like undifferentiated phenotype,[16] through an epithelial-to-mesenchymal transition-like reprogramming.[17] In addition to the tumourigenic genetic abnormalities, it has been shown that interactions between melanoma cells and surrounding stromal environment are significant. Melanoma cells are embedded in a cell-rich

tissue microenvironment and surrounded by multiple cell types including keratinocytes, fibroblasts, endothelial cells and immunoregulatory cells. In malignant melanoma, tumour-stroma interactions involve several biological mechanisms, including changes in intercellular and cell-matrix adhesions, up-regulation of autocrine/paracrine growth factors and their receptors and stimulation of angiogenesis and immune cell response that cooperate in a concerted action to rise up the growth and invasion of malignant melanoma cells.[18]

Melanoma can arise as a pigmented lesion or less frequently, as non-pigmented or amelanotic lesions (2% of melanomas).[19] Melanocytes are cells specialized in the synthesis of melanin pigments. Although the main function of melanin is to protect against UV-induced damage, synthesis and accumulation of abnormal melanin pigment and dysfunctional or fragmented melanossomes, usually altered in pigmented melanoma lesions,[20] is generally associated with aggressiveness, oxidative stress, and resistance to treatment.[21–23] However, and in spite of significant research efforts, the relationship between melanin content and metastatic phenotype and prognosis of melanoma still remains controversial.

Along melanoma progression, tumours acquire and sustain a dense vascular network, enabling their adhesion to the vascular bed, favouring tumour cells extravasation and metastasis.[18] Melanoma neovascularization has been correlated with ulceration, poor overall survival and increased rate of relapse.[24] The degree of tumour vascularity is one of the most important histopathologic factors determining overall survival. Besides angiogenesis, vasculogenic mimicry provides an alternative, angiogenic-independent tumour microcirculation.[16,25,26] It is well established that melanoma cell-lined vascular networks sustain a redundant blood supply, with a viable blood flow between tumour-cell-lined vascular spaces and endothelium-lined and/or mature vasculature, required for both growth and metastasis.[25,26] The presence of these functional vascular mimetic channels by the tumour itself stands a predictor of poor prognosis in human melanoma patients[27,28], but little is known about the biological relevance of this phenomenon.

1.1.2 Molecular Basis of Melanoma Pathogenesis

Melanoma etiopathogenesis is heterogeneous; it partly depends on genomic mutations, which lead to the activation of proto-oncogenes or to the inactivation of suppressor genes as well as the amplification/deletion and translocation of parts or whole chromosomes. None of the oncogenes or tumour suppressor genes identified in melanoma is thought to be deregulated in stand-alone events, even though some of the critical mutations in melanoma cells are mutually exclusive.

Several altered intracellular signaling pathways have been identified in melanomas so far, the best known of which is the mitogen activated protein kinase (MAPK) pathway or RAS-RAF-MEK-ERK pathway (Fig. 1.1).[29] The intracellular MAPK pathway can be activated by various extracellular signals. Growth factors such as epidermal growth factor (EGF), insulin-like growth factor (IGF)-I, or transforming growth factor (TGF)-ß induce signal transduction by binding to the respective recep-

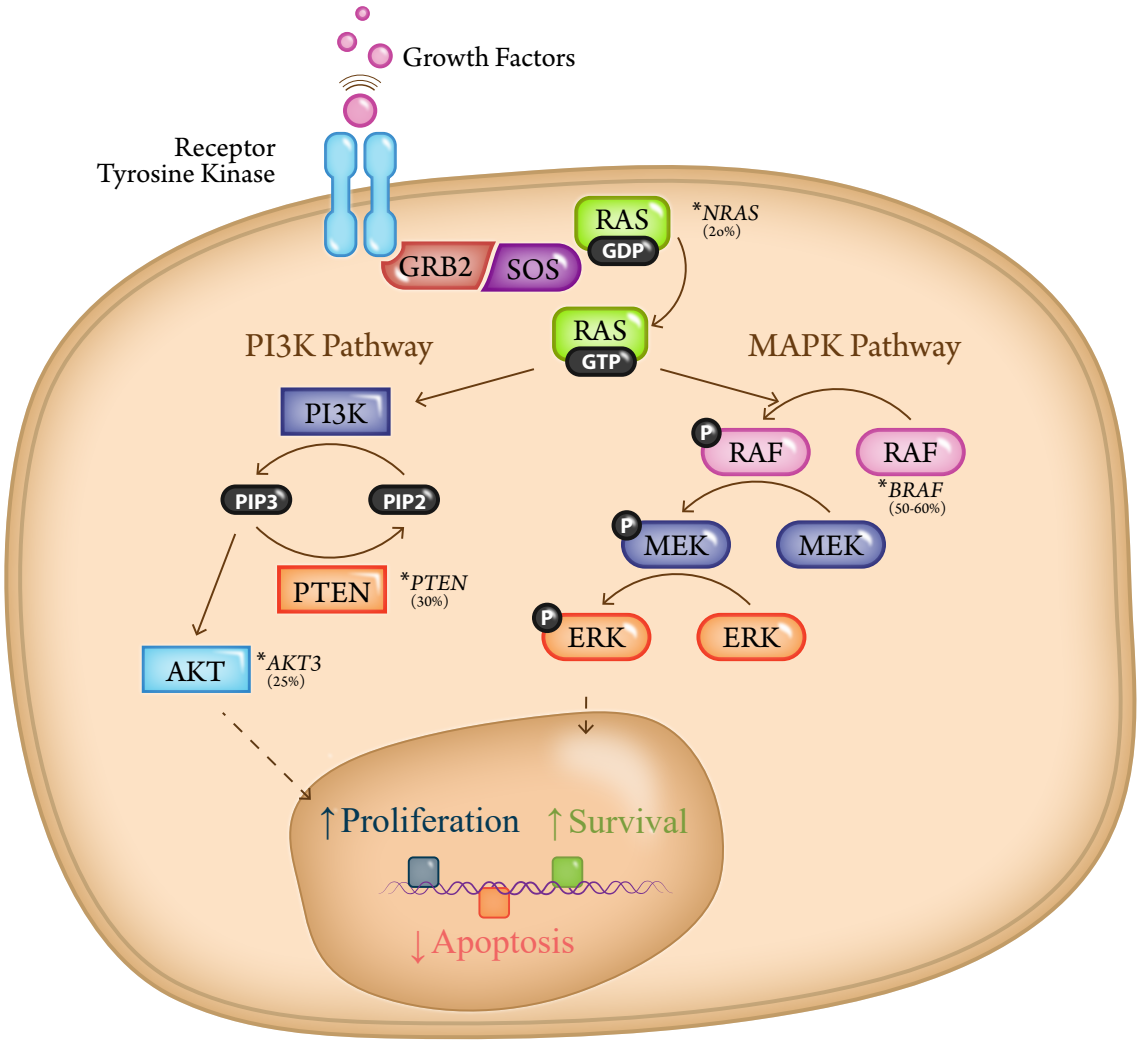

Figure 1.1: The MAPK and PI3K-AKT signalling pathways in melanoma. Diagram of key activators, regulators and critical mutations of the MAPK and PI3K-AKT signaling cascades in malignant melanocytes.

tors located on the cell surface. This, in turn, leads to the activation of the RAS protein which transducts the signal to the RAF group of serine-threonine kinases, including ARAF, BRAF, and CRAF. Each of those three kinases may activate MEK kinases. In turn, MEK kinases activate the following stage of the pathway - ERK kinases, that either phosphorylate cytoplasmic proteins or migrate into the cell nucleus influencing the transcription factors regulating genes connected with proliferation, differentiation and apoptosis.[30]

It has been estimated that about 50-60% of melanomas contain MAPK pathway activating mutations, rendering this pathway as the most important therapeutic target.[29] NRAS harbours activating mutations in 15–20% of melanomas. Several somatic mutations in the *BRAF* gene have been described so far. The most commonly observed mutation in melanomas is BRAF-V600E, which ranges in frequency from 30% to 72%.[31] As BRAF mutations confer RAS-independent activation of the MAPK pathway, concomitant BRAF and NRAS mutants are rarely found.[32]

Melanomas also harbour abnormalities in the PI3K/AKT signalling pathway, but they are observed at lower frequencies. The PI3K-AKT pathway is activated by a number of different factors, including ligands binding to tyrosine kinases receptor and G protein-coupled receptors and GTP binding of RAS proteins. These signals activate the catalytic activity of PI3K, which phosphorylates inositol molecules found on phospholipids in the plasma membrane, resulting in the generation of phosphatidylinositol-(3,4,5)-P3 (PIP3). PIP3 activates downstream signaling effectors, the most notable one being the serine-threonine protein kinases AKT1, AKT2, and AKT3, which activate downstream anabolic signaling pathways required for cell growth and survival. Protein phosphatase PTEN dephosphorylates PIP3 to phosphatidylinositol-(4,5)-P2 (PIP2) and directly antagonizes the activity of PI3K kinase.[33]

The PI3K-AKT pathway has been shown to complement activation of the MAPK pathway in melanocyte transformation. Mutations involving PI3K itself are rare in melanoma. However, significantly increased expression of p-AKT was observed in melanomas with complete loss of PTEN. Deleterious mutation or loss of PTEN have been described in 10% to 30% of melanomas. These events also seem to coincide with BRAF mutation and are mutually exclusive with NRAS mutations.[34–36] Alterations of *AKT1* and *AKT2* genes are rare, but genetic gain of AKT3 is seen in 25% of melanoma tumours.[37,38]

Less common genetic alterations, such as cyclin D1 amplification and cyclin-dependent kinase 4 mutation have also been identified in association with BRAF mutation. Other genomic aberrations, such as amplification of microphthalmia-associated transcription factor, loss of expression of the p16 also represent oncogenic events in melanomas.[36,39] Still, 30–40% of melanomas do not bear identifiable driver mutations by conventional clinical assays and are considered to be 'pan-negative'.[40] The lack of clearly detectable mutations or available targeted therapies makes this a challenging cohort in the clinic.

Nevertheless, melanoma still remains a paradox among all solid tumours. Despite the fact that many critical mutations and prognostic markers have already been identified, there is very little understanding of their biological role and interplay in the transformation of melanocytes into melanoma cells, as well as their contribution to the metastatic phenotype. In fact, the prognosis of malignant melanoma relies mainly on histological criteria such as tumour size, thickness, ulceration and mitotic activity. However, the identification of novel critical driving mutations and signalling pathways represents potential new therapeutic targets for human melanoma treatment.

1.1.3 Management of Melanoma

Malignant melanoma is among the most notoriously aggressive and treatment-resistant human cancers. Melanoma therapy remained the same for several decades: surgical excision of the malignant mass remains the mainstay of primary melanoma treatment at all sites. An early diagnosis followed by the appropriate surgical technique is currently the only demonstrated effective treatment.

In theory, surgery allows locoregional disease control without severe functional and/or aesthetical impairments.[41] However, the prognosis for melanoma patients with distant metastases is generally poor, with historical 5-year survival rates of less than 10%.[42]

1.1.3.1 Chemotherapy, Targeted Therapy and Immunotherapy

Cytotoxic chemotherapy has been used for the treatment of advanced melanoma for over 4 decades. Dacarbazine still is the chemotherapeutic agent of choice in metastatic melanoma. Temozolomide, another alquilating agent, is preferred when central nervous system metastases are present.[43] However, the overall success of chemotherapy in metastatic melanoma is quite limited. Metastatic melanoma has historically carried an especially poor prognosis, with an average survival of 6-9 months.[42,43] In recent years, however, major breakthroughs in both immune-based therapies and molecularly targeted inhibitors brought great advancements and expanded the treatment options for patients with this disease.[44]

One the most important milestones was the approval of immune-checkpoint inhibitors that target the mechanisms of tumour immunosuppression, including cytotoxic T lymphocyte-associated antigen (CTLA)-4 and programmed death (PD)-1 receptors. CTLA-4 and PD-1 are immune checkpoint receptors expressed by T-cells that upon binding to its ligands, which are expressed on melanoma cells, negatively regulate T-cell activation thereby causing immunosuppression and preventing the immune system from triggering an immune T-cell response to the tumour.[45] Ipilimumab, an inhibitor of CTLA-4, and nivolumab and pembrolizumab, both PD-1 inhibitors, are monoclonal antibodies approved as immunotherapies for melanoma that target these receptors resulting in increased activation of inflammatory tumour-cell removal responses.[36,45]

The discovery of many critical mutations in melanoma led to the introduction of targeted molecular inhibitors in melanoma therapy. BRAF protein inhibitors such as vemurafenib and dabrafenib or MEK inhibitors cobimetinib and trametinib are approved drugs that combine the inhibition of intracellular MAPK signal transduction. Inhibition of NRAS, ERK, AKT and other intermediaries of the major altered signaling pathways identified in melanomas is an emerging therapeutic strategy and represents another major leap in melanoma treatment.[36,44]

Moreover, there are many ongoing clinical trials testing the efficacy and safety of new molecules and treatments. The results of various combinations of approved drugs, treatment modalities and new promising agents keep emerging in the literature. Researchers continue working on new possible methods of treatment and combinations of adjuvant therapies as resistance to the immuno and targeted therapy drugs is a commonly observed complication.[46]

1.1.3.2 Radiation Therapy

RT is frequently employed as a treatment option for the majority of malignancies. However melanomas reputation as a prototypical RT-insensitive cancer still discourages the use of ionizing

radiation as an adjuvant therapy in melanoma patients. Wide local surgical resection has proved effective at low risk for primary melanoma lesions, so RT is not a first-line treatment.[41] Radiation therapy (whole-brain irradiation and/or stereotactic radiosurgery) is particularly useful in the management of brain metastases, as most systemic chemotherapeutic drugs have limited penetration into the central nervous system or when adequate surgical margins cannot be guaranteed, such as with melanoma lesions of the head and neck.[47]

The role of adjuvant RT in melanoma therapy has generally been limited to palliative care because melanoma has historically acquired a biased reputation as a radioresistant tumour.[48] However, recent clinical trials combining appropriately fractionated higher delivered doses of radiation with immunotherapy and chemotherapy agents improved the outcome of treatment and palliation of symptomatic melanoma metastases, endorsing RT to play a greater role in melanoma management.[44,49,50]

1.1.4 Final Remarks

Malignant melanoma is an aggressive and clinically complex malignancy. Melanoma can arise from very distinct anatomic locations with numerous, and sometimes rare, subtypes. Distinguishing ambiguous dysplastic nevi from those true melanoma represents a challenge in histopathologic diagnosis. Most diagnostic biomarkers of melanoma rely on detection of melanocytes rather than melanoma itself and currently there are no serologic markers for the early detection of melanoma. Melanoma etiology results from an intricate combination of environmental factors and genetic abnormalities. However, there is very little understanding of their biological role in disease progression. Melanoma unique biology challenges clinical control of the disease and improvement in patient survival has been an arduous path. However, poor prognosis for patients with metastatic melanoma has changed radically over past few years. The medical approaches in practice are becoming more and more promising as several novel agents designed for patients with advanced melanoma appeared just a few years ago. Numerous clinical studies present clinical benefit of treatment with new biological agents and molecular inhibitors over standard chemotherapeutics, but melanoma management still is a major challenge for clinicians. Participation in clinical trials remains a mainstay for patients with melanoma. Nevertheless, patients diagnosed with melanoma today are given a chance to access sophisticated treatment that has never been available before.

1.2 Obesity and Melanoma

Adipose tissue (AT) has long been recognized as a mere reservoir of energy. When the caloric intake surpassed the body daily needs, extra-energy is converted to high-caloric fatty acids, and later stored in adipocytes. When extra energy is required, or over long periods of fasting, the fatty acids stored in adipocytes are mobilized to provide energy for other tissues. With the "modern lifestyle",

obesity has become prevalent and novel functions for AT have been unveiled. Parallel to the fat-storage specialization, adipocytes are secretory cells that produce a panoply of molecules, generally named as adipokines. Adipokines mediate vast functions in our organisms, from appetite to inflammation, including angiogenesis. Nowadays, the knowledge about AT is accumulating, changing our view on adiposity and raising it to an inflammatory and endocrine organ.[51]

The excessive accumulation of fat and AT expansion are serious risk indicators for metabolic impairment. Obesity is implicated in the development of metabolic syndrome, contributing to the onset of hypertension and dislipidemia, the development of atherosclerosis and cardiovascular complications, and the establishment of glucose intolerance, peripheral insulin resistance and the pathogenesis of type 2 *Diabetes mellitus*.[52–54] AT dysfunction, along the development of obesity, promotes the instalment of a chronic low-grade inflammatory state in metabolic tissues, that is accompanied by a parallel increase in systemic oxidative stress.[55–58] However, the spaciotemporal interdependency of these biological hallmarks in the pathogenesis of obesity has yet to become better understood.

In 2003, a new epidemiologic link between between obesity and several types of malignancies raised the alarm in the scientific and medical communities.[59] The risk of obesity-associated cancer is now well established by more than a decade of scientific research.[60] Obesity is not only associated with the onset of cancer, but has also a negative impact in the disease progression leading to a worsened prognosis and a higher mortality risk from the most common forms of cancer in overweight patients.[61,62]

Not all cancers are associated with obesity and the relative risk varies among different cancer types. In epidemiologic studies, obesity-associated cancer risk is often quantified as the ratio of the probability change in risk per 5 kg/m^2 increase in body mass index, a measure of adiposity. Using this formula, recent meta-analysis estimate a malignant melanoma relative risk in between 1.17-1.31,[63–65] however other prospective cohort studies showed no significant association between obesity and risk for malignant melanoma.[62,66]

1.2.1 Mechanisms Linking Obesity and Melanoma

AT expansion, during the development of obesity, shares several biological similarities with malignant neoplasms. Both tissues exhibit considerable and rapid expansion and cause deleterious effects on the organism. Any expanding tissue is challenged to vascularize the growing mass in order to provide access to sufficient O_2 and nutrients, overcoming hypoxia. Both diseases share significant alterations in immune responses and adipose/cancer cells have the capacity to establish interactions and modulate immune cells. Finally, dysfunctional adipocytes and neoplasic cells have abnormal gene expression profiles and factor secretion patterns, with similar modulation of parallel signaling/metabolic pathways during adipogenesis and oncogenesis.[67,68]

Taking into account the overlapping characteristics of both pathologies, several molecular intermediaries and biological processes have been investigated in an attempt to disclose the contribution

of obesity to the initiation, development and progression of malignant melanoma. Adipose growth-factors, hypoxia, angiogenesis, inflammation, oxidative stress and energetic metabolism have all been postulated as possible biological candidates in the cross-talk between fat deposition and the pathogenesis of melanoma and will be reviewed in the following sections (Fig. 1.2). Yet, the rationale behind obesity-associated melanocyte carcinogenesis is a problem that is far from being completely understood.

1.2.1.1 Adipokines and Growth Factors

Nowadays, AT is considered an endocrine organ due to the production of multiple bioactive molecules. These adipose-derived secreted factors can exert effects at both local and systemic levels. The great majority of these factors are cytokines, chemokines and inflammatory mediators, but a role in growth regulation as a new aspect of adipokines has been revealed by novel adipocyte-released molecules.[69] Deregulated production and/or secretion of these adipokines, caused by excess

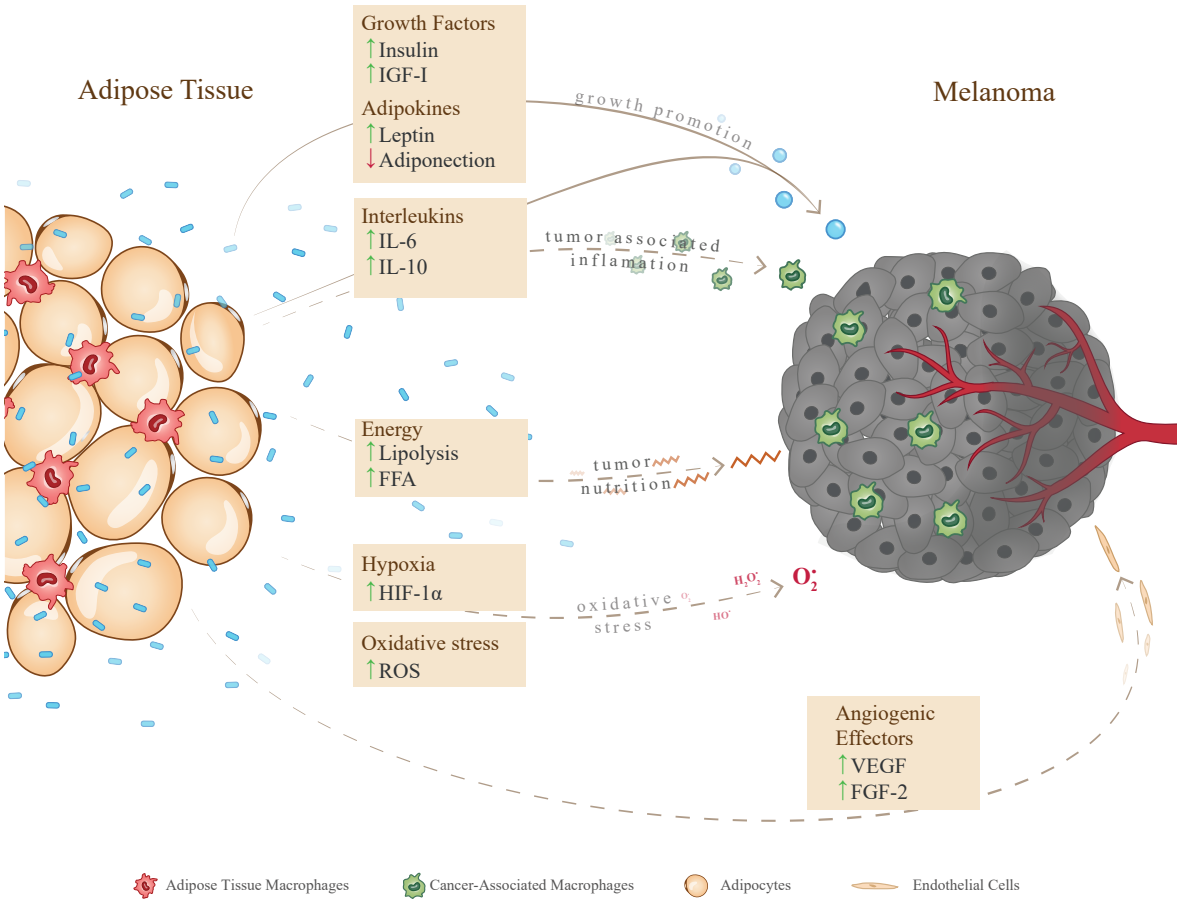

Figure 1.2: Mechanisms linking obesity and melanoma. Adipose growth-factors, hypoxia, angiogenesis, inflammation, oxidative stress and energy metabolism have all been postulated as possible players in the cross-talk between fat deposition and the pathogenesis of melanoma.

Legend: FFA: free fatty acids; FGF-2: fibroblast growth factor 2; HIF-1α: hypoxia inducible factor 1α; IGF-I: insulin-like growth factor I; IL: interleukin; ROS: reactive oxygen species; VEGF: vascular endothelial growth factor.

adiposity and AT dysfunction, has been linked to the pathogenesis of various obesity-linked diseases, including cancer.[62,70]

A number of biological changes associated with obesity have been identified as predictors of a poor prognosis in melanoma, including hyperinsulinemia, insulin resistance[71,72] and IGF-I activity, changes in the production of adipokines, including increased circulating leptin[73,74] and resistin[74] and decreased serum levels of adiponectin.[71,75] Although not expressed by melanocytes, IGF-I and insulin are essential mitogens for normal and malignant melanocytes involved in the proliferation and strong evasion of apoptosis.[76] Leptin and resistin serve as angiogenic/mitogenic factors in melanoma tumour growth and metastasis,[73,74,77,78] while adiponectin exerts primordially anti-proliferative and anti-inflammatory effects.[72,79] In fact, the increased circulating levels of insulin and leptin as well as the IGF-I signalling axis have already been proposed as a molecular link that might aggravate melanoma carcinogenesis in obese individuals.[80]

Additionally, endocrine-mediated consequences of obesity also renders an increase in serum levels of adipose-secreted growth factors. Elevated circulating levels of EGF, TGF-β, hepatocyte growth factor (HGF), fibroblast growth factor (FGF)-1, FGF-2 and FGF-21, platelet-derived growth factor (PDGF) have been reported in obese individuals. Interestingly, melanoma cells are very sensitive to FGF-2 and EGF signaling.[81] Moreover, HGF is expressed in most melanomas and activates various cellular signaling pathways involved in proliferation, migration, and invasion in a paracrine manner.[16] HGF, IGF-I, EGF, FGFs and TGF-β are involved in phenotype switching in melanoma and epithelial-to-mesenchymal-like transition,[82] while PDGF, HGF, TGF-β and EGF act as angiogenesis promotors as well.[83–85]

Adipose-derived secreted factors accumulation can induce signal transduction upon binding to the respective receptors located on the surface of the melanoma cell. Overexpression of numerous G-protein-coupled receptors and receptor tyrosine kinases has long been recognized to play central roles in the metastatic melanoma phenotype.[86,87] This in turn leads to the activation of their downstream signalling cascades, most of them converging at the PI3K/AKT and MAPK pathways. However, most melanomas already harbour constitutively activating mutations in MAPK and PI3K/AKT pathways and raise doubts about the magnitude of the effects of these adipose-derived factors in promoting melanoma carcinogenesis. Conversely, overexpression of some of these growth factors, by malignant melanocytes, promotes adaptive resistance to targeted therapies in melanoma[88] and pharmacological receptor-inhibition, even though located upstream in the signaling cascade, revealed some sort of effectiveness in reducing tumour growth in human melanoma.[89]

In fact, obesity-associated superfluous AT could be an important additional source of extracellular mitogenic factors that provide paracrine stimulation and activation of intracellular pathways involved in proliferation, migration, and invasion of melanoma cells.

1.2.1.2 Angiogenesis

With few exceptions, the majority of tissues in adult life are in a quiescent state. Their capacity to expand is limited and, in non-pathological conditions, they remain in a homeostatic growth steady-state. Unlike most other tissues, AT exhibits high plasticity in adulthood, with permanent growth potential and almost unlimited expansion. AT humongous expansion potential allows it to account for 40% of total body mass and expand or shrink up to 10 times its mass. Concomitantly with AT expansion or reduction, the growth, maintenance and remodeling of a supporting network of vessels must occur. Therefore, adipocytes must be capable of tightly regulating the angiogenic process.

In fact, decades ago surgeons have already realized that AT can improve wound healing by stimulating angiogenesis.[90] This vascular growth-stimulating effect has been initially attributed to the ability of adipocytes to produce vascular endothelial growth factor (VEGF). Nowadays, more and more adipokines are known to have direct and indirect effects on AT vascularization. Adipocytes are able to stimulate and/or inhibit angiogenesis, thus controlling and fine-tuning vascular remodeling.

AT secretes numerous angiogenic modulators including leptin, VEGF, FGF-2, HGF, tumour necrosis factor (TNF)-α, TNF-β, interleukin (IL)-1β, IL-6, IL-8, placental growth factor (PlGF), PDGF, visfatin, resistin, neuropeptide Y, leptin and angiopoietins, as well as antiangiogenic factors thrombospondin-1, plasminogen activator inhibitor (PAI)-1 or adiponectin, whose expression balance will determine the triggering or halting of the angiogenic switch.[91–94] In addition to adipocytes, AT contains diverse cell types including adipose stromal cells (ASC) and adipose tissue macrophages (ATM) that also contribute to angiogenesis. ASC also produce a pleiade of angiogenic factors (VEGF, HGF, GM-CSF, FGF-2, and TGF),[95,96] while macrophages also produce VEGF and the angiogenic cytokines TNF-α, FGF-2, IL-1β, IL-6, and IL-8.[97] AT also produces several matrix metalloproteinase (MMP)s including MMP-2 and -9,[96] which could potentially affect preadipocyte differentiation and microvessel maturation by modulating the extracellular matrix. Moreover, MMPs release the matrix-bound VEGF and indirectly induce angiogenesis.

Angiogenesis is a pivotal process in neoplasic progression and metastasis. The *de-novo* formation of blood vessels is typically perceived as the tumour's response to the low O_2 pressures or hypoxic conditions. Several pro-angiogenic factors were discovered, which play a pivotal role in tumour angiogenesis, including melanomas. Among these are VEGF, FGF-2, EGF and IL-8 as well as PlGF, and PDGF.[83,84] However, hypoxia-independent drivers of melanoma angiogenesis have also been described.[98] Hypoxia-independent expression of VEGF, IL-8 and FGF-2 may in fact be more important than hypoxia-induced upregulation of these factors in the angiogenesis of melanoma xenografts.[99].

Triggering pro-angiogenic events even before a critical tumour mass is reached, in an hypoxia-independent manner, allows small tumour cell colonies to recruit blood vessels, providing the first entry point into the vasculature, which produces the appropriate signals to metastasise. Adipose-derived angiogenic factors might be a source of these premature angiogenic stimuli. The induction of an early

switch to the vascular phenotype contributes to the acceleration of tumour growth, accompanied by a deleterious impact in the disease metastatic onset in overweight individuals.

1.2.1.3 Hypoxia

The labile expansion of fat mass combined with the large hypertrophic adipocytes is not accompanied by a proper expansion of the capillary network, disrupting the oxygen supply to adipocytes.[100] Hypoxia in AT of obese individuals has been proposed a causal role in triggering the inflammatory response in AT, with the release of cytokines, chemokines, and angiogenic factors, that would serve to increase blood flow and stimulate angiogenesis, as well as the associated systemic metabolic complications.[100–104]

Cells under low-oxygenation must express numerous genes to properly adapt. Hypoxia inducible factor (HIF)s are a family of well characterized heterodimeric factors that establish the main hypoxia-responsive cellular sensors and molecular mediators.[105] HIF-1α has been found to be elevated in AT hyperplasia and has a putative role in adipocyte differentiation and function.[103,106,107] Adipocytes exhibit extensive functional changes in culture in response to hypoxia and HIF-1α, which alters the expression of up to 1,300 genes. These include genes encoding key adipokines such as leptin, IL-6, VEGF, and MMP-2 and MMP-9, which are upregulated, and adiponectin, which is downregulated.[106,108] Hypoxia also inhibits the expression of genes linked to oxidative metabolism while stimulating the expression of genes associated with glycolysis.[108]

HIFs are key regulators of the vasculature homeostasis.[109] HIF-1α is a very powerful pro-angiogenic stimulator, with recognized roles in numerous hypervascularization disorders and cancer neovascularization. In fact, activation of HIF-1α is upregulated by hyperinsulinemia and adipogenesis, but not by hypoxia in adipocytes,[110] suggesting that AT angiogenesis and VEGF expression is neither HIF-1α nor hypoxia dependent.[110,111] Human AT samples from obese patients have, in fact, pronounced greater levels of VEGF-A and other pro-angiogenic factors,[112,113] but there is no significant increase in the number of capillaries formed and no organized vascular response to the increased stabilization of HIF-1α has been observed.[114]

Studies from Bedogni *et al.* have previously demonstrated the importance of hypoxia of the skin in melanocyte transformation and the development of melanoma.[115] Oncogenes such as *RAS* can increase the expression of both VEGF and FGF-2. This effect is likely due to increased stabilization/activity of HIF-1α, a transcription factor that plays an essential role in tumour angiogenesis and tumour progression.[109] Specifically, the mild hypoxic microenvironment of the skin contributes to melanocyte transformation, and hypoxia-mediated melanoma proliferation occurs via the PI3K/AKT and MAPK kinase pathways.[116]. Simultaneously, hypoxia promotes both melanoma growth and metastasis in addition with the accumulation of IL-10-secreting M2-like macrophages within tumours.[117] Hypoxia also increases the heterogeneity of melanoma cell populations, indicating that a subset of cells rests as a treatment-resistant pool that confers incomplete response to treatment.[118]

Hypoxia is able to induce vasculogenic mimicry channel formation and promote tumour invasion-related protein expression, such as MMP-2 and MMP-9, in melanoma, strengthening the invasive and metastatic potential.[119] Silencing of HIF-1α protein production induced the apoptosis of hypoxia-tolerant and hypoxia-resistant melanoma cells *in vitro*,[118,120] further reinforcing the putative role of hypoxia in melanoma etiology.

Actually, AT hypoxia in human obesity has been challenged. Despite the lower oxygenation of AT in obese patients,[121] the low oxygen demand by adipocytes[122,123] might undermine the expected hypoxic state of the fat mass. Unlike in the diet induced obesity mouse models, adiposity gain, in humans, develops over long periods of time. The slower expansion of the adipose mass, allied to an larger vascular remodeling timeframe, that allows partial vascularization of at least some of the expanding fat depots, can also account to the observed discrepancies, weakening the theory of hypoxia-triggered angiogenesis-dependent metabolic dysfunction of AT in obesity. Additionally, BRAF/MEK/ERK signaling[124] and the PI3K pathway[125] are involved in an hypoxia-independent regulation of HIF-1α in cancer. HIF-1α accumulation can also take place in presence of increased levels of reactive oxygen species (ROS) and nuclear factor-κB (NF-κB) in melanoma,[126,127] both being commonly deregulated in this cancer type.

Given the anatomical vicinity of melanocytes to subcutaneous fat, obesity-associated hypoxia might render a great impact in exacerbating the hypoxic microenvironment of the skin, endorsing melanoma development. Additionally, the aberrant hypoxia-induced adipocyte secretome includes several factors known to play a role in tumour cell proliferation, apoptosis, migration, inflammation, and aggressiveness that might paracrinally induce changes directly in malignant cells or in the tumour milieu.

1.2.1.4 Inflammation

Macrophages play a key role in inflammatory diseases.[128] Visceral adiposity low-grade chronic inflammation and ATM accumulation are pivotal in the deleterious effects for the obesity-associated metabolic syndrome and insulin resistance.[57,129] In fact, macrophages and other inflammatory cells in the AT cellular content ranges from up to 10% in lean subjects, compared to nearly 40% in overweigh individuals.[129] The massive infiltration of macrophages into AT leads to chronic inflammation that not only modifies local metabolism, but also influences systemic energy.

Generally, ATM have been characterized into two sub-populations: M1 and M2 macrophages. While the M1 macrophages are associated with more pro-inflammatory cytokines, M2 macrophages display an anti-inflammatory profile.[130] In obesity, it has been proposed that a phenotypic switch inducing a M2 to M1 polarization of the ATM occurs and could account for the metabolic impairments and chronic inflammation of AT.[131,132] In addition to their immunological function macrophages also modulate tissue growth and angiogenesis through the production of growth factors and pro-angiogenic cytokines, respectively. This dual role of macrophages is well known in tumour angiogen-

esis.[133] In tumours, M1 macrophages are associated with pro-inflammatory tumour-cell removal responses, whereas M2 macrophages exhibit tumour-promoting properties including the production of proteolytic enzymes, the suppression of anti-tumour immune responses and act as tumour-associated angiogenic sponsors.[133,134]

In most advanced tumours, and in contrast to ATM pool, tumour-associated macrophages (TAM) have been reported to be preferentially shifted towards an M2-like anti-inflammatory phenotype.[135] In malignant melanoma, TAM and their secreted mediators may be involved in all steps of invasion and metastasis, correlating in most cases with poor outcomes.[136] On the contrary, the presence of tumour-infiltrating lymphocytes is regarded as the host immune anti-tumour response and is associated with improved survival.[137] Additionally to TAM-released cytokines, IL-1, IL-6, IL-8, and IL-10, TNF-α and TGF-β are also produced by melanoma cells to stimulate proliferation in autocrine loops,[138,139] while paracrinally they modulate the microenvironment, via M2-macrophages, to the benefit of tumour growth and invasion.[117,140,141] IL-6, IL-10, TNF-α, and TGF-β also regulate anti-melanoma immune responses, further increasing the immunosuppressive environment in the tumour stroma.[142]

Nevertheless, TAM and ATM produce an overlapping collection of cytokines, such as TNF-α, IL-1, IL-6, IL-8, monocyte chemotactic protein (MCP)-1 and TGF-β.[97,143] The mutual obesity-associated ATM and TAM-released inflammatory factors mentioned above are involved in the regulation of tumour growth, angiogenesis, invasion, and/or promotion of cancer metastasis,[143] and may in fact be a linking rationale in the contribution of AT-inflamation to worsen tumour progression and melanoma risk. Recent studies revealed that high-fat diet-induced obesity and peritumoural AT increases tumour progression and angiogenesis in B16-F10 melanoma allografts, with concomitant accumulation of M2-macrophages and IL-6 and IL-10 signalling, further reinforcing these assumptions.[144,145]

1.2.1.5 Oxidative Stress

Excessive cellular production of ROS such as superoxide anions, peroxides and hydroxyl radicals, imbalances redox homeostasis with the depletion of antioxidant defences, culminating in oxidative stress. Oxidative stress, which has long been recognized as an adverse event for promoting tumourigenesis and cancer progression, plays a fundamental role in melanocytes UV-induced photocarcinogenesis.[146,147] Exacerbated levels of ROS can irreversibly modify protein, lipid and DNA molecules, and permanently or temporarily change their cellular behavior, leading to the accumulation of somatic DNA mutations, proto-oncogenes activation and epigenetic alterations.[148] At the same time, increased signaling via AKT, RAS/RAF/ERK and NF-κB pathways, constitutively activated signaling cascades in melanomas, stimulate endogenous ROS production, further enhancing oxidative damages in melanoma cells.[127,149]

Besides their harmful effects, ROS and oxidative stress are key mediators in the regulation and

homeostasis of several signal transduction pathways in normal and cancer cells.[150] ROS-mediated PI3K/AKT activation,[151] and NF-κB[149] signaling promote cell proliferation and apoptosis suppression. ROS and reactive nitrogen species (RNS) are also implicated in HIF-1α stabilization,[152] the expression of VEGF and VEGF receptors,[152,153] angiogenesis[153,154] and vasculogenic mimicry[155] in melanomas.

However, both malignant and non-malignant melanocytes bear higher basal levels of ROS compared to keratinocytes and epidermal fibroblasts. Recently, melanin, melanogenesis and melanoma aberrant melanossomes have been found as another source of ROS,[21] which seems counter-intuitive at first. Melanin acts as a scavenger of active oxygen species and is in general regarded as protective pigment.[156] However, melanin pigment plays a double role in the etiology of melanoma acting as a two-edged sword: protecting the melanocytes against UV radiation and oxidative stress, but at the same time melanossomes accelerate melanoma progression and resistance to the effects of ROS-generating treatment therapies, specially RT,[22,23,157] rendering melanomas ionizing radiation resistant.

In addition to endogenous melanoma ROS production, other cells in the tumour microenvironment can generate various ROS and RNS. TAM are effective producers of ROS and RNS and further contribute to a pro-oxidant environment.[140] ROS produced from inflamed peritumoural AT and cancer-associated adipocytes also accelerate oxidative stress within tumour cells and might contribute to cancer progression in overweight patients.[144]

In fact, oxidative stress has been proposed as a mechanistic link between obesity and cancer.[64] Central adiposity is characterized by a general increase in systemic oxidative stress, in part through the inflammatory process but also by enhanced levels of reactive oxygen and nitrogen species.[56,70] Obese patients also have impaired antioxidant defences[55] that further increase oxidative damage to DNA, RNA, lipids and proteins in a process that enhances carcinogenesis.

1.2.1.6 Energy Metabolism

The main metabolic function of AT is to store energy as triglycerides and provide fatty acids for other tissues and organs. In fact, fatty acids are the main secretion product of adipocytes. Tumour cells display progressive changes in metabolic activity that correlate with malignancy, including *de novo* lipid biosynthesis and the development of lipogenic phenotype.[158] Still, the fatty acids stored in fat tissue can be an important reservoir of energy to sustain the rapid tumour growth.

Recent studies show the transfer of lipids from adipocytes to melanoma cells. In melanoma cell line B16-F10 adipocyte-released palmitic acid has a positive proliferative effect in melanoma growth and palmitic acid-pretreated B16-F10 cells resulted in larger tumours upon inoculation in mice.[159] The fatty acid synthesis pathway is activated in various types of cancers and seems to be an important mediator in the link between obesity and melanoma.[160] Both palmitic acid and fatty acid synthase have an impact on the activation status of AKT with a concomitant stimulation of AKT signaling cascade in a PTEN-independent way, although the underlying mechanisms are not fully elu-

cidated.[159,160] In melanoma, reducing intracellular palmitic acid/fatty acid levels by lipase activity blockage[161] or by inhibiting fatty acid synthase[74,162] induces cancer apoptosis and reverses obesity-induced rapid melanoma progression and metastasis.

These effects not only suggest the importance of fat-stored lipids as fuel to tumour growth, but also suggest that both exogenous and endogenous fatty acids are mediators in critical signaling pathways in melanoma. Thus, melanoma tumourigenesis involves communication between tumour cells and neighboring adipocytes, posing as another molecular link in the melanoma-obesity rationale.

1.2.2 Final Remarks

Obesity has long been recognized as a risk factor for metabolic impairment, contributing to hyperlipidemia, atherosclerosis, cardiovascular complications and type 2 *Diabetes mellitus*. Last few years brought a novel view on the possible deleterious contributions of high adiposity to cancer onset and progression, including melanomas. Obesity and cancer have complex etiologies and pathophysiological mechanisms. However, both morbidities exhibit undoubtedly too many similarities, from molecular and cellular players to biological processes and signalling pathways, even similar microenvironments. Adipose growth-factors, adipokines, cytokines, hypoxia, angiogenesis, inflammation, oxidative stress and energy metabolism are all possible candidates in the cross-talk between obesity and cancer. In fact, obesity is a complex, multifactorial and multi-system disease and a "one mechanism fits all" is unlikely to exist.

The obesity-carcinogenesis relation is not fully elucidated and still remains controversial for malignant melanoma. Nevertheless, sufficient evidence exists to support ongoing and planned research studies to further acquire in-depth knowledge and evidence to attain a more clear understanding of this rationale.

1.3 Rationale

The incidence of melanoma has been increasing steadily over the past few decades in most western countries and obesity has been postulated to be one of the causes for the increased incidence of melanoma. However, literature on this subject is scarce, with limited and scant in-depth evidence about the obesity-associated melanoma carcinogenesis. Indeed, many questions still need an answer in the relationship between obesity and melanoma. High adiposity is associated with a dysfunctional secretion profile of multiple bioactive molecules as well as with a more pro-oxidant status. Oxidative stress, in turn, is a major player in radiotherapy. Herein, we aim to unravel the biological role of adipose derived factors, focusing on fat-released adipokines, growth factors and angiogenic modulators, in our search for mechanisms of obesity-enhanced melanoma progression. Our research efforts were divided in three separate and specific milestones with inherent specific objectives defined as follows:

- evaluate the biological roles and direct paracrine effects of both adipocyte and adipose tissue secretomes towards malignant melanocytes proliferation and plasticity *in vitro*;
- investigate the effects of fat-derived growth factors in melanoma cell survival, oxidative stress and radioresistance employing an *in vitro* radiotherapy cell culture model;
- elucidate the *in vivo* effects of high-fat diet feeding in melanoma progression and metastasis, focusing on tumour vascularization and vasculogenic mimicry;

2

Effect of Adipocyte Secretome in Melanoma Progression and Vasculogenic Mimicry

Coelho P, Almeida J, Prudêncio C, Fernandes R and Soares R

Journal of Cellular Biochemistry 2016; **117**(7):1697–1706

ABSTRACT

Obesity, favored by the modern lifestyle, acquired epidemic proportions nowadays. Obesity has been associated with various major causes of death and morbidity including malignant neoplasms. This increased prevalence has been accompanied by a worldwide increase in cutaneous melanoma incidence rates during the last decades. Obesity involvement in melanoma aetiology has been recognized, but the implicated mechanisms remain unclear. In the present study, we address this relationship and investigate the influence of adipocytes secretome on B16-F10 and MeWo melanoma cell lines. Using the 3T3-L1 adipocyte cell line, as well as *ex vivo* subcutaneous (SAT) and visceral (VAT) adipose tissue conditioned medium, we were able to show that adipocyte-released factors play a dual role in increasing melanoma cell overall survival, both by enhancing proliferation and decreasing apoptosis. B16-F10 cell migration and cell-cell and cell-matrix adhesion capacity were predominantly enhanced in the presence of SAT and VAT released factors. Melanocytes morphology and melanin content were also altered by exposure to adipocyte conditioned medium disclosing a more dedifferentiated phenotype of melanocytes. In addition, exposure to adipocyte-secreted molecules induced melanocytes to rearrange, on 3D cultures, into vessel-like structures, and generate characteristic vasculogenic mimicry patterns. These findings are corroborated by the released factors profile of 3T3-L1, SAT, and VAT assessed by microarrays, and led us to highlight the mechanisms by which adipose secretome from subcutaneous or visceral depots promote melanoma progression.

2.1 Background

Obesity prevalence has significantly increased worldwide,[163] leading to a public health concern and branded as "the modern epidemic".[53,163] The prevalence of obesity in Europe has increased by approximately 30% over the past 10 years and this phenomenon is corroborated by data from several other countries.[164] It has long been recognized that excess adipose tissue (AT) increases the risk of cardiovascular disease, type 2 diabetes and metabolic syndrome,[53,163] but only in the past few decades it became widely accepted that augmented body adiposity is a risk factor for several types of malignancies.[165,166] Additionally, obesity can lead to worsened prognosis, poorer treatment outcome and increased cancer-related deaths.[61]

Cutaneous melanoma incidence rates have increased in the last decades worldwide from 3% to 7% annually.[2] These statistics suggest a doubling of rates every 10-20 years,[3,4] raising melanoma to the most rapidly increasing cancer in Caucasians.[4] Several reports showed positive associations between increased body fat and the risk of cutaneous melanoma later in life,[65,167–169] suggesting that the increasing incidence of melanoma may be related to the enlarged obesity prevalence.

In vivo adiposity-related stimulation of melanoma growth has been demonstrated.[77,144,145,160] Tumour-associated macrophages[144,145] and endothelial cells[145] have been pointed out as possible mediators in the growth-promoter effect of adipose tissue towards melanomas. In fact, tumour stroma comprises many different cell types, including fibroblasts, adipocytes, immune and endothelial cells that, along with the extracellular matrix, are key players in cancer development and progression.[18,170] However, we hypothesize that adiposity might also exert a direct effect over melanocytes without the involvement of stromal cells in a paracrine or endocrine manner. Herein, we explored the biological role of adipocytes secretome in B16-F10 and MeWo melanoma cell survival and plasticity.

2.2 Materials & Methods

2.2.1 Cell Culture and *In Vitro* Treatments

The mouse melanoma B16-F10 cells exhibit *in vitro* a mixed morphology of spindle-shaped and epithelial-like cells. It was originally isolated from melanoma of the C57BL/6J mouse strain. B16-F10 is a metastatic variant of B16 melanomas with high tropism for lung invasion. The human melanoma cell line MeWo was originally derived and established in culture from a lymph node metastasis from a 78-year-old male patient. MeWo is also a metastatic cell line. Similarly to B16-F10 it also resembles moderate lung invasion ability.

B16-F10 murine melanoma cell line (ATCC CRL-6475), MeWo human melanoma cells (ATCC HTB-65), and 3T3-L1 pre-adipocytes (ATCC CL-173) were maintained in Dulbeco's modified Ea-

gle's medium (DMEM; Sigma-Aldrich), human dermal microvascular endothelial cells (HMEC)-1, ATTC CRL-3243) were cultured in RPMI-1640 (Sigma-Aldrich) containing 10 ng/mL epidermal growth factor (BD Biosciences) and 1 µg/mL cortisone (Sigma-Aldrich). Both media formulations were supplemented with 10% heat inactivated fetal bovine serum (FBS; Sigma-Aldrich), 1% penicillin/streptomycin/amphotericin B (Sigma-Aldrich). Cells were grown at 37 °C under a humidified 5% CO_2 atmosphere. Cells were serum-deprived during 16h before incubation with each treatment for every experiment. Unless otherwise specified, all treatments and controls were carried out in serum-free conditions.

2.2.2 Adipocyte Differentiation and Conditioned Medium Collection

3T3-L1 pre-adipocytes were harvested and allowed to reach confluence. After 2 days (day 0), the differentiation was initiated by addition of a hormonal mixture composed of 2 µM insulin (Sigma-Aldrich), 1 µM dexamethasone (Sigma-Aldrich) and 0.25 mM isobutylmethylxanthine (Fluka) in complete medium. Three days later (day 3), the induction medium was replaced by complete medium supplemented with insulin only. At day 7, cultures with a differentiation yield higher than 80% were washed with phosphate buffered saline (PBS) and incubated in serum-free DMEM. After 24h (day 8), the conditioned medium (CM) was harvested from the adipocytes cultures, spun for 5 minutes at 300*g* and the supernatant was stored at -80°C for the subsequent treatments.

2.2.3 Adipose Tissue Organ Culture

Fragments (8-10 mg) from visceral adipose tissue (VAT) and subcutaneous adipose tissue (SAT) depots were collected from 8-week-male C57BL/6J mice. The fragments were then washed with 1% penicillin/streptomicyn/amphotericin B (Sigma-Aldrich) in PBS and cultured afterwards in 1 mL of DMEM supplemented with 10% FBS. The fragments were serum-deprived and 24h later the CM harvested and centrifuged at 300*g* for 5 minutes.

2.2.4 Mouse Adipokine Array Analysis

Mouse adipokine antibody arrays (# ARY-013; R&D systems) were performed using 1 mL of 3T3-L1, SAT and VAT CM and following the manufacturer's protocol. The pixel density of each spot was calculated with the microarray profiler plugin of the ImageJ software (NIH). The relative adipokine levels were calculated upon normalization with the adipokine levels of B16-F10 CM.

2.2.5 Cell Viability Assay

To measure B16-F10 metabolic activity, after a 24h incubation of 1×10^4 cells/mL with the different treatments, 20 µL of the MTS reagent, from CellTiter 96 Aqueous assay (Promega), was added

into each 96-plate well followed by a 3 hour incubation period. Color development was determined by measuring absorbance at 490nm.

2.2.6 Apoptosis Assay

Terminal deoxynucleotidyl transferase-mediated deoxyuridine triphosphate nick-end labelling (TUNEL) assay was performed in B16-F10 cells (1×10^4 cells/mL), after 24h incubation with the different treatments using the In Situ Cell Death Detection Kit (Roche Diagnostics) following the manufacturer's protocol. Nuclei were counter-stained with DAPI (Roche Diagnostics) and immunofluorescence was visualized under a fluorescence microscope (Nikon). The percentage of TUNEL-positive cells was evaluated by counting the cells stained with TUNEL divided by the total number of DAPI-stained nuclei at a 200× magnification field. One thousand nuclei were evaluated. The results are presented as mean±standard error of the mean (SEM).

2.2.7 BrdU Proliferation Assay

B16-F10 cells (1×10^4 cells/mL) were cultured with standard treatments in serum-free conditions for 20h. Then bromodeoxyuridine (BrdU; Roche Diagnostics), at a final concentration of 0.01 mM, was added to each well for 4h. The detection was performed using the colorimetric Cell Proliferation ELISA, BrdU (Roche Diagnostics), according to the manufacturer's instructions.

2.2.8 Cell Spreading and Adhesion Determination

To determine cell spreading and adhesion,[171] B16-F10 cells were re-suspended in the different treatments at a final concentration of 5×10^4 cells/mL, seeded in a 24-well microplate and allowed to adhere and spread for 3 hours and then washed with PBS to remove non-adherent cells. Fixation was performed with 4% (w/v) *p*-formaldehyde in PBS. Afterwards 200 µL of crystal violet 0.1% (w/v) was added to each well for 20 minutes and later washed with H_2O. To evaluate the morphologic parameters (cell area, sphericity, size and perimeter) 1000 cells were analysed by CellProfiler software (Broad Institute) on photographs of random fields, for each treatment, captured under an inverted microscope (Nikon) at a 200× magnification. To determine cell adhesion, the above protocol was reproduced but only allowing cells to adhere for 30 minutes. Afterwards, crystal violet dye was solubilized in 100 µL 10% (v/v) acetic acid (Fluka) and the absorbance measured at 570nm using a plate reader.

2.2.9 Adhesion to Endothelium Evaluation

HMEC-1 cells were cultured in a 24-well microplate with glass coverslips and allowed to reach confluence. Media was aspirated and the monolayers were washed with PBS. Afterwards 1×10^5 cells/mL

B16-F10 cells, in the different treatments, were added to the wells for 30min. To remove non-adherent cells, the wells were washed with PBS. Fixation was performed with 4% (w/v) *p*-formaldehyde for 10 minutes. Coverslips were then stained with Giemsa's stain, thoroughly washed in Sorensen's phosphate buffer and mounted on a microscope slide. Using a light microscope (Nikon) the number of cells adherent to the endothelial monolayer were counted in 5 random fields.

2.2.10 Melanin Content Determination

B16-F10 cells (5×10^5 cells/mL), were incubated with the different treatments for 24 hours. Following detachment with 0,5% trypsin, cell density was assessed on a haemocytometer. After 300*g* centrifugation for 10min, the pellet was washed twice with PBS and the melanin was solubilized in 1.0 mL of 1M NaOH (Panreac) containing 10% (v/v) dimethyl sulfoxide (Merck). Next, the absorbance at 475nm was recorded. Results represent the mean absorbance (±SEM) of 1×10^6 cells.

2.2.11 Transwell Migration

Migration capacity was quantified on 24-well plates with 8 µm-pore transwell inserts (BD Biosciences). B16-F10 cells (5×10^4 cells/mL) were harvested on inserts in serum-free medium and placed on wells containing the standard treatments plus 10% fetal bovine serum (FBS) for 24h. Membranes were then stained with crystal violet 0.1% (w/v) and visualized under a light microscope (Nikon). Five random fields of each membrane were counted on the microscope (Nikon) at a 100× magnification.

2.2.12 Injury Assay

To perform the injury assay, melanoma cells at confluence were scrapped from the culture dish using a pipette tip, which left a void space. Cells were then incubated for 24h following the standard treatments. After this period, damage recovery was then visualized and photographed under an inverted microscope (Nikon) at a 200× magnification. The wound closure was determined by measuring the wound area and by subtracting this value from the initial void space (CellProfiler software; Broad Institute). Shown are the means values (±SEM) of nine measurements for each time point and condition.

2.2.13 Matrigel Cultures

To perform Matrigel cultures, 24-well plates were coated with 250 µL per well of Matrigel Basement Membrane Matrix (Corning). Afterwards, B16-F10 (5×10^4 cells/mL) or MeWo (20×10^4 cells/mL) melanocytes harvested in the respective treatments were fed on top of the Matrigel layer.

Cell growth was then monitored and photographed under an inverted microscope (Nikon) at a 200× magnification for 24h.

2.2.14 Soft-Agar Colony Formation

The bottom of each 12-well plate was coated with 2 mL of 0.5% agarose and DMEM 2×. After polymerization the wells were fed with 5×10^3 B16-F10 cells in 2 mL of 0.2% agar and DMEM 2×. The medium was changed every 2-3 days. After 15 days, the wells were stained with 0.01% crystal violet and photographed. The number and area of the colonies was assessed with ImageJ software (NIH).

2.2.15 Hanging-Drop Cell Cultures

Generation of melanoma spheroids was conducted as previously described.[172] Briefly, 2.5×10^6 B16-F10 or MeWo cells/mL were collected in the respective treatments and pippeted to the lid of a 60mm non-adhesive petri dish leaving 10 µL drops onto the bottom of the lid. The lids were inverted, placed on top of the PBS-filled bottom chamber of the dish and incubated for 3 days.

2.2.16 Statistical Analysis

Results are expressed as mean±SEM. Data were analysed with GraphPad Prism 6.0 (GraphPad Software Inc.). Differences between samples and parameters among two experimental groups were evaluated by Student's *t*-test. When three or more conditions were evaluated, statistical analysis was conducted through one-way ANOVA with Sidak post-hoc test. Significance was set at $P < 0.05$.

2.3 Results

2.3.1 3T3-L1 Secretome Increases Melanocytes Survival, Proliferation and Melanin Content, and Decreases Apoptosis

3T3-L1 preadipocytes are a commercially available cell line for studying adipogenesis.[173,174] Their differentiation, in culture, into mature adipocytes is well widespread and can be achieved by established protocols. We used CM from fully differentiated 3T3-L1 cells to explore the potential effects of adipocytes secretome over malignant melanoma B16-F10 cells viability, proliferation, and apoptosis.

We first analyzed the effects of this conditioned medium in melanoma cells viability by the MTS assay. After a 24h exposure to adipocyte CM, melanoma cells showed a 48% increase in their metabolic activity (Fig. 2.1A). We found as well that the fraction of proliferating B16-F10 cells was signif-

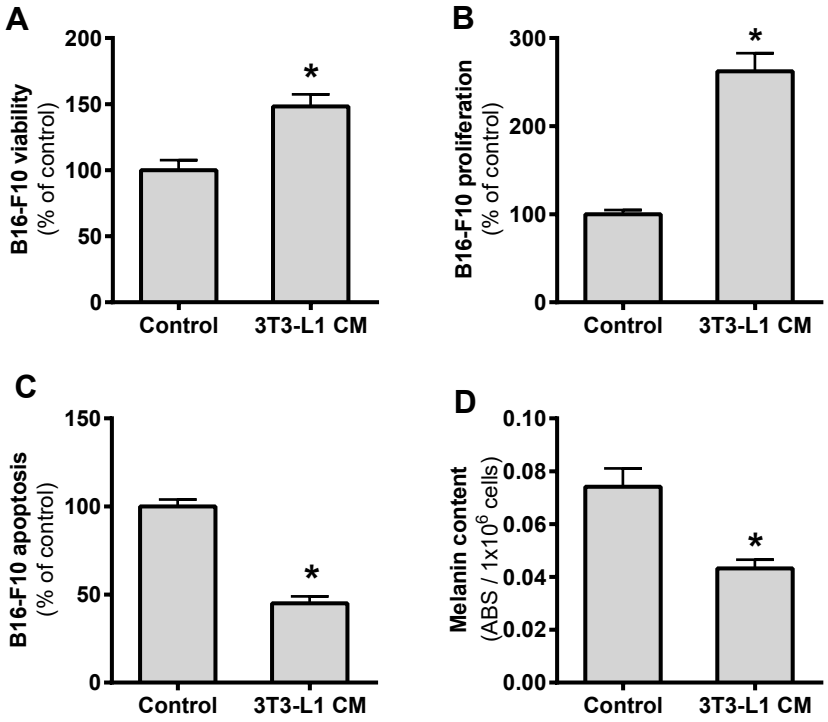

Figure 2.1: 3T3-L1 secretome increases melanoma cell survival. B16-F10 cells were incubated with CM from differentiated 3T3-L1 cells cultures (3T3-L1 CM) or untreated (Control) for 24h. **A)** An increase in the percentage of viable melanoma cells was observed when compared with control. Results represent the percentage of viable cells normalized by the absorbance of control. **B)** The number of proliferating cells, incorporating BrdU, increased in the presence 3T3-L1 CM. Results represent the percentage of proliferating cells normalized over the absorbance of control. **C)** A significant decrease in the percentage of apoptotic cells was observed when melanocytes were treated with 3T3-L1 CM. Results represent the percentage of apoptotic cells evaluated by the ratios of TUNEL-positive cells versus total DAPI-counterstained nuclei. **D)** The melanin content per cell was significantly decreased when melanocytes were cultured in presence of 3T3-L1 CM. Melanin concentration was calculated by determination of OD 475. Results represent the absorbance of 1×10^6 cells. ($*P < 0.05$ *vs* Control; n=9)

icantly increased, as shown by the higher BrdU incorporation, in the presence of these adipocyte-released factors (Fig. 2.1B). The effect of 3T3-L1 secretome on apoptosis was examined using TUNEL analysis. Concomitantly, 3T3-L1 CM medium decreased B16-F10 programmed cell death by approximately 50% (Fig. 2.1C). These effects were further accompanied by a significant reduction in melanin content per cell (Fig. 2.1D).

2.3.2 Adipocyte Secretome Profile Characterization

The previous findings imply that adipocytes released factors stimulate melanoma cell viability and aggressiveness. Therefore, we then assessed the secretion profile of adipocytes to further elucidate the involvement of adipose tissue in melanoma behavior (see Supplemental data). Given the well-established distinct biological and metabolic roles of subcutaneous (SAT) and visceral (VAT) adipose tissue, microarray assay was performed not only in 3T3-L1 cells, but also in organ cultures of SAT

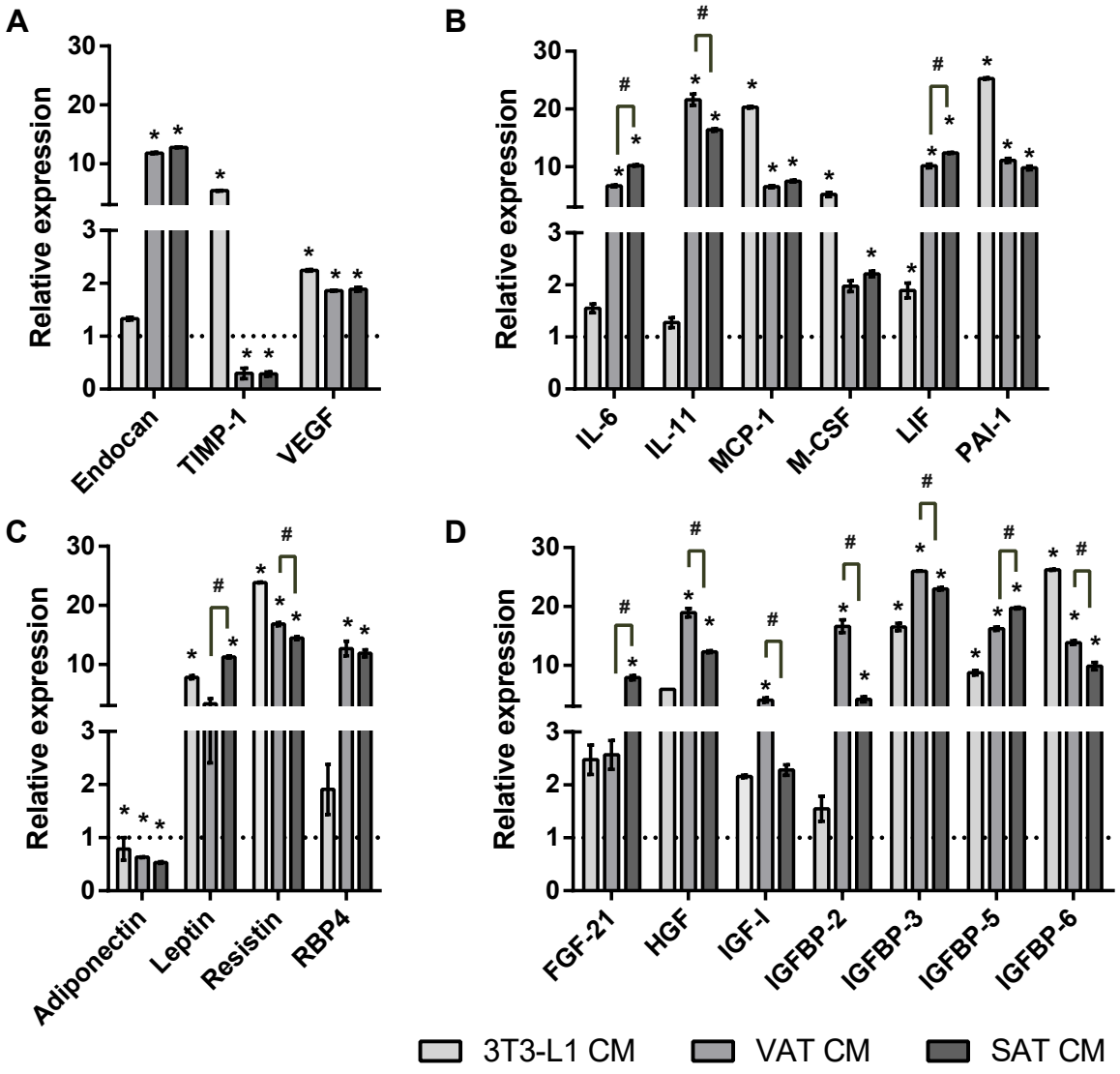

Figure 2.2: Secretion profiles of 3T3-L1 cells and subcutaneous and visceral AT organ cultures. **A)** Both SAT and VAT CM exhibit greater levels of vascular endothelial growth factor (VEGF) and endocan with a concomitant reduction in the expression of tissue inhibitor of metalloproteinases (TIMP)-1. **B)** Distinct relative levels of interleukin (IL)-6, IL-11, and leukaemia inhibitory factor (LIF) were found among SAT and VAT CM. **C)** Adipokines leptin and resistin are overexpressed in all CM, whereas adiponectin levels are significantly reduced. **D)** Numerous cellular growth factors were present at considerably higher concentrations in both VAT and SAT CM. ($*P < 0.05$ *vs* Control; $\#P < 0.05$ SAT CM *vs* VAT CM; n=2).

and VAT fragments.

As illustrated in Figure 2.2, the secretion patterns of numerous growth-factors, adipokines, cytokines, and angiogenesis-related molecules are different among the different CM. Greater levels of VEGF and endocan were found in SAT and VAT CM, whereas TIMP-1) levels were significantly reduced in these two CM (Fig. 2.2A). On the other hand, 3T3-L1 CM exhibited higher levels of VEGF, TIMP-1, and endocan than B16-F10-CM (Fig. 2.2A). The levels of the IL family of cytokines: IL-6, IL-11, and LIF were also significantly overexpressed within SAT and VAT, although no substantial differences were found in the 3T3-L1 CM (Fig. 2.2B). Nonetheless, monocyte chemotactic pro-

tein (MCP)-1 and plasminogen activator inhibitor (PAI)-1 expression was upregulated in every CM (Fig. 2.2B). AT hormones were also identified. Resistin and leptin relative expression levels were higher in 3T3-L1, SAT, and VAT CM. In addition, retinol binding protein (RBP)-4 was significantly released in SAT and VAT, but not in 3T3-L1 CM. Interestingly enough, a significant reduction in adiponectin levels was observed in all CM (Fig. 2.2C). The levels of several growth factors involved both in metabolism and in cell behavior were also analyzed. VAT CM revealed the higher expression of fibroblast growth factor (FGF)-21, insulin-like growth factor-binding protein (IGFBP)-5, hepatocyte growth factor (HGF), insulin-like growth factor (IGF)-1, IGFBP-2, IGFBP-3, and IGFBP-6 levels were significantly higher in SAT than VAT CM (Fig. 2.2D).

2.3.3 SAT and VAT Distinctively Modulate Melanocyte Migration and Cell Spreading

According to the previous secretome profile, TIMP-1, an inhibitor of extracellular matrix degradation was significantly decreased, whereas several inflammatory cytokines and angiogenic growth factors were upregulated particularly in SAT and VAT. These findings led us to evaluate the influence of CM in melanocytes motility. We first analyzed whether 3T3-L1 CM mechanically induced a wound to B16-F10 confluent cultures by injury assay. As illustrated in Figure 2.3A, the resulting void area was promptly occupied by melanocytes upon 3T3-L1 CM incubation in comparison to untreated B16-F10 cultures. Following a 24h incubation with CM, the migrated distance is almost twice the distance of the control treatment as seen by the microscopic examination of the wounds (Fig. 2.3B). We then examined the effect of SAT and VAT fat depots secretome in B16-F10 cells motility. In the double-chamber migration assay, the number of migrating cells following a chemotactic gradient was significantly enhanced in every treatment as compared to untreated B16-F10 cultures (Fig. 2.3C). However, SAT CM exerted this effect into a much larger extent. Cell spreading evaluation revealed that VAT and 3T3-L1 secreted molecules, but not SAT, induced spreading dynamic of B16-F10 cells (Fig. 2.3D). In addition, VAT CM-treated B16-F10 cells exhibited significantly higher areas and perimeter, whereas a smaller number of round shaped cells were observed. In contrast, SAT secreted factors did not significantly alter B16-F10 spread plasticity (Fig. 2.3E). These findings highlight a distinct paracrine role of AT depots regarding B16-F10 locomotive behavior: although SAT-released factors boost melanoma cell chemotaxis, VAT CM signalling enhance cell morphological plasticity and haptotactic spreading.

2.3.4 AT Secretome Modulates Melanoma Cells Adhesion and Tumourigenesis

Decreased cell-cell adhesion and anchorage-independent growth are prominent features necessary for successful metastization.[170,175] Therefore, we evaluated the adhesion of CM-treated B16-

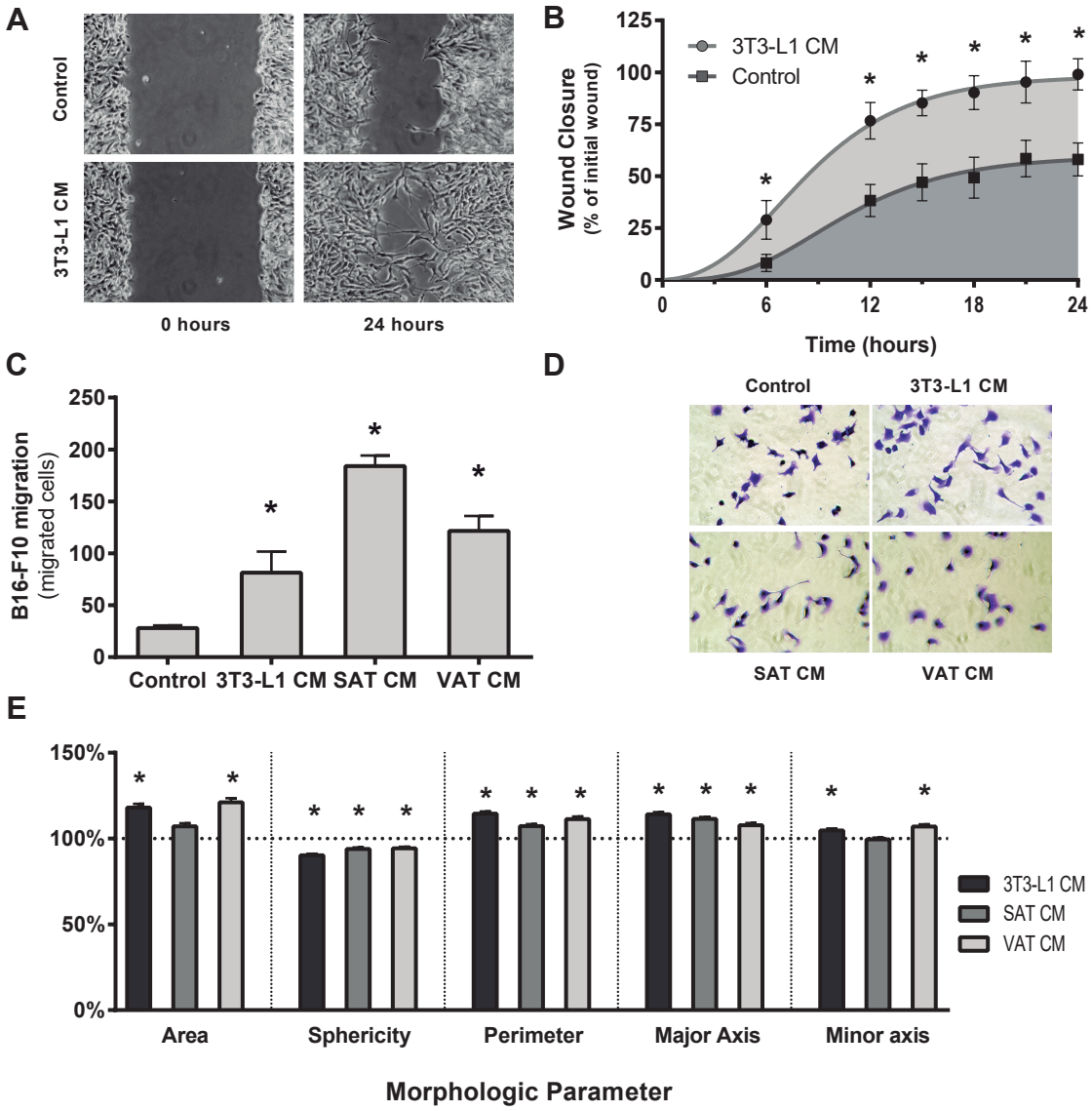

Figure 2.3: *In vitro* motility, migration and spreading analysis of B16-F10 melanocytes. **A)** A rapid B16-F10 cell migration was observed after incubation with 3T3-L1 CM in comparison to untreated (Control) for 24h. Cell cultures were visualized under an inverted microscope at a 200× magnification. **B)** When exposed to 3T3-L1 CM, melanocytes rapidly occupied the injury-created void area. The wound closure was determined by measuring cultures void area and by subtracting it from the initial area of the wound. Bars show the means values (±SEM) of nine measurements for each time point/condition. **C)** The effects of AT secretome on cell migration were quantified in a double-chamber assay using FBS as a chemoattractant. The number of cells that invaded the membrane was significantly higher when treated with 3T3-L1, and particularly with SAT and VAT CM. Mean values (±SEM) of three independent measurements are shown ($*P < 0.05$ *vs* Control; $\#P < 0.05$ SAT CM *vs* VAT CM; n=3). **D)** B16-F10 cells were allowed to adhere and spread for 3h in the standard treatments. Representative images of crystal-violet stained melanocytes are shown (200×). **E)** Morphologic analysis of B16-F10 cells revealed that VAT and 3T3-L1 CM significantly enhanced cell spreading. Bars are the means values±SEM, represented as percentage of Control, of 1000 evaluated cells ($*P < 0.05$ *vs* Control; n=9)

F10 cells to standard cell culture plates. Interestingly, B16-F10 cells adhesion was significantly increased after incubation with every CM, being higher upon VAT medium exposure (Fig. 2.4A).

Identical findings were observed in B16-F10 cells adhesion to endothelial cells (Fig. 2.4C). The number of B16-F10 cells adherent to HMEC-1 monolayers was significantly enhanced both after SAT and VAT CM treatments as compared to untreated cells or to cells treated with 3T3-L1 CM (Fig. 2.4B), being the highest increase found upon VAT CM incubation. These findings confirm that VAT improves B16-F10 adhesive properties. Conversely, in the soft-agar clonogenic assay, SAT soluble factors promoted the anchorage-independent proliferation of B16-F10 cells upon culture in non-adherent conditions (Fig. 2.4D and E), whereas exposure to VAT CM did not exert any effect. SAT released factors increased the number of colonies formed, but not in a statistically significant manner (Fig. 2.4F). These results further emphasize the divergent roles of SAT and VAT towards melanocytes malignancy.

2.3.5 Adipocytes Secreted Factors Induce Malignant Melanocytes Vasculogenic Mimicry

Given that malignant melanomas are highly vascularized tumours[85,176] and metastatic melanoma cells actively participate in tumour vascularization,[16,176] we next addressed whether CM from 3T3-L1 adipocytes prompted B16-F10 melanoma cells toward vasculogenic mimicry.

In comparison to untreated cells, 3T3-L1 CM-treated B16 cells rapidly assembled into capillary-like structures when cultured in Matrigel basement matrix (Fig. 2.5A). To further confirm the three dimensional growth and spatial arrangement of the melanoma cells, B16-F10 cells were cultured in hanging-drops for 72h. Microscopic observation of the generated spheroids upon incubation with 3T3-L1 CM revealed the formation of large and diffused aggregates of B16-F10 cells, whereas in the control treatment, a spherical and compact mass of melanocytes was observed (Fig. 2.5B). Next, we used MeWo cell line to additionally examine the vasculogenic mimicry inducer effects of 3T3-L1 CM in human melanoma cells. MeWo cells, when cultured on top of Matrigel and in the presence of 3T3-L1 CM displayed the same vessel-like rearrangement already observed for B16-F10 melanocytes (Fig. 2.5A). MeWo spheroids further revealed a loophole growth pattern when exposed to 3T3-L1-released factors (Fig. 2.5B). Altogether, these findings regarding cell-cell adhesion and reorganization into vessel-like structures formation provide additional support and reinforce the deleterious effects of fat-secreted molecules on melanoma tumour progression.

2.4 Discussion

Emerging evidence indicates that systemic factors, including inflammatory, angiogenic or metabolic markers, significantly influence tumour behavior.[177]

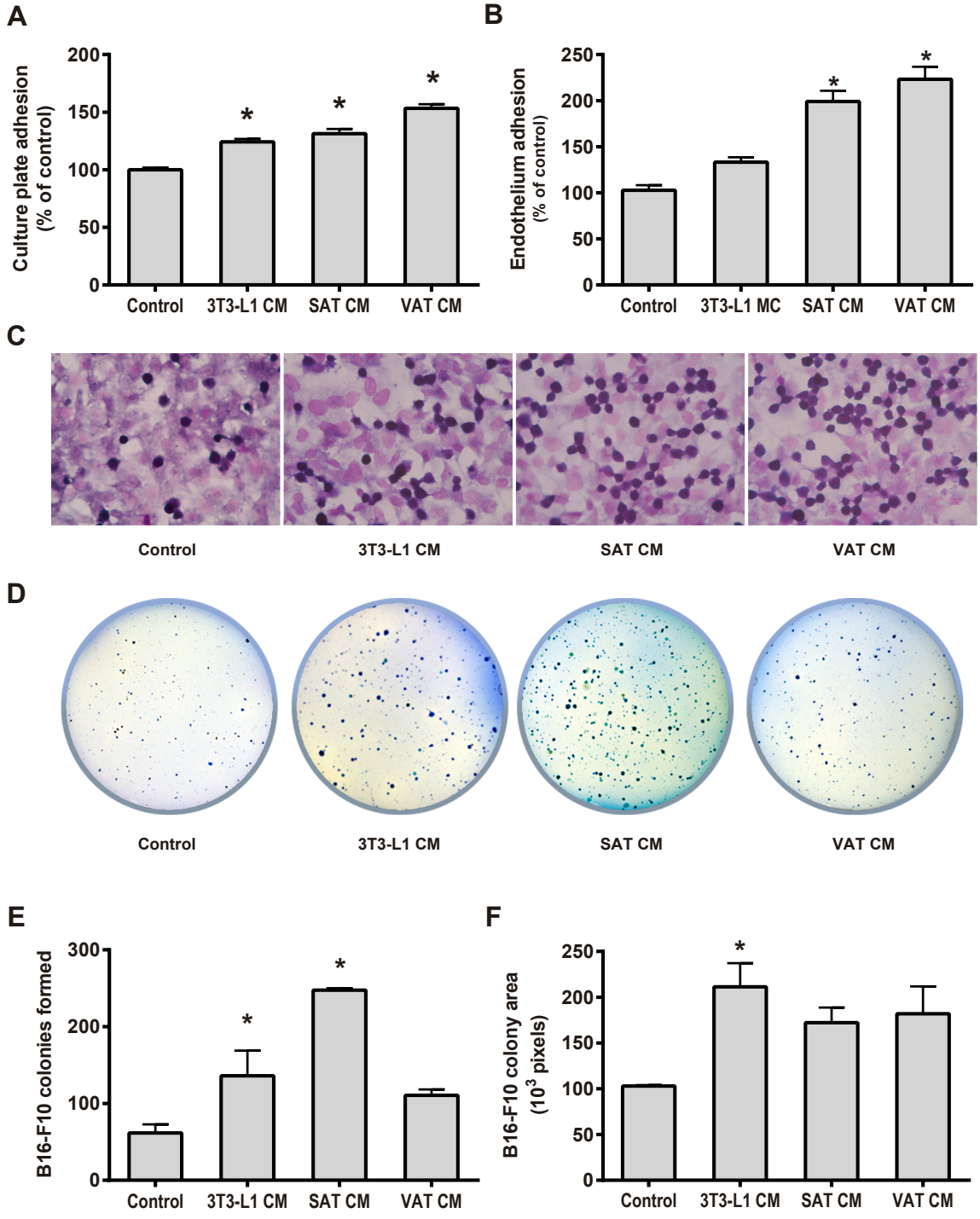

Figure 2.4: Melanoma cells adhesion and achorage-independent growth were increased after incubation with AT CM. **A)** Adhesion to culture plates for 30 min. **B)** Adhesion to HMEC-1 monolayers for 30 min. VAT-released factors were prominent in enhancing melanocytes adhesive potential both to cultures plates and endothelial cells. Results are expressed as percentage of Control (±SEM). **C)** Representative images (800×) of Giemsa stained slides showing B16-F10 cells (dark blue) adherent to HMEC-1 monolayers (pink). **(D)** Evaluation of anchorage-independent proliferation of B16-F10 melanocytes was conducted by soft-agar colony formation assay. **E)** The number of colonies formed was significantly higher in both 3T3-L1 and SAT CM treatments but not in VAT CM. **F)** Mean B16-F10 colony area was significantly increased after 3T3-L1 CM incubation, but not after VAT or SAT CM treatment. Bars represent means±SEM ($*P < 0.05$ *vs* Control; $\#P < 0.05$ SAT CM *vs* VAT CM; n=3-9).

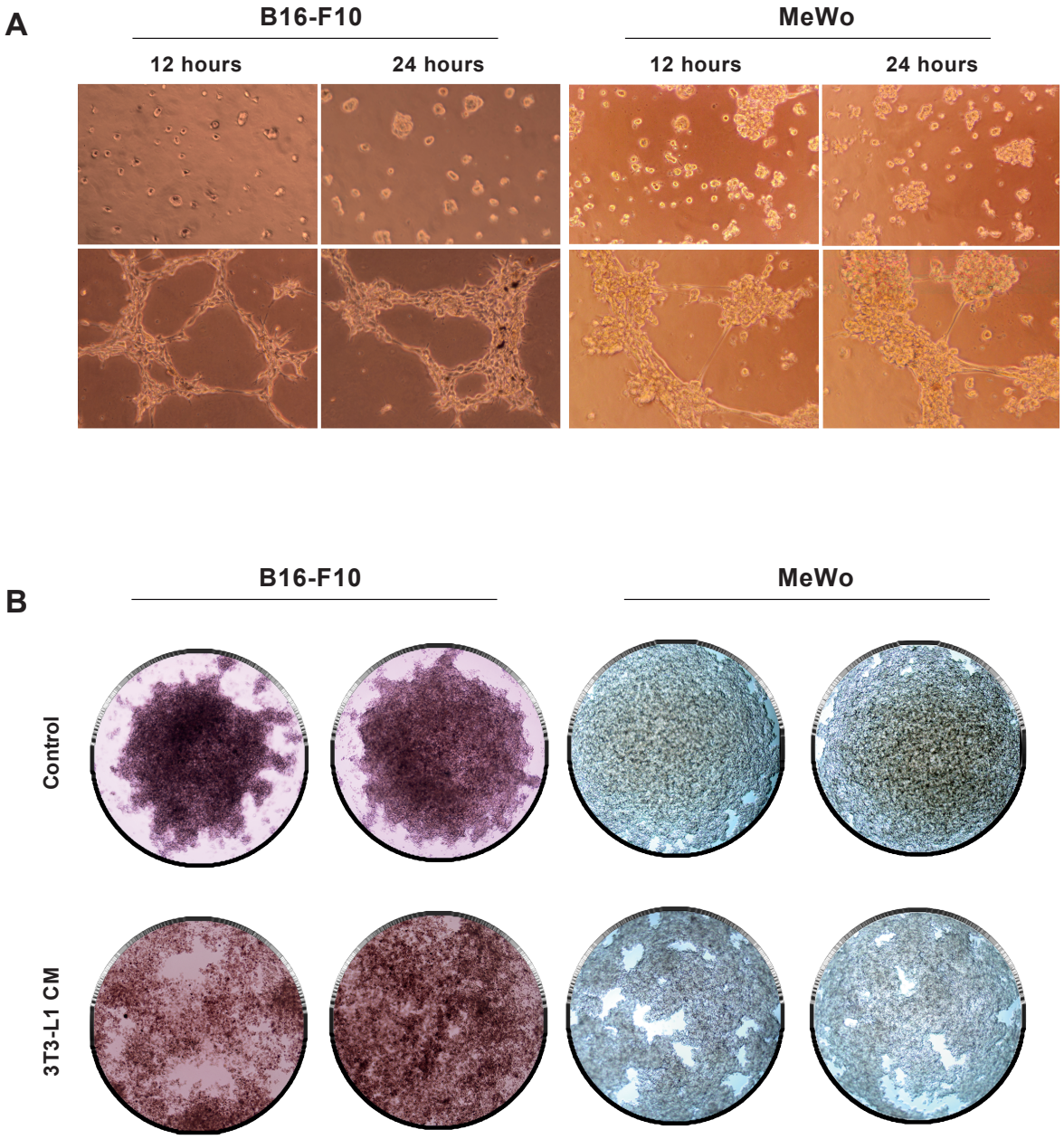

Figure 2.5: Vasculogenic mimicry by melanoma cells was stimulated by AT CM. **A)** B16-F10 and MeWo cells were cultured on top of Matrigel layers. Upon treatment with 3T3-L1 CM, melanocytes acquired a vessel-like tubular phenotype. Images were captured under an inverted microscope (200×) at 12 and 24h post treatment. **B)** Microscopic examination of B16-F10 and MeWo spheroids in hanging-drop cultures. The presence of 3T3-L1 secreted factors inhibited the formation of a compact spheroid cellular mass. Shown are representative light-microscopy photographs (80×) of the spheroids.

The current study reveals that adipocyte-released factors increase B16-F10 melanoma cells viability, proliferation, and reduces apoptosis and melanin content. Exposure to adipose tissue CM of these cells further resulted in increased motility, enhancing the capacity to migrate and spread. These findings were accompanied by an augmented adhesion capacity, in particularly to endothelial cells, and anchorage-independent proliferation as assessed by soft agar assays. We further identified the

factors that are released by adipocyte cells of different depots, and revealed that several pro-inflammatory factors (IL-6, IL-11, LIF, and PAI-1), metabolic markers (IGFBPs, FGF-21), angiogenic growth factors (endocan, HGF, VEGF, IGF-I), and hormones (leptin, resistin, RBP-4) were secreted to the medium into a high extent, whereas TIMP-1, an inhibitor of ECM degradation, and adiponectin were significantly downregulated.

Adipose tissue is no longer considered a mere lipid store depot, but also an inflammatory and endocrine organ.[52,60] Accordingly, obesity provides a chronic low grade inflammatory condition, further potentiated by the presence of hormone cues and cytokines, which are strongly associated with disease. Therefore, the presence of high amounts of pro-inflammatory cytokines and hormones in adipocyte CM is expected. Remarkably, the majority of these factors are known to play a role in cell proliferation, apoptosis, migration, and invasiveness, as well as adhesion capacity. Recently, it has been reported that both leptin and resistin, two adipocyte-released hormones, were able to stimulate melanoma cell growth and proliferation through AKT and fatty acid synthase modulation.[74] In addition to these hormones, FGF-21, a metabolic regulator also increases cell proliferation *in vitro* and increased tumourigenesis and invasive potential *in vivo*.[178] Likewise, FGF and IL-6 are known to be produced by melanoma cells and stimulate proliferation in a autocrine manner, although other paracrine growth factors (HGF, IGF-I, and VEGF) modulate the microenvironment and potentiate tumour growth and invasion.[138,179] We have found that adipose tissues CM have significant higher levels of the above growth factors, reinforcing our findings concerning the effect of CM from the distinct adipose tissue depots studied in augmenting B16-F10 cell proliferation, migration, ability to invade, and decreasing apoptosis.

Along with the progression of melanoma, malignant melanocytes dedifferentiate losing most of their epithelial characteristics through a process similar to epithelial-mesenchymal transition,[180] leading thus to more aggressive phenotypes.[181] Melanogenesis is an inherent process in melanocytes. Melanocytes respond to the inflammatory cytokines, namely IL-6, with a dose-dependent inhibition of melanogenesis.[182] Nevertheless, whenever these cells exhibit a more malignant phenotype, melanocytes decrease melanin synthesis.[20] Our findings show that when treated with CM from adipocytes, the melanin content per B16-F10 melanocyte was significantly reduced, further enlightening the growth-promoter and dedifferentiation paracrine effects of adipocytes.

Furthermore, active locomotion of tumour cells is fundamental to malignant invasive and metastatic capacity.[183–185] By crossing tissue stroma and the vascular bed, tumour cells interact with both extracellular matrix and soluble tropic factors. Our findings showed that chemotactic migration of B16-F10 cells was enhanced upon exposure to SAT released factors although cell spreading and haptotactic migration of tumour cells were positively modulated by visceral-fat secretome. Intercellular adhesion is reduced in many aggressive tumours,[175] allowing cells to detach from the primary lesion and metastasize to distant organs. Again, we found discrete effects among subcutaneous and visceral fat depots on B16-F10 adhesive properties. In fact, several biological, metabolic,

and secretory differences distinguish intra-abdominal visceral adipocytes from peripheral subcutaneous adipose tissue.[186,187] In agreement, our results unveiled distinct effects of SAT and VAT upon melanocytes aggressiveness. SAT CM enhances B16-F10 locomotion and anchorage-independent proliferation. In turn, VAT prominently improves melanocytes cell-substratum adhesion. Despite the higher release of visceral-fat pro-inflammatory cytokines,[186] subcutaneous fat depots, which are located close to melanoma lesions, influence the malignant transformation of melanocytes. Nevertheless, our microarray assay revealed that the secretome profile of SAT and VAT is significantly different regarding some of the inflammatory, hormonal, and metabolic molecules addressed. TIMP-1 and IGF-I are chemotactic agents for human melanoma cells that mediate motility.[179,188] IGF-I was significantly higher in SAT CM although TIMP-1 was under expressed in the adipose tissues CM. PAI-1 is also known to modulate cell adhesive properties and its overexpression is correlated with the metastatic capacity of melanomas.[189] Antagonistically, IGFBPs inhibit melanoma migratory and invasive behavior, and induce melanocytic differentiation[190] counterbalancing the IGF-I effects and most likely contribute to the discrete differences observed between subcutaneous and visceral CM. The effect of the different AT depot secretome in tumour cells behavior is beyond the scope of this study, however, our results reinforce the need for additional molecular studies to investigate how SAT and VAT affect tumour progression.

Accumulating data point out mechanisms associating obesity to melanoma.[77,80,160,167,168,191] Recent reports unveiled the involvement of high-fat diet-induced increased cytokines and angiogenic factors in the crosstalk between tumour cells and macrophages.[60,144,145,192] Recruitment of the immune system cells, which release factors that enhance tumour plasticity and the maintenance of stromal microenvironment, has already been described for other malignancies.[193,194] In contrast, our *in vitro* results disclose a direct effect of adiposity on melanoma cells, without the influence of either tumour-associated cell-mediated immunity or endothelium.

Vascularization plays a central role in tumour development and progression. Besides angiogenesis, vasculogenic mimicry provides an alternative, angiogenic-independent tumour microcirculation.[16,25,26] Melanoma cell-lined vascular networks sustain a redundant blood supply required for both growth and metastasis.[25,26] The presence of these functional vascular channels by the tumour itself is a predictor of poor prognosis in human melanoma patients[27,28] and might circumvent the effectiveness of anti-vascular drugs and antiangiogenic therapies.[195] Fully differentiated 3T3-L1 adipocytes CM were able to induce malignant melanocytes to rearrange on Matrigel cultures into vessel-like structures typically reported for endothelial cells.[196] Moreover, microscopic inspection of B16-F10 and MeWo spheroids, obtained by hanging-drop cultures, revealed the same pattern of vasculogenic mimicry observed in cultures of human melanoma cell lines.[25,197] Data confirming melanoma angiogenesis stimulation by AT tropic factors has recently been highlighted.[144,145] However, we report for the first time supporting evidence endorsing the potential adipocyte secretome inducer effects of tumour vasculogenic mimicry. Accordingly, several angiogenic growth factors were

significantly higher in CM, including HGF and VEGF. HGF was involved in vascular mimicry of hepatocellular carcinoma.[198] Additionally, VEGF signalling was found to be involved in vascular mimicry through activation of VEGFR1 expression in melanoma cells,[199] explaining the increased capacity of melanoma cells to form vasculogenic structures after treatment with adipocyte CM. Endocan, in turn, is a new tumour invasion and angiogenic marker, being overexpressed in tumour vessels.[200] The fact that it is upregulated in both SAT and VAT conditioned medium may also explain the involvement of adipose tissues in tumour aggressiveness.

Altogether, our results indicate that adipocytes secretome induce malignant melanocytes aggressiveness. The synergic increase in melanocyte survival, adhesion, motility, and plasticity allied to the stimuli for cell-cell networks of vasculogenic mimicry patterns, support the deleterious effects that adiposity partakes directly in melanoma progression.

2.5 Acknowledgments

We would like to thank Professor Conceição Calhau (Faculty of Medicine of the University of Porto) and Professor Paula Soares (I3S, Institute of Research and Innovation in Health, University of Porto) for kindly providing the 3T3-L1 and MeWo cell lines, respectively. We are also in debt to the "Fundação para a Ciência e a Tecnologia" (FCT) and FEDER-COMPETE for the financial support through the research unit PEst-OE/SAU/UI0038/2011, UID/BIM/04293/2013 and the PhD grant attributed to PC (SFRH/BD/80434/2011).

2.6 Supporting Information

Table 2.S1: Gene expression profile of secretomes from 3T3-L1, SAT and VAT by microarray

Adipokine	**3T3-L1**	SEM	**SAT**	SEM	**VAT**	SEM
Adiponectin	0,79	0,30	0,63	0,01	0,53	0,02
AgRP	1,53	0,04	1,04	0,00	1,15	0,02
ANGPT-L3	1,35	0,10	1,58	0,03	1,14	0,13
C-Reactive Protein	1,53	0,10	1,95	0,00	1,72	0,11
DPP-IV	1,73	0,00	4,13	1,33	4,60	2,45
Endocan	1,33	0,04	11,80	0,19	12,76	0,10
Fetuin A	1,05	0,00	1,19	0,12	1,23	0,02
FGF acidic	1,32	0,00	1,11	0,08	1,18	0,02
FGF-21	2,48	0,39	2,57	0,39	7,88	0,51
HGF	5,89	0,02	18,93	1,03	12,28	0,25
ICAM-1	1,36	0,05	1,36	0,02	1,36	0,01
IGFBP-1	1,73	0,48	1,09	0,05	1,14	0,06
IGFBP-2	1,55	0,34	16,62	1,57	4,20	0,61
IGFBP-3	16,50	0,87	26,01	0,06	22,99	0,33
IGFBP-5	8,71	0,54	16,21	0,43	19,71	0,21
IGFBP-6	26,24	0,15	13,84	0,45	9,84	0,86
IGF-I	2,16	0,03	4,06	0,52	2,28	0,14
IGF-II	3,25	0,14	1,01	0,05	1,06	0,06
IL-10	1,18	0,05	1,10	0,15	1,10	0,07
IL-11	1,28	0,13	21,61	1,39	16,38	0,33
IL-6	1,55	0,12	6,68	0,23	10,22	0,16
Leptin	7,81	0,38	3,31	1,28	11,24	0,25
LIF	1,89	0,20	10,14	0,47	12,40	0,14
Lipocalin-2	48,38	3,70	1,91	0,64	1,14	0,15
MCP-1	20,31	0,23	6,53	0,28	7,49	0,25
M-CSF	5,19	0,51	1,98	0,15	2,21	0,08
Oncostatin M	1,75	0,35	1,67	0,04	1,17	0,03
Pentraxin 2	1,43	0,02	1,12	0,08	1,08	0,05
Pentraxin 3	5,78	0,18	1,72	0,16	2,32	0,12
Pref-1	6,21	0,02	1,42	0,06	1,36	0,13
RAGE	1,70	0,12	1,27	0,00	1,30	0,06

Continued on next page

Table 2.S1: Gene expression profile of secretomes from 3T3-L1, SAT and VAT by microarray

Adipokine	**3T3-L1**	SEM	**SAT**	SEM	**VAT**	SEM
Continued from the previous page						
RANTES	4,79	0,18	0,93	0,00	1,43	0,04
RBP4	1,91	0,67	12,67	1,74	11,87	0,86
Resistin	23,87	0,09	16,82	0,37	14,43	0,38
Serpin E1	25,29	0,20	11,09	0,50	9,79	0,47
TIMP-1	5,39	0,08	0,30	0,14	0,29	0,06
TNF-α	3,21	0,23	1,69	0,59	1,80	0,12
VEGF	2,24	0,02	1,86	0,02	1,89	0,05

Values are fold-increase relative to fresh medium of each culture. Intensity values are averages of two measurements.

Legend: AgRP: Agouti-related peptide; ANGPT-L3: angiopoietin-like 3; DPP-IV: dipeptidyl peptidase 4; FGF: fibroblast growth factor; HGF: hepatocyte growth factor; ICAM-1: intercellular adhesion molecule 1; IGFBP: insulin-like growth factor-binding protein; IGF: insulin-like growth factor; IL: interleukin; LIF: leukemia inhibitory factor; MCP-1: monocyte chemotactic protein 1; M-CSF: macrophage colony-stimulating factor; Pref-1: preadipocyte factor 1; RAGE: receptor for advanced glycation endproducts; RANTES: regulated upon activation normal T cell expressed and presumably secreted; RBP4: retinol binding protein 4; TIMP-1: tissue inhibitor of metalloproteinase 1; TNF-α: tumour necrosis factor alpha; VEGF: vascular endothelial growth factor.

3

Adipocyte Secretome Increases Radioresistance of Malignant Melanocytes by Improving Cell Survival and Decreasing Oxidative Status

Coelho P, Silva L, Faria I, Vieria M, Monteiro A, Pinto G, Prudêncio C, Fernandes R and Soares R

Radiation Research 2017; in press

ABSTRACT

Radiotherapy is a treatment option for the majority of malignancies. However, because melanoma is known to be radioresistant, the use of ionizing radiation as an adjuvant therapy in cutaneous melanoma patients is ineffective. Obesity has now been recognized as a risk factor for melanoma. High adiposity is generally associated with a more pro-oxidative status. Oxidative stress is a major player in radiation therapy and also a common link between obesity and cancer. Several adipocytes-released proteins are known to have a role in controlling cellular growth and pro-survival signaling. For that reason, we investigated the influence of 3T3-L1 mature adipocyte secretome in B16-F10 malignant melanocyte radiosensitivity. We evaluated B16-F10 cell survival and redox homeostasis when exposed to four daily doses of ionizing radiation (2 Gy per day) up to a total of 8 Gy in a medical linear accelerator. B16-F10 melanocytes exhibited slight alterations in survival, catalase activity, nitrative stress and total oxidant concentration in the first 2 Gy irradiation. The motility of the melanocytes was also delayed by ionizing radiation. Subsequent irradiations of the malignant melanocytes led to more prominent reductions in overall survival. Remarkably, 3T3-L1 adipocyte-secreted molecules were able to increase the viability and migration of melanocytes, as well as lessen the pro-oxidant burden induced by both the single and cumulative X-ray doses. *In vitro* adipocyte-released factors protected B16-F10 malignant melanocytes from both oxidative stress and loss of viability triggered by radiation, enhancing the radioresistant phenotype of these cells with a concomitant activation of the AKT signalling pathway. These results both help to elucidate how obesity influences melanoma radioresistance and support the usage of conventional medical linear

accelerators as a valid model for the *in vitro* radiobiologic study of tumour cell lines.

3.1 Background

Melanoma is one of the world's most rapidly increasing malignancies.[1] The number of reported cases has been increasing for the last few decades. Over 176000 new cases of melanoma are reported annually in Europe and the US.[5,6] Melanoma treatment has remained the same for the last decades: surgical excision of the malignant mass is still the most effective treatment in primary melanomas.[2]

Radiation therapy (RT) is frequently used to treat the majority of malignancies, and has a direct impact in the proliferative phenotype of both normal and cancer cells. Radiation-induced ionization of regulatory proteins and DNA might render the cells unviable and culminate in cellular death.[201] Ionizing radiation can also indirectly cause cellular damage. The formation of highly reactive oxygen and nitrogen radicals increases the intracellular oxidative stress, depleting the antioxidant defences, which subsequently react with many cellular components (DNA, proteins, lipids) leading to unrecoverable damage.[202]

However, melanoma is known to be radioresistant, which discourages the use of ionizing radiation as an adjuvant therapy in melanoma patients.[48] Recently, the use of radiation in higher delivered doses, hypofractionated and in combination with immunotherapy has led to some positive outcomes in melanoma metastasis treatment and palliation.[44,49,50] Nonetheless, obesity, particularly high visceral adiposity, presents a problem in treatment planning and the delivery of radiation to internal metastases. Generally, higher body adiposity is associated with both cancer initiation and progression.[203] Obesity itself is a risk factor for several types of neoplasms, including melanomas.[63,65] High adiposity can be a contraindication for (and may limit the extent of) cancer surgery, since it contributes to the inadequate dosing of chemotherapeutic drugs and complicates the planning and delivery of radiation.[204–206]

Adipocytes secrete a variety of factors that exert effects at both local and systemic levels.[51] The grand majority of these factors are cytokines, chemokines and inflammatory mediators, but a role in growth regulation as a new aspect of adipokines has been revealed by novel adipocyte-released molecules.[69] Fat-derived molecules stimulate melanoma progression and aggressiveness and act as mediators of proliferation in melanoma cells.[160,207]

Resistance to oxidative stress appears to be a key mechanism of tumour radioresistance.[208] Obesity is linked to a more pro-oxidative status, with a concomitant systemic increase in reactive oxygen species (ROS), acting as an additional source of oxidants.[55]

For the current study, we hypothesize that adipocytes might lead to two antagonistic outcomes towards melanocyte radiosensitivity. Although the fat-derived growth factors might protect melanocytes from radiation-induced loss of survival by stimulating their overall proliferation, the adipocyte-generated oxidants can further increase the oxidative burden, aggravating the radiation-induced

damages. In this study, we irradiated cell cultures at standard doses investigate the action of adipocyte secretome in melanoma radioresistance.[209]

3.2 Material & Methods

3.2.1 Cell Cultures

B16-F10 melanocytes and 3T3-L1 pre-adipocytes were maintained in high-glucose Dulbeco's modified Eagle's medium (DMEM; Sigma-Aldrich) supplemented with 10% fetal bovine serum (FBS) and 1% penicillin/streptomycin/amphotericin B (Sigma-Aldrich). Cells were culture at 37°C in an incubator with a 5% CO_2 humidified atmosphere.

B16-F10 melanocytes were cultured in 96 well plates (1×10^4 cells/mL) for viability determination and in 24 well plates (10×10^4 cells/mL) for the other assays. All treatments were conducted in serum-free conditions and following a 16 hour FBS-starving period.

3.2.2 Adipocytes Differentiation and Conditioned Medium Collection

Two days after 3T3-L1 pre-adipocytes cultures reached confluence, a mixture of 2 µM insulin (Sigma-Aldrich), 1 µM dexamethasone (Sigma-Aldrich) and 0.25 mM isobutylmethylxanthine (Fluka) was added to the cultures. The medium was replaced and the cells maintained with 2 µM insulin every two-three days. On the seventh day post-induction, cultures were washed with phosphate buffered saline (PBS) and incubated in serum-free DMEM. On the next day, the conditioned medium (CM), enriched with adipocytes secretome, was harvested from the adipocytes cultures, centrifuged for 5 minutes at 300*g* and the supernatant was collected for the subsequent treatments.

3.2.3 Irradiation of Cells

Prior to irradiation, computed tomography scans were performed to obtain three-dimensional images and calculate the density of both the 24 and 96-well plates. To simulate a biologic structure, the plates were placed in between two 5cm-height water phantoms (Supplementary Fig. **??**).

The three-dimensional conformal RT dosimetric plan comprised two fields (one anteroposterior and one posteroanterior) and was performed using the software XIO-Release 4.70.02 (Supplementary Fig. **??**). A total dose of 8 Gy in 4 daily fractions of 2Gy, prescribed to the isocenter, was delivered in a PRIMUS, Siemens® linear accelerator with a 6 MV photon beam.

3.2.4 Metabolic Activity Assay

The (4,5-dimethylthiazol-2-yl)-2,5-diphenyltetrazolium bromide (MTT, Sigma-Aldrich)was used to assess the metabolic activity of malignant melanocytes (B16-F10) submitted to RT under the influence of adypocytes secretome (3T3-L1). B16F10 cells were seeded in 96-well plates and cultured for 24 hours. Afterwards, cells were treated with the mature adipocytes CM and submitted to RT treatment. Next, 20 µL of MTT was added to each well and incubated for 3 hours. After this period, the violet formazan precipitate was dissolved in 100 µL of dimethyl sulfoxide (Merck) and the absorvance at 550 and 650nm recorded. The results were calculated by the formula $ABS_{(final)} = ABS_{(550)} - ABS_{(650)}$ and normalized by diving over the absorbance of the control.

3.2.5 Total Antioxidant Status Determination

The *in vitro* determination of the total antioxidant status (TAS) was done with the TAS kit (Randox Laboratories) following the manufacturers instructions. Briefly, 5 µL of the sample were mixed with a 200 µL of the chromogenic solution and the substrate was added to a final volume of 250 µL. The appearance of the radical cation $ABTS^{\bullet+}$ was monitored for 15 minutes at 600nm. Antioxidants suppress the blue-green color production to a degree that is proportional to their concentrations. Calibration was performed using Trolox (6-hydroxy-2,5,7,8-tetramethylchroman-2-carboxylic acid) standards and the results were expressed as $TAS_{mmol/mL} = \frac{Concentration_{Trolox\ standards}}{(\Delta ABS_{samples} - \Delta ABS_{Trolox})}$ where $\Delta ABS = ABS_{final} - ABS_{initial}$, according to the manufacturer instructions.

3.2.6 Catalase Activity

Catalase activity was determined based on the rate of decomposition of H_2O_2, which is proportional to the reduction of the absorbance at 240nm. A volume of 100 µL of each sample was added to 400 µL of 5 mM hydrogen peroxide substrate solution in 0.05 M phosphate buffer (pH 7.0). The decay kinetics for absorbance was determined in a Jenway 6505 Uv/Vis spectrophotometer for one minute. Results are expressed as $|\Delta ABS/min| \times 10^6$.

3.2.7 TBARS Determination

To determine thiobarbituric acid-reactive substances (TBARS), 100µL of thiobarbituric acid 10% (w/v) (Merk) were added to 500 µL of cellular extract and placed in a boiling water bath for 30 minutes. Afterwards, the amount of malondialdehyde (MDA) present was determined by measuring the absorbance at 535 nm. The standard curve was performed with standard solutions of malonaldehyde bis(dimethyl acetal)(Sigma).

3.2.8 Nitrotyrosine Quantification

B16 cell lysates were prepared in PBS and sonicated for 10 min (Silent Crusher S; Heidolph Instruments GmbH). Proteins and other cellular components were precipitated with 15% (v/v) ice-cold trifluoracetic acid upon centrifugation at 10000 rpm for 10 minutes. Chromatographic detection of 3-nitrotyrosine (3-NT) was performed as described by Dulce Teixeira and colleagues (in press; see Supplementary Table **??** for detailed chromatographic conditions). 3-NT standards were prepared from lyophilized 3-Nitro-L-tyrosine (Santa Cruz Biotechnology). The reverse-phase HPLC VWR-Hitachi Elite LaChrom (VWR) chromatographic system used consisted of a quaternary pump model HTA L-2130, an autosampler L-27200, a ODS-Hypersil C18 analytical column (200 cm × 4 mm i.d.; 5 µm particle size) (Merck) in a L-2300 column oven and a diode array detector model L-2455. The resulting chromatograms (Supplementary Fig. **??**) were analyzed using Agilent EZChrom Elite 3.3.2 software (Agilent Technologies).

3.2.9 *In Vitro* Scratch Assay

Using a pipette tip, an injury was inflicted in B16-F10 confluent cultures. Cells were then incubated following 3T3-L1 conditioning and/or RT treatment. At 4, 12 and 24 hours *post*-treatment, the migrated distance was photographed under an inverted microscope (Nikon) at a 200× magnification and the scratch closure was determined by measuring the injury width with Image J software (NIH). Shown are the normalized values ±standard error of the mean (SEM) of nine measurements.

3.2.10 Western Blotting Analysis

Proteins were extracted using RIPA buffer from B16-F10 cell lysates. Equal volumes of protein extracts were loaded onto a 10% SDS-PAGE with a 5% stacking gel. After electrophoretic separation, proteins were blotted into a nitrocellulose membrane (Amersham Biosciences). Immunodetection for total AKT, phosphorylated AKT (Ser473), and β-actin (all Cell Signaling) was accomplished with enhanced chemiluminiscence (Clarity ECL kit, BioRad).

3.2.11 Statistical Analysis

Statistical analysis was conducted in GraphPad Prism 6.0 (GraphPad Software Inc.). Differences between treatments were evaluated by Student's *t*-test or two-way ANOVA with Sidak multiple comparisons test accordingly to the number of conditions and treatments. Significance level was set to $P < 0.05$.

3.3 Results

3.3.1 3T3-L1 CM Protects B16-F10 Cells from Radiation Damage

To access the susceptibility of B16-F10 cells to the direct effects of ionizing radiation, B16-F10 melanocytes were irradiated with a single 2 Gy dose of X-rays and the cellular viability was then evaluated by the MTT assay. Upon irradiation, B16-F10 cells shown a slight (10%) decrease in their metabolic activity. However, 12 hours after the metabolic activity of the melanocytes exposed to RT was improved to control values (Fig. **??**A). When cultured with 3T3-L1 CM the malignant melanocytes significantly increased their metabolic activity by more than 30% whether irradiated or not (Fig. **??**A).

Ionizing radiation imbalances the cellular redox homeostasis.[202] Accordingly, we next evaluated oxidative stress markers and antioxidant status of the irradiated B16-F10 melanocytes.

Lipid oxidation by ROS gives rise to a number of byproducts. MDA is one of the principal end-products of fatty acid peroxidation in cells.[210] We evaluated the MDA levels by the TBARS assay but found no significant differences in lipid peroxidation with either irradiation or 3T3-L1 secreted factors at the two time points studied (Fig. **??**B).

Catalase is an oxidative stress protective enzyme that neutralizes hydrogen peroxide formed during oxidative stress. The activity of this enzyme in B16-F10 melanocytes was not altered after exposure to ionizing radiation. However, a significantly lower activity was observed when cells were treated with 3T3-L1 secreted molecules (Fig. **??**C). Incubation with adipocyte 3T3-L1 CM resulted in a significant increase in catalase activity in the melanocytes 4 h postirradiation.

Although the total antioxidant capacity of 3T3-L1 CM is significantly higher than fresh culture medium (Fig. **??**D), when fed to B16-F10 cultures and irradiated, the number of antioxidants present in the 3T3-L1 CM is no different from the control 12 h after treatment (Fig. **??**E). Interestingly, the intracellular production of redox scavenger mechanisms is stimulated by the adipocyte secretome and counterbalances the lower radiation-induced antioxidant defence status (Fig. **??**F).

To address the ability of melanocytes to migrate, a mechanical damage was inflicted to confluent melanocytes cultures and the scratch closure was microscopically inspected (Fig. **??**B). Melanocytes rapidly occupied the injured area when incubated with 3T3-L1 CM. Exposure to radiation (2 Gy) slowed down B16-F10 motility towards the injury void space, particularly 4 h postirradiation, but this effect was reversed when 3T3-L1 CM were also present (Fig. **??**A).

These results indicate that adipocyte-released molecules can protect melanoma cancer cells from X-ray radiation damages, both reducing antioxidant status and enhancing cell migration.

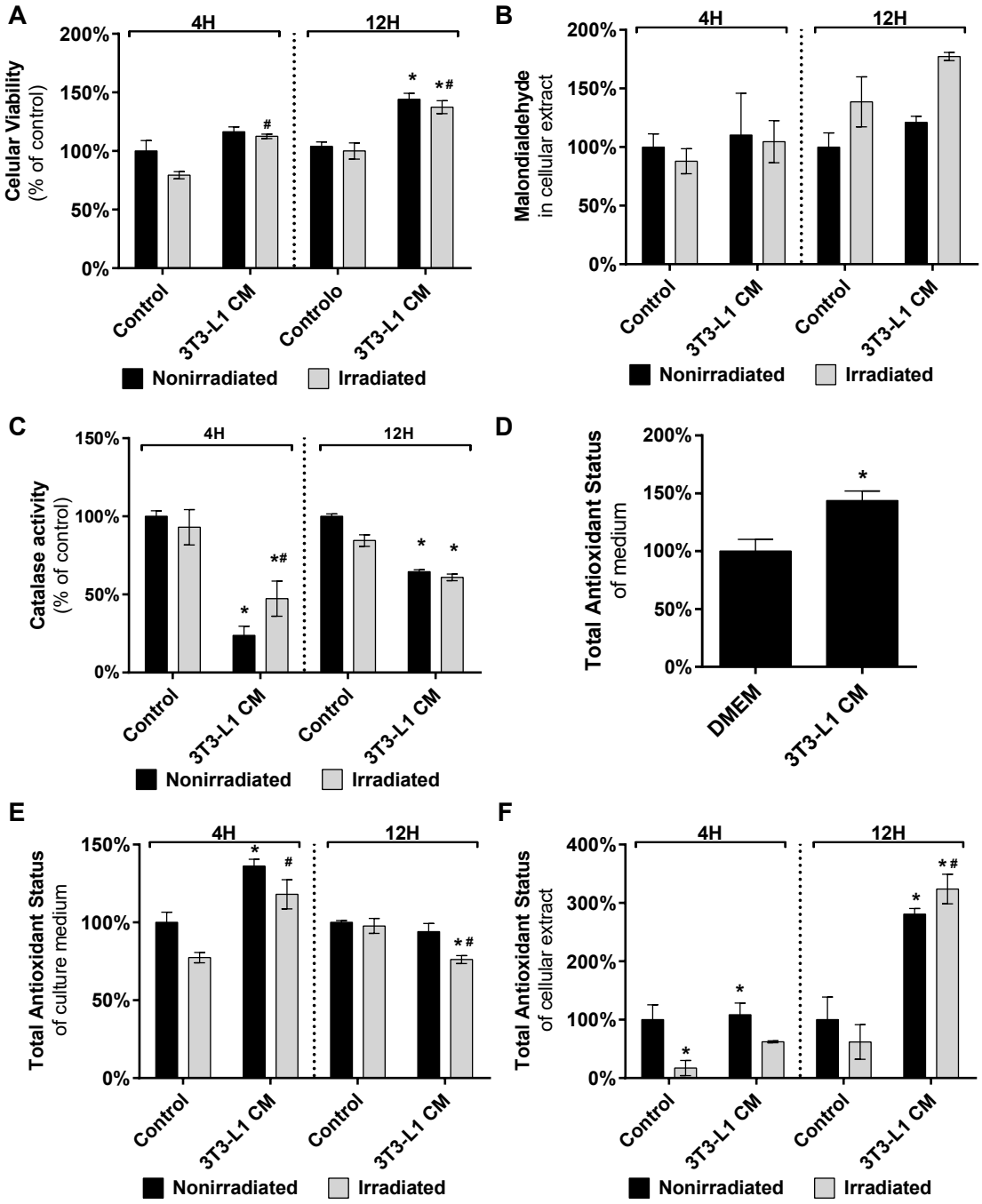

Figure 3.1: B16-F10 survival and antioxidant status upon single 2 Gy irradiation and treated with 3T3-L1 CM. Controls were treated with serum-free DMEM. **A)** Metabolic activity of melanoma cells by MTT reduction assay. Results represent the percentage of viable cells normalized by the absorbance of control. **B)** Levels of MDA by TBARS determination in B16-F10 cell lysates. **C)** Catalase activity was determined based on the reduction of absorbance at 240 nm.
Total antioxidants concentration in fresh 3T3-L1 CM and DMEM **(D)** and in the treated B16-F10 culture supernatant **(E)** and cellular extract **(F)** was determined enzymatically by the TAS assay. Shown are mean values (±SEM) of three measurements for each time point/condition. Results are normalized as a percentage of the control treatment ($*P < 0.05$ *vs* Control treatment; $\#P < 0.05$ *vs* irradiation).

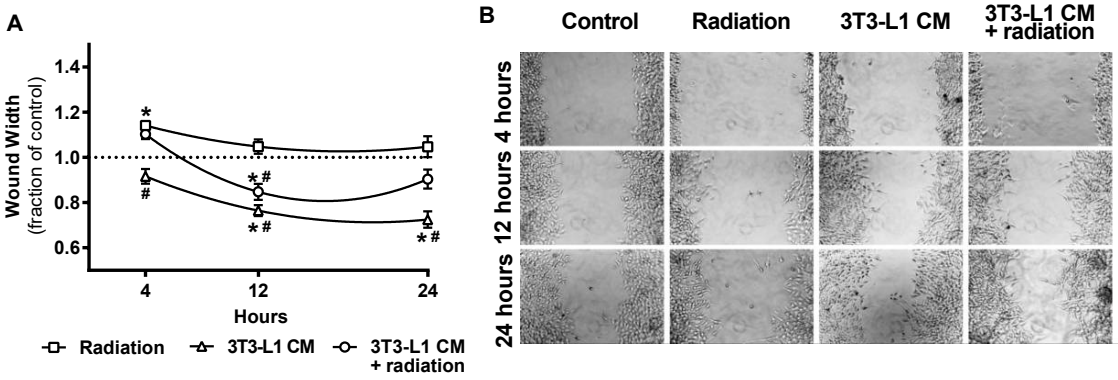

Figure 3.2: Migration of B16-F10 melanocytes exposed to 3T3-L1 CM and/or radiation (2 Gy). **A)** Injury closure fraction was determined by diving over the width of the void space of the control. Bars show mean values (±SEM) of nine measurements for each time point/condition. ($*P < 0.05$ *vs* Control treatment; $\#P < 0.05$ *vs* irradiation). **B)** Representative microscopy images of the injuries for each treatment and time point (200×).

3.3.2 Adipocyte Secretome Contributes to Melanoma Radioresistance

As radiation exposure increases, the amount of direct and indirect oxidative stress-mediated cellular damages increases proportionally. Our next approach was to determine the effects of cumulative radiation of B16-F10 melanocytes. A total dose of 8 Gy was delivered in four daily 2 Gy irradiations to melanoma cells in the presence of the 3T3-L1 adipocyte derived factors.

The metabolic viability of the irradiated melanocytes displayed a constant decrease, of approximately 20%, for radiation doses greater than 4 Gy. However, 3T3-L1 CM treatment of B16-F10 cells significantly increased the survival of the melanocytes suppressing the radiation-induced cytotoxic effects (Fig. **??**A). Catalase activity followed a similar trend: radiation promotes a diminished basal catalase activity but when in the presence of the 3T3-L1 CM, catalase activity is highly enhanced (Fig. **??**B).

Reactive nitrogen species (RNS) lead to oxidative protein modifications. Free 3-NT is a biomarker of the turnover of radiation-induced nitrated proteins.[211] The levels of 3-NT rapidly increased with the first cumulative radiation doses, but by the end of the experiment the levels of 3-NT approximated to those of the control group. 3T3-L1 released factors protected irradiated B16-F10 cells from oxidative nitration primarily in the first radiation fractions (Fig. **??**C).

Activation of the PI3K-AKT signaling pathway has been correlated with radiation resistance.[212,213] To investigate whether these radioresistant inducer effects of 3T3-L1 CM were due to activation of the PI3K-AKT signaling pathway, immunoblotting for AKT and Ser473 phospho-AKT was performed in B16-cell lysates. The expression of the active form of AKT was only detected in treatment groups containing the 3T3-L1 CM (Fig. **??**D), confirming the stimulation of this pathway by adipocyte-released factors.

These findings further underscore the protective effects of the adipocyte secretome in shielding

melanocytes from oxidative stress and loss of viability triggered by repetitive fractions of ionizing radiation.

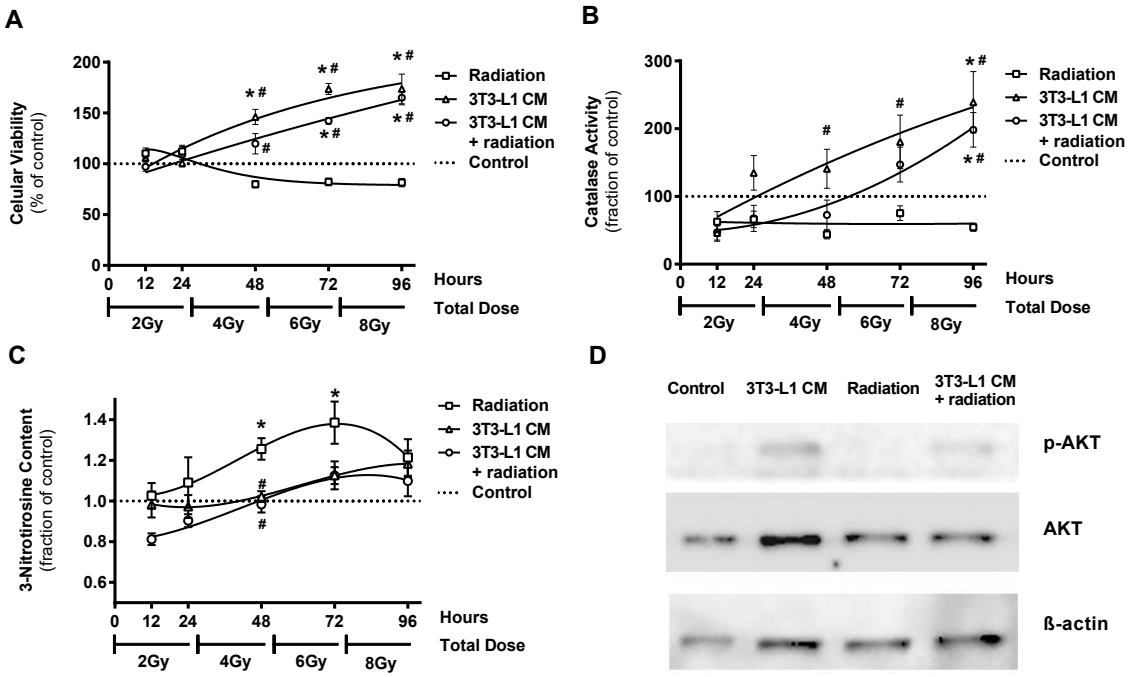

Figure 3.3: Adipocyte released factors protect B16-F10 melanocytes from fractionated radiation damage. Melanocytes were treated with 3T3-L1 CM, irradiated daily (2Gy) for four consecutive days or received both treatments (3T3-L1 CM + irradiation). At 12, 24, 48, 72 and 96 h after the first irradiation, cellular metabolic activity **(A)**, catalase activity **(B)** and 3-nitrotirosine content **(C)** were determined. Results are represented as percentage of control. Bars show mean±SEM ($*P < 0.05$ *vs* Control treatment; $\#P < 0.05$ *vs* irradiation; n=6). **D)** Immunoblot detection of AKT and Ser473 phosphorylated-AKT. β-actin was used as a loading control. A representative Western blot is shown.

3.4 Discussion

Cell survival response and (anti)oxidant status are good indicators of radiation susceptibility. Our results disclosed an increased metabolic activity of irradiated melanocytes when treated with adipocyte CM. Low-dose irradiation (2 Gy) was only able to induce significant alterations in B16-F10 viability in the early hours after treatment. However, repeated irradiation of melanocytes, up to a total of 8 Gy, led to a constant decrease in metabolic activity. On the other hand, when 3T3-L1 adipocyte secreted molecules were present, radiation-induced loss of viability was overturned and melanocytes had higher metabolic activities.

Melanocytes are considered to be resistant to radiation damage.[214] Ionizing radiation increases the oxidative burden in tumour cells.[215] The mild decrease in catalase activity and antioxidant capacity combined with the temporary increase in protein nitrative stress observed corroborate the low

radiosensitivity of B16-F10 melanocytes. Nevertheless, adipocyte-released factors enhanced the capacity of melanocytes to fight radiation-induced oxidative stress further contributing to melanomas radioresistance.

In obese patients there is a shift in the delivery of external-beam radiation, resulting in the target location not receiving the full dose.[216] In addition to the physical constraints to dose planning and delivery, our data further reinforce that the adipokine-rich environment might further contribute to the radioresistance of the melanocytes, culminating in a global underdosing effect. In addition to careful planning and dose delivery, which must take into account the higher body mass index of the patients, consideration must also be given to the more pro-inflammatory status and the adipokine and chemokine-rich environment that can protect malignant cells from the radiation damages.

Oxidative stress has been proposed as a common link between obesity and cancer. The increased levels of circulating oxidants and ROS produced from peritumoural adipose tissue accelerate oxidative stress within tumour cells and might contribute to the increased risk for cancer progression in obese patients.[55] ROS production also increases along the differentiation of 3T3-L1 cells into mature adipocytes,[56] however, our results showed a higher antioxidant capacity of 3T3-L1 CM. Given the short half-life of radicals, this ROS-mediated effect might be less significant in our cell culture model. In fact, numerous 3T3-L1 adipocyte-secreted proteins have implications in growth regulation and act as cell mitogens.[69,207,217] We believe these pro-proliferative and anti-apoptotic effects overcome the adipocyte-derived ROS.

Several signaling pathways involved in the radioprotective mechanisms of melanoma have been identified. MEK, ERK and PI3K-AKT cell survival cascades are known to play important roles in overcoming the radiation-induced damage[218] and have implications for radioresistance mechanisms in cancer.[212,213] Blockage of these pathways has been shown to radiosensitize melanocytes to ionizing radiation.[219] We have already demonstrated that 3T3-L1 CM is rich in numerous growth factors,[207] such as insulin-like growth factor (IGF)-I and hepatocyte growth factor (HGF), which have been linked to cancer radioresistance. Downregulation of IGF-1 receptor in mouse melanoma B16-F1 cells improved radiosensitivity[220] and, in some malignancies, radioresistance phenotypes were aggravated by HGF.[221] IGF-I and HGF signaling activates PI3K-AKT pro-survival pathways.[222] These findinds led us to assume that the growth-factors present in the 3T3-L1 CM and the up-regulation of the AKT signaling cascade are contributing to the radioresistant phenotype of B16-F10 cells observed in our results. Nevertheless, given the vast number of growth factors and bioactive molecules released by adipocytes, it is our belief that a "one mechanism fits all" approach is unlikely to exist and other signalling pathways certainly are co-activated and contribute to the enhanced radioresistance of melanoma .

Radiation also induces vascular damage that potentiates tumour hypoxia.[223] In a recently published study, our group showed that adipocyte secretome enhances vasculogenic mimicry in B16-F10 cells.[207] Therefore, reducing the vascular network dependence of the tumour for blood supply,

which allied with the radiation-desensitizing effect, plays a cumulative role towards melanoma aggressiveness.

In summary, our results indicated that an environment rich in adipocyte-released factors contributes to the protection of melanocytes from radiation-induced oxidative stress and viability loss, circumventing the efficacy of radiation, with a contribution of adipocyte-released factors PI3K-AKT activation.

Although further *in vivo* studies are of paramount importance to elucidate the molecular players involved, the current study demonstrates the importance of taking into consideration the role of adiposity when planning RT regimens.

3.5 Acknowledgments

We are immensely grateful to the personnel from "Serviço de Radioterapia, Centro Hospitalar de São João" who assisted us along the radiotherapy procedures. We are also in debt to the "Fundação para a Ciência e a Tecnologia" (FCT) and FEDER-COMPETE for financial support through the research unit PEst-OE/SAU/UI0038/2011, UID/BIM/04293/2013 and the PhD grant attributed to PC (SFRH/BD/80434/2011).

3.6 Supplementary Data

Table 3.S1: Detailed chromatographic conditions for 3-nitrotyrosine detection

HPLC Running Conditions	
Solvents:	Methanol, ultrapure water and 2,5% acetic acid (70:15:15)
Elution:	Isocratic
Flow:	1,0 mL/min
Injection volume:	30 µL
Column Temperature:	25 °C
Detection:	UV @ 356 nm
Runtime:	15 minutes

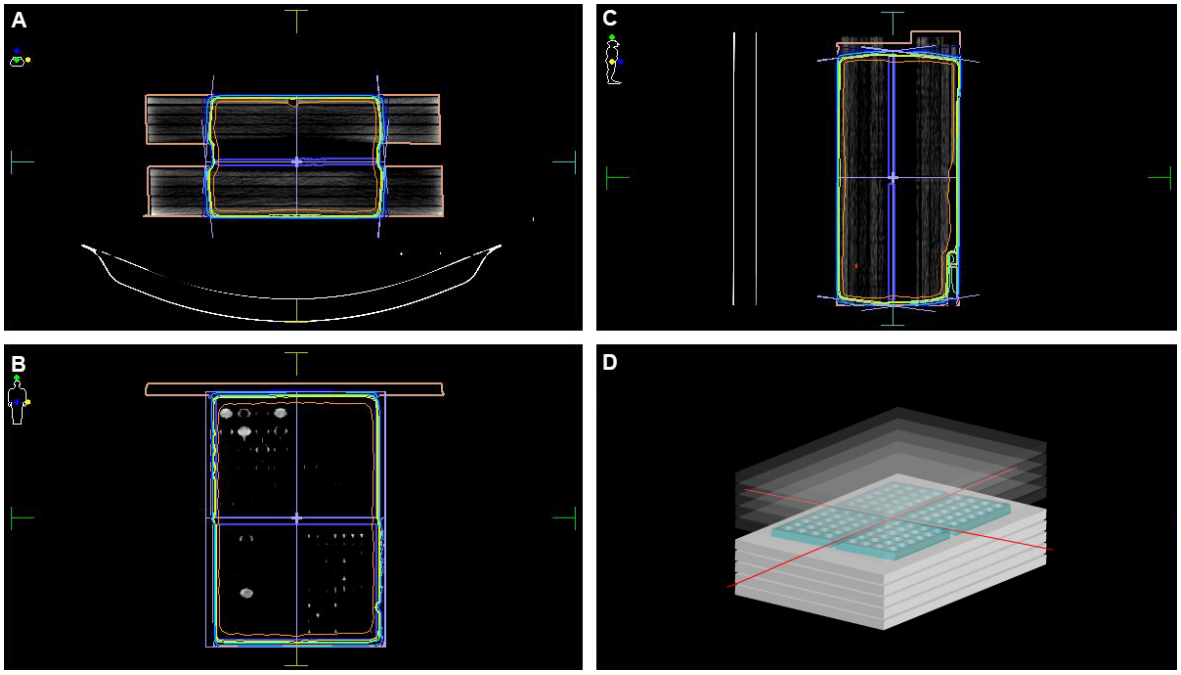

Figure 3.S1: 3D Conformal radiotherapy planning CT for the multi-well cell culture plates. **A)** Axial plane planning CT with overlay of radiation isodose lines. Coronal **(B)** and sagittal **(C)** images. **D)** Schematic representation of the plates arrangement in between the water phantoms. The red lines represent the laser-guided alignment to the radiation isocenter.

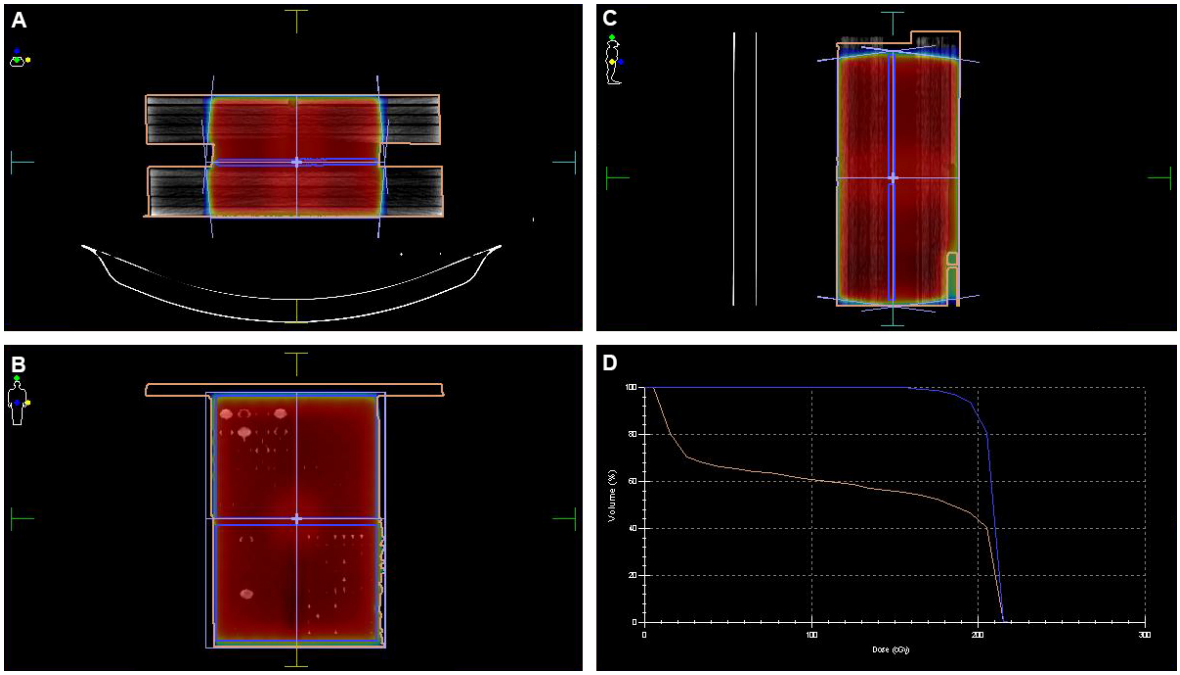

Figure 3.S2: Conformal radiotherapy simulation for the multi-well cell culture plates. Axial **(A)**, coronal **(B)** and sagittal images **(C)**. The red isodose area represents the fraction dose - 2 Gy. **D)** Dose volume histogram summarizing the radiation dose coverage to the target volume.

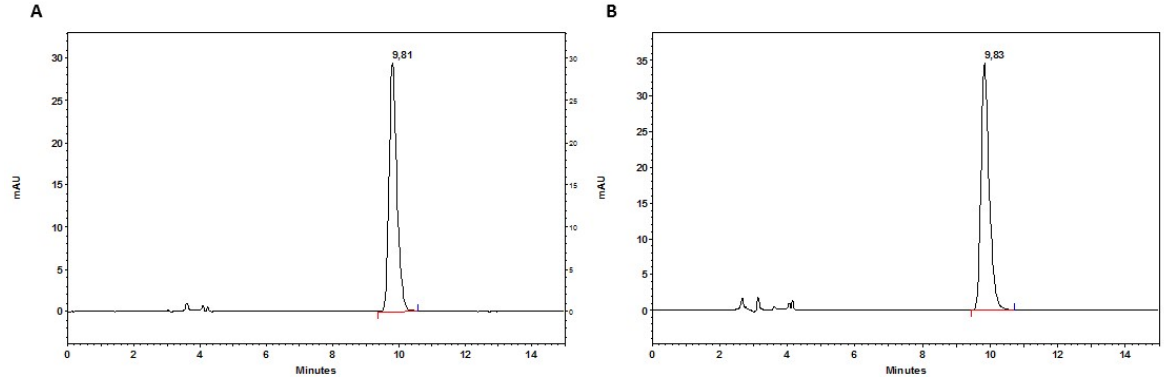

Figure 3.S3: Representative chromatograms of 3-nitrotyrosine (3-NT) standards **(A)** or samples **(B)**. 3-NT elution was detected at 356 nm and displayed a retention time of approximately 9,8 minutes.

4

Adipose-Derived Factors Increase B16-F10 Tumour Vascularization but Decrease Metastatic Potential

Coelho P, Almeida J, Prudêncio C, Fernandes R and Soares R

Unpublished Work

ABSTRACT

Melanoma has one of the most rapidly increasing cancer prevalences and obesity has been pointed out as a potential melanoma-promoting factor. A small group of reports in the literature demonstrate that adiposity and fat-released molecules play a role in melanoma vascularization, including angiogenesis, lymphangiogenesis, and more recently vasculogenic mimicry (VM). Both angiogenic vessels and VM channels represent entry points into the vasculature, allowing tumour cells to hematogenous spread and metastasise. However, the relationship between obesity and melanoma VM/metastasis is largely unknown. Herein, we employed a high-fat diet (HFD)-induced obese mice melanoma allograft model, where C57Bl/6J mice were either subcutaneously or intravenously inoculated with B16-F10 melanoma cells, to investigate the action of adiposity in melanoma angiogenesis, VM density and lung colonization. HFD-feeding enhanced melanoma burden, with tumour volume positively correlating with weight gain. Tumour growth was accompanied with increased microvessel density and area. However, tumour VM density was not significantly altered upon high-fat feeding. Weight gain was inversely correlated with lung metastatic potential. Significantly fewer lung metastasis were found in HFD animals than their standard diet (SD)-fed counterparts, still they exhibited more melanin pigmentation. *In vivo* fat-released circulating factors enhanced skinfold melanoma growth and vascularization but, on the other hand weakened the metastasizing capacity of circulating malignant B16-F10 cells. Distinct circulating profiles of adipokines, growth factors and angiogenic modulators, assessed by microarrays, were associated to weight gain and led us to highlight possible molecular players for the observed discrepancies.

4.1 Background

Malignant melanoma is among the most notoriously aggressive and treatment-resistant human cancers. Even though melanomas comprise less than 10% of all diagnosed skin cancers, melanoma represents nearly 80% of skin cancer deaths.[80] The incidence of melanoma is continuing to increase year by year in the last decades,[2] with an estimate doubling of incidence rates every 10 to 20 years,[3,4] raising melanoma to the most rapidly increasing cancer in white populations.[4]

Both high-adiposity and obesity have been pointed out as possible underlying causes for the increasing prevalence of human melanoma. Even though systematic reviews estimate a 1.17-1.31 risk ratio of developing melanoma for overweight and obese populations,[63–65] other reports found no significant association between obesity and risk for malignant melanoma.[62,66] Therefore, obesity influence in melanoma still remains controversial.

Nevertheless, *in vivo* adiposity-related stimulation of melanoma growth has already been demonstrated.[77,144,145,160] Diet-induced obesity, in rodent models, enhances both melanoma angiogenesis and lymphangiogenesis, with the commitment of lymph node metastasis,[145] while *in vitro* adipocyte-released factors act as sponsors of melanoma vasculogenic mimicry (VM).[207] Metastasis in melanoma xenografts is associated with primary tumour microvascular density.[99] Moreover, VM is another characteristic microcirculation pattern in melanomas.[25] Melanoma cell-lined vascular-mimetic networks constitute an additional entry point into the vasculature. However, the relationship between obesity and melanoma VM and metastasis is largely unknown.

Dysfunctional adipose tissue production of many adipokines and growth factors is involved in the growth-promotion and metastatic potential of human cancers.[36,64] Moreover, there is increasing evidence that adipokines play a pivotal role in the dissemination and establishment of melanoma metastasis.[138,224] Accordingly, we propose to address the relationship between high adiposity and melanoma progression. Employing an high-fat diet (HFD)-induced C57Bl/6J mice model and B16-F10 murine malignant melanoma cells we explored the effects of diet-induced obesity on melanoma progression, focusing on tumour angiogenesis, vasculogenic mimicry and lung metastasising capacity.

4.2 Materials & Methods

4.2.1 Cell Culture

Mouse melanoma B16-F10 cells, originally isolated from C57Bl/6J melanoma lung metastasis, are metastatic skin melanoma cells line with high tropism for lung invasion. B16-F10 cells (ATCC CRL-6475) were maintained in Dulbecco's modified eagle's medium (Sigma-Aldrich) supplemented with 10% heat inactivated fetal bovine serum (Sigma-Aldrich) and 1% penicillin/streptomycin/amphoter-

icin B (Sigma-Aldrich). Cells were maintained at 37 °C in a humidified 5% CO_2 incubator. Cells were serum deprived for 24 hours before inoculation into the animals.

4.2.2 Animals and Diets

Five-week-old male C57Bl/6J mice were purchased from Charles River (France) and housed at the animal research facility of Faculty of Medicine of University of Porto. Mice were acclimatized to the laboratory conditions and provided free access to rodent chow and water. The mice stayed in quarantine for 10 days before use and were maintained throughout the study in a controlled and specific-pathogen-free environment: 23 ± 5°C, 35 ± 5% relative humidity, and a 12-hour light/dark cycle. Afterwards, mice were randomly split and subsequently fed with one of two diets: the standard diet (SD) and the HFD. The SD (#2014; Teklad Diets) used in this study contained 13%, 67% and 20% of kcal from fat (soybean oil), carbohydrates and protein respectively. The purified HFD (EF R/M acc. D12451 (I) mod; ssniff Spezialdiäten) contained 45%, 35% and 20% of kcal from fat (lard), carbohydrates and protein respectively. Fresh diet was freely provided and the animals weight and food/water intake was monitored throughout the study.

4.2.3 B16-F10 Cell Inoculation

After 26 weeks of diet feeding, both HFD and SD-fed mice were randomly split intro 3 groups: subcutaneous (SC; 6 animals/diet), intravenous (IV; 6 animals/diet) and control (CT; 3 animals/diet). Subcutaneous (SC) mice were subcutaneously inoculated with 1×10^6 B16-F10 melanoma cells suspended in 0.1 mL phosphate buffered saline (PBS) into the dorsal skinfold and monitored for the development of palpable tumours for 14 days. Afterwards, mice were sacrificed, the tumours were excised and paraffin-embedded for histological analysis. Tumour dimensions were determined along the major (*length*) and minor axis (*width*) with an digital caliper and tumour volume was calculated according to the formula: $0.52 \times length \times (width)^2$. IV animals were intravenously injected in the tail vain with 2×10^5 B16-F10 cells in 0.25 mL 0.9% saline. Three weeks later, mice were sacrificed, the lungs were excised and paraffin-embedded for histological analysis. Control animals were not injected with B16-F10 cells and were melanoma free. Blood was collected from all animals, spun at 14,000 rpm for 5 mins at 4ºC and the supernatant stored for molecular analyses. All procedures were conducted by accredited personnel, in accordance with the European Community policy for Experimental Animal Studies [European Community law dated from November 24th 1986 (86/609/CEE) with addendum from June 18th 2007 (2007/526/CE)] and under the supervision of the animal facility veterinary.

4.2.4 Histologic Analysis

Tissues were fixed in 10% neutral buffered formalin, dehydrated and embedded in paraffin. Histological 4 μm thickness sections were stained with hematoxylin and eosin (H&E) for histopathological analyses.

4.2.5 CD31 Immunohistochemistry

Sections of paraffin-embedded tumour tissues were deparaffinized and rehydrated. Thermal antigen retrieval was done in 10 mM sodium citrate (Merck) buffer (pH 6) at 98°C for 20 min. Afterwards, slides were incubated in 3% H_2O_2, and blocked with a solution of 2% bovine serum albumin (Sigma) and 10% normal swine serum in PBS. Immunohistochemistry was conducted with the rabbit anti-CD31 primary antibody (1:100; Abcam), biotinylated goat anti-rabbit secondary antibody (1:200; Santa Cruz Biotechnology), streptavidin-horseradish peroxidase (Vectastain Elite), 1,3-diaminobenzidine tetrahydrochloride (Abcam) and counterstained with hematoxylin. Microvessel area was determined by measuring CD31 endothelial vessels area with the help of ImageJ software (NIH) and normalizing by dividing over the total tissue area.

4.2.6 Periodic Acid–Schiff Reaction

The periodic acid-Schiff (PAS) reaction in tissue sections was conducted as previously described. Briefly, slides were deparaffinized, rehydrated and immersed for 10 minutes in a 10% (w/v) periodic acid solution (Merck) followed by 20 minutes incubation with Schiff reagent (Panreac) in a dark chamber. Afterwards, slides were counterstained with hematoxylin and mounted for microscopic observation.

4.2.7 Melanin Staining and Quantification

Melanin staining was conducted according to the Fontana-Masson method. Briefly, slides were deparaffinized, rehydrated and incubated with the ammoniacal silver solution at 56°C for 40 minutes. The precipitate was fixed with a 5% (w/v) sodium thiosulfate solution and the cells counter-stained with nuclear fast red for 5 minutes. Melanin-positive areas were photographed at 200× magnification and staining intensities were quantified with ImageJ software (NIH).

4.2.8 Metastasis Assessment

Three random H&E-stained paraffin-embedded lung sections from each IV animal were microscopically inspected for metastasis presence. The number of metastasis found was reconfirmed for the presence of melanin deposits in Fontana-Masson stained slides.

4.2.9 Microvessel and Vasculogenic Mimicry Density Determination

Tumour allograft microvessel and VM density were evaluated under a light microscope at 400× magnification. In consecutive CD31 immunohistochemistry-stained and PAS-stained tumour sections, the number of endothelial vessels (CD31-positive and PAS-positive) and VM channels (CD31-negative and PAS-positive) were counted throughout the whole section. Three CD31/PAS tissue sections for each SC tumour were analyzed and normalized to the total tissue area. A negative control was included. Both positive-stained endothelial cells or clusters that were separated from adjacent vessels were considered an individual vessel. VM channels were double checked for the presence of lumen erythrocytes in H&E stained sections.

4.2.10 Adipokine and Angiogenesis Antibody Arrays

Mouse adipokine and angiogenesis antibody arrays (# ARY-013 and ARY-015, repectively; R&D systems) were performed using 500 µL of pooled serum from both SD and HFD control animals and following the manufacturer's protocol. The relative pixel density of each spot was calculated with the microarray profiler plugin of ImageJ software (NIH).

4.2.11 Statistical Analysis

When analysing the influence of the diet (SD or HFD) in only one parameter an unpaired two-tailed Mann-Whitney nonparametric test was used. Statistical dependence of two variables was computed by Spearman's rank correlation. To test for differences in animal weight gain and tumour volume progression among the groups repeated measures two-way ANOVA with the diet as the categorical independent variable and time as the repeated measure factor was executed. If a significant interaction occurred, Sidak post-hoc multiple comparisons test was subsequently performed. All data are presented as mean ± standard error of the mean (SEM). Differences with a P value less than 0.05 were considered statistically significant. All analyses were carried out in GraphPad Prism 7.0 Software (GraphPad Software Inc.).

4.3 Results

4.3.1 High-Fat Diet Causes Significant Weight Gain and Increases Serum Levels of Growth and Angiogenic Factors in C57Bl/6J Mice

High-fat feeding significantly increased body weight gain in C57Bl/6J mice to a great extent than standard-fed animals. Mice weight began to increase as soon as 7 weeks after HFD feeding and the weight differences between SD and HFD groups became more prominent. At the beginning of the

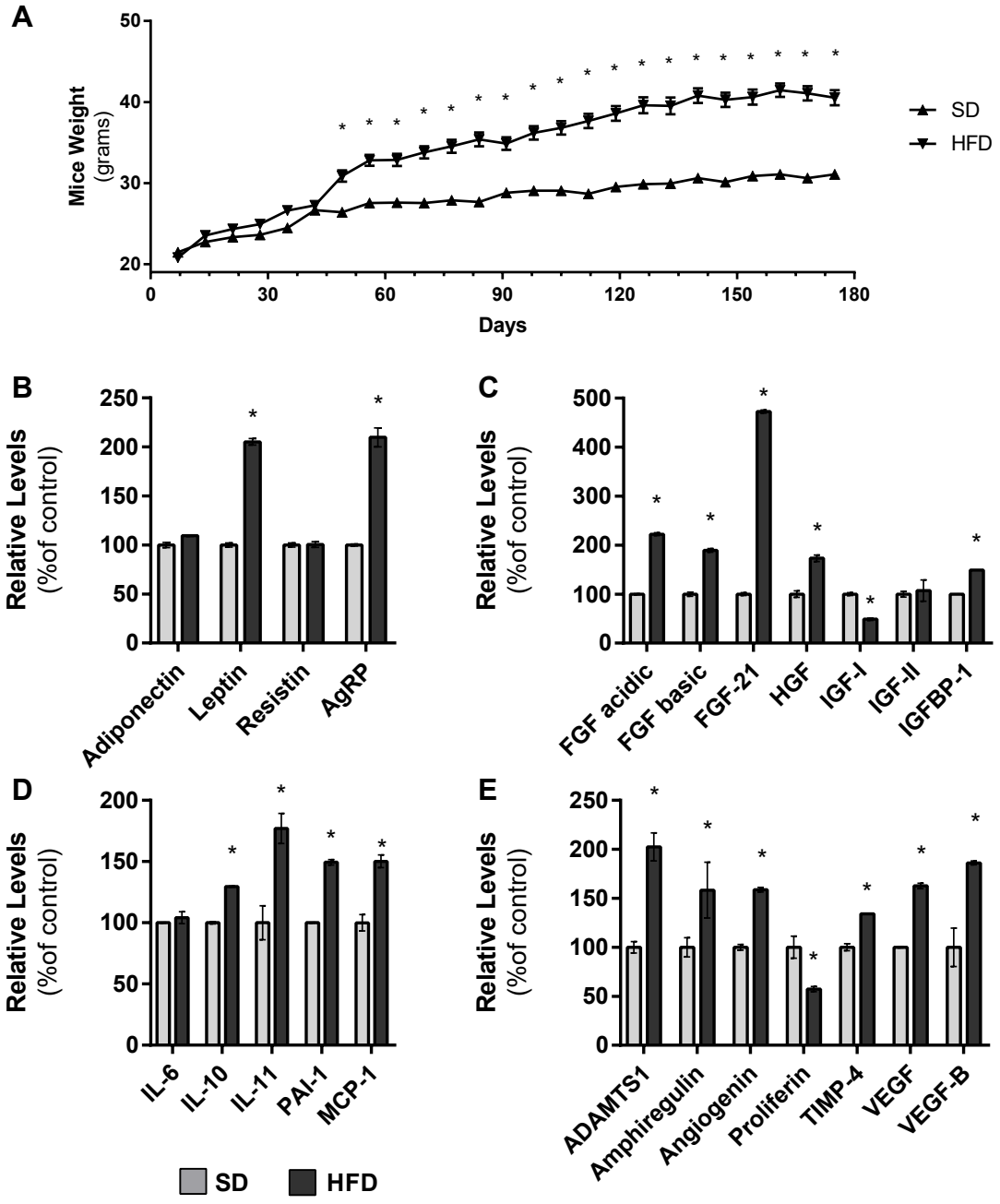

Figure 4.1: Weight gain and serum profiles of HFD and SD challenged C57Bl/6J mice. **A)** HFD feeding significantly increased the weight of HFD animals as compared to SD-fed animals. **B)** Leptin and AgRP adipokines are elevated in HFD animals, whereas adiponectin and resistin levels are not significantly altered. **C)** HGF and FGFs, particularly FGF-21, were present at considerably higher concentrations in HFD animals serum. **D)** Increased relative levels of IL-10, IL-11, PAI-1 and MCP-1 were found within serum of HFD mice. **E)** Obese animals exhibit greater levels of angiogenin, VEGF-A, and VEGF-B and other angiogenic factors. Bars represent mean values (±SEM) ($*P < 0.05$ HFD *vs* SD)

tumour challenge, 26 weeks after diet introduction, SD mice average weight was 31.07 g as compared to 40.53 g in HFD animals (Fig. 4.1A).

The relative abundance of numerous adipokines and angiogenic factors in pooled serum collected from both SD and HFD-fed CT animals was accessed by antibody microarrays (see Supplemental data). Adiposity gain was accompanied by changes in the serum levels of several circulating molecules in C57Bl/6J mice. Serum profiles of growth-factors, adipokines, cytokines, and angiogenesis-related molecules were different between animals on SD and HFD regimens. HFD mice showed a noticeable increase (∼2.0-fold) in leptin as well as Agouti-related protein (AgRP) levels, but no significant decrease in serum adiponectin or resistin levels (Fig. 4.1B). The levels of several growth factors were also analyzed. HFD animals had higher circulating levels of fibroblast growth factor (FGF)s, in particular FGF-21 (∼5.0-fold), hepatocyte growth factor (HGF) and insulin-like growth factor-binding protein (IGFBP)-1, whereas insulin-like growth factor (IGF)-I levels were significantly decreased (Fig. 4.1C). The levels of the interleukin (IL)-10, IL-11 were also significantly higher within HFD animals and accompanied with no significant alteration in the concentration of IL-6 (Fig. 4.1D). Angiogenesis stimulators A disintegrin and metalloproteinase with thrombospondin motifs (ADAMTS)-1, amphiregulin, angiogenin, and vascular endothelial growth factor (VEGF)-A and VEGF-B were significantly more abundant in overweight animals, as well as anti-angiogenic tissue inhibitor of metalloproteinases (TIMP)-4 was also significantly elevated. Conversely, proliferin was significantly decreased in overweight animals as compared to lean mice (Fig. 4.1E).

4.3.2 Fat-Rich Diet Promotes Melanoma Progression and Vascularization

Our previous studies showed that adipocyte secretome was particularly rich in pro-angiogenic factors and these adipose-derived factors favoured the *in vitro* development of VM structures as well.[207] Therefore, we next examined the effects of the HFD in vascular and VM microcirculation of C57Bl/6 SC-implanted melanomas. Upon inoculation, B16-F10 tumours became palpable from day 8 and 9 onwards for the HFD and SD groups, respectively. SC tumours from HFD-fed mice displayed a marked expansion, with an average volume approximately twice the size of melanomas in SD animals (∼2.7 cm^3 and ∼1.3cm^3, respectively; Fig. 4.2A). Moreover, tumour volume positively correlated with weight gain ($r = 0.83, P = 0.0049$; Fig. 4.2B). Analysis of Fontana-Masson stained tumour tissue sections (Fig. 4.2D) indicated that the melanin pigmentation was not different between tumours from HFD and SD diet regimens (Fig. 4.2C).

VM tubules characteristically have tumour cells, but not endothelial cells, covering the lumen of channel-like structures.[225] To distinguish VM from endothelial-lined vessels, we performed immunostaining for the CD31 endothelial marker and PAS reaction for basal membrane in consecutive tumour sections. While endothelium vessels are lined by spindle-shape endothelial cells and surrounded by basement membrane, thus staining positive for both CD31 and PAS, VM tumour

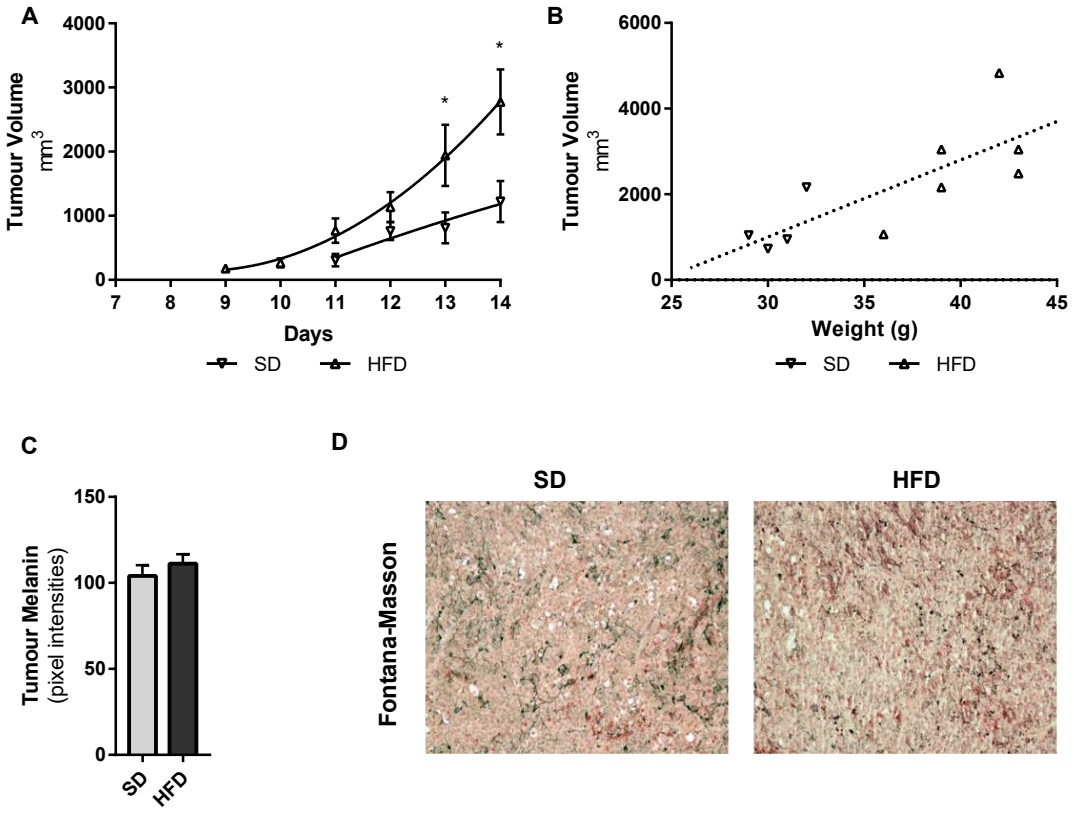

Figure 4.2: A) C57Bl/6J tumours from HFD and SD-fed animals became measurable from day 9 and 10 onwards, respectively. Tumours from HFD mice progressed more rapidly and had significant higher volumes than SD-fed animals. **B)** Melanoma volume was significantly correlated with weight gain. **C)** Tumour melanin content from both SD and HFD groups. **D)** Representative images of Fontana-Masson stained melanoma sections are shown (100×). Bars represent mean values ±SEM ($*P < 0.05$ HFD *vs* SD; n=6)

cell-lined blood channels are CD31-negative and only the basement membrane is positive for PAS staining (Fig. 4.3D).

Enhanced tumour growth, in HFD-fed animals, was accompanied by a significantly higher microvessel density in SC tumours (Fig. 4.3A). Not only the number of endothelium-lines vessels was elevated in HFD tumour-bearing animals, but also a parallel increase in the microvessel total occupied area was observed (Fig. 4.3B). Moreover, PAS-positive VM channels were detected in both HFD and SD melanomas. However, in comparison to SD-fed animals, only a small increase in the number of cell-lined vessel-like structures was observed in HFD-treated mice (Fig. 4.3C).

4.3.3 High-Fat Diet Decreases B16-F10 Lung Metastasis

Malignant melanocytes lung colonization potential is associated with tumour microvascular density.[99] To evaluate the *in vivo* effects of HFD and adipose-derived circulating factors in the ability of melanoma cells to metastasise, we intravenously injected B16-F10 cells into the tail vein of C57Bl/6J

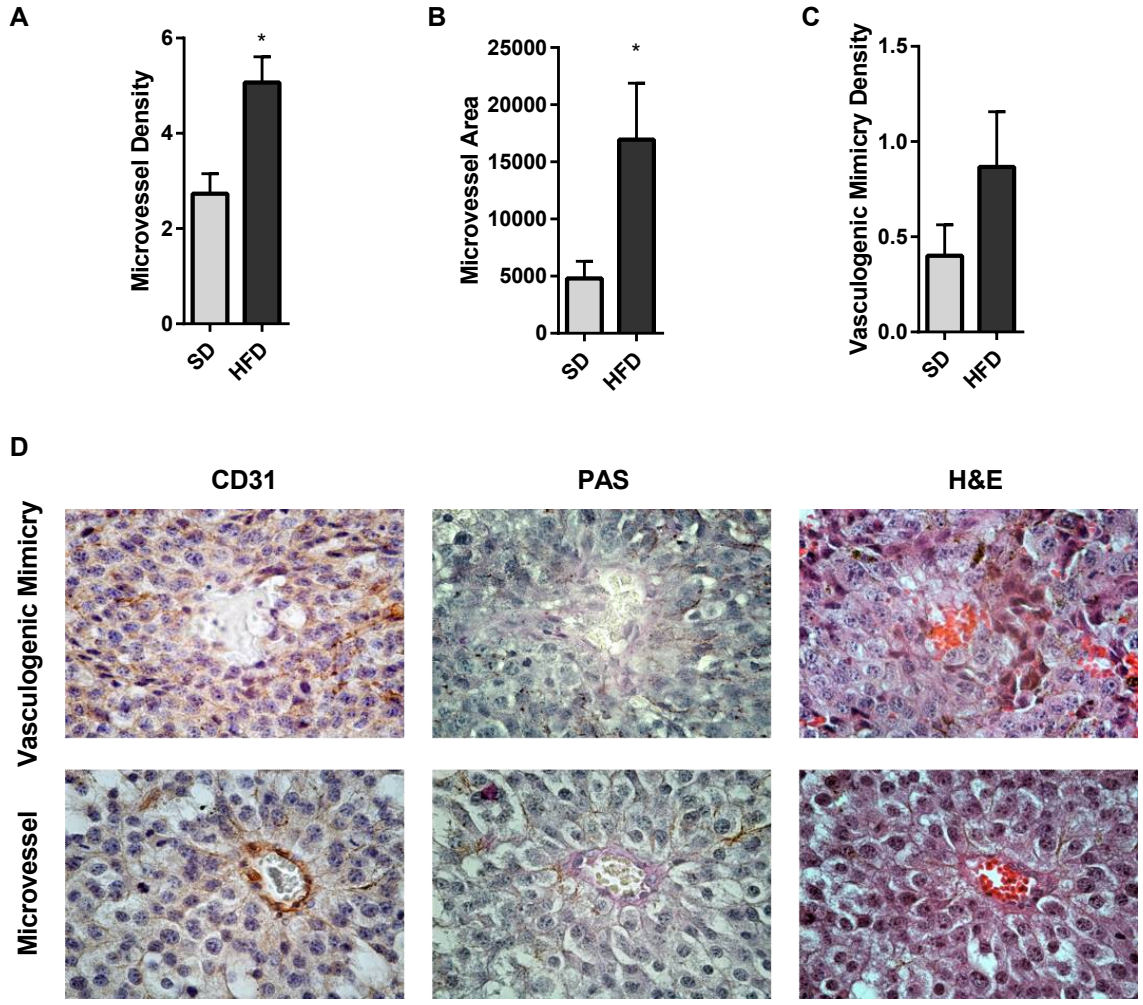

Figure 4.3: Microvessel density **(A)**, microvessel area **(B)** and VM density **(C)** was accessed in consecutive CD31 immunohistochemistry, PAS and H&E stained tumour sections. **D)** Representative images of spindle-shape endothelial cell-lined microvessels (CD31-positive and PAS-positive) and B16-F10 VM channels (CD31-negative and PAS-positive). Endothelial cell are stained by CD31 immunohistochemistry (brown) and basement membrane is positive for PAS staining (pink). H&E staining revealed the presence of lumen erythrocytes in the center of both tubular structures (400×). Show are means±SEM ($*P < 0.05$ HFD *vs* SD; n=6)

mice. Three weeks upon inoculation, lungs from both CT and IV mice were collected and processed for further microscopic observation. Histopathologic analysis of H&E lung sections revealed a more inflamed environment, with increased septal thickening, intra-alveolar hemorrhages, peribronchial lymphocytic infiltrate accumulation, abnormal deposition of hemosiderin and a notorious decrease in total alveolar volume in the lungs of both CT and IV diet-induced obese animals. No significant parenchymal alterations were found in the lungs of SD animals (Fig. 4.4D).

In B16-F10 IV-inoculated mice, 5 out of 6 SD animals (∼83%) developed lung metastases by the end of the metastasis challenge, however in only 2 out of 6 HFD-fed animals (∼33%) lung metastases were present (Fig. 4.4A). In fact, not only less HFD animals exhibited metastases, but they

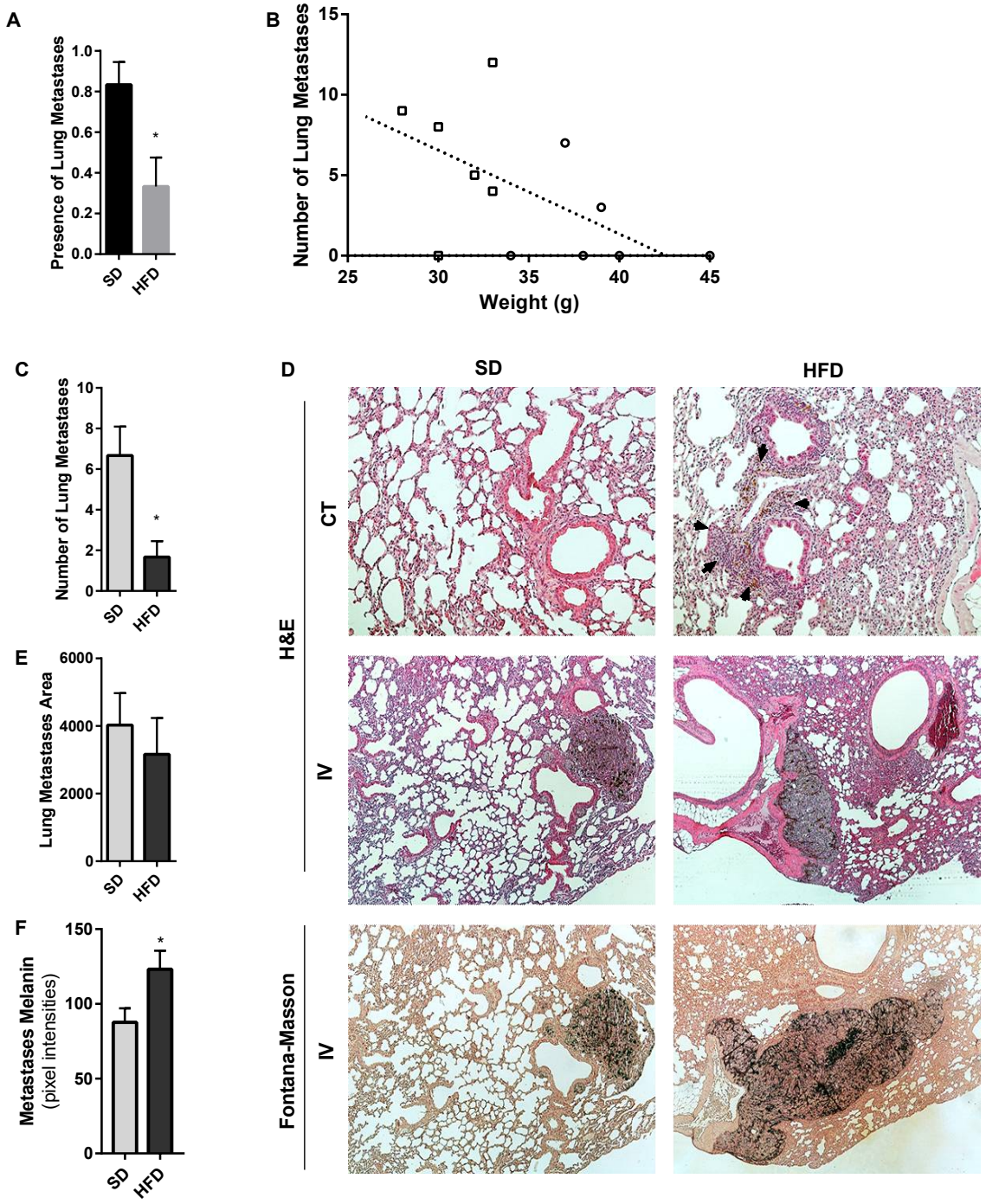

Figure 4.4: Intravenous injection of B16-F10 cells more readily formed lung metastases in lean animals **(A)** and the number of developed metastases correlates inversely with the animal weight **(B)**. The number of metastases found is significantly higher in SD *vs* HFD groups **(C)**, however no differences were found in the mean metastases area **(E)**. **D)** Representative images of H&E and Fontana-Masson stains in lung sections from SD and HFD animal (200×). Black arrows represent histological changes of lungs (peribronchial inflammatory cells and hemosiderin deposition). **F)** Melanin pigmentation in lung metastases was evaluated by Fontana-Masson stain. Bars are the means values ±SEM ($*P < 0.05$ HFD *vs* SD; n=6)

also had significantly fewer metastases per lung than their leaner counterparts (6.7 and 1.7 respectively; Fig. 4.4C). Interestingly, the number of metastases found inversely correlates with the weight of the animal ($r = -0.61, P = 0.038$), in a diet-independent manner (Fig. 4.4B). The melanoma metastases present in HFD animals were located in more peripheral regions of the lung and in the pleural space, while in SD animals most metastases were perivascular. Moreover, one subcutaneous metastasis was found in one of the HFD animals along the necropsy (data not shown). Fontana-Masson stain (Fig. 4.4D) revealed a higher melanin content in lung metastases from overweight animals (Fig. 4.4F). The average area of the metastases was not significantly different among HFD and SD animals (Fig. 4.4E).

4.4 Discussion

Vascularization plays a central role in tumour development and progression.[177] The awareness that different stages of melanoma growth are associated with distinct tumour microcirculation patterns[209] led us to investigate the influence of high-fat feeding in melanoma VM and angiogenesis.

Melanoma angiogenic development of endothelium-lined networks is mediated by a complex multistep process comprising a series of molecular mediators that lead to tumour neovascularization. Among these are VEGF, FGF-2, epidermal growth factor (EGF) and IL-8 as well platelet-derived growth factor (PDGF).[83,84] In the present study, plasma concentration of VEGF-A, -B and FGF-2 was significantly increased in non-tumour-bearing HFD-fed mice compared to those fed the SD diet. Moreover, high-fat feeding enhanced the circulating levels of ADAMTS-1, amphiregulin and angiogenin. Besides their angiogenesis-stimulating potential, these factors are known to be involved in several aspects of tumourigenesis, including growth-promoting signals, tissue invasion and metastasis, and resistance to apoptosis.[226–228] Genetic ablation of ADAMTS-1 in C57Bl/6 mice resulted in a drastic decrease of B16 tumour growth and metastasis via an anti-tumourigenic microenvironment-modulation effect.[229] ADAMTS-1 does not seem essential for melanoma growth, but contributes to the acquisition of an endothelial-like phenotype by tumour cells and might be eliciting endothelial mimicry by B16-F10 tumour cells.[230] Furthermore, FGF-2 confers VM features and increases *in vivo* metastasising of melanoma cells.[231] In fact, induction of VM overcomes VEGF-A angiogenic signaling conferring melanomas adaptive resistance to anti-angiogenic therapies,[232] rendering VM one of the major aggressive features of human metastatic melanoma.

In addition to angiogenic endothelium-dependent vessels, VM is another characteristic microcirculation pattern in melanomas.[25] In both overweight and lean tumour-bearing mice, we detected CD31-negative PAS-positive tumour cell-lined blood vessels. However, high-fat feeding had no significant net effect in the number of VM channels formed. In fact, vasculogenic mimicry and endothelium-lined vessel densities vary along melanoma growth. In early stages of tumour growth, vasculogenic mimicry predominates but, as the malignant mass expands the number of true endothelium-

lined vessels increases and vascular microcirculation predominates.[209] Accordingly, HFD tumour-bearing mice had a more pronounced tumour expansion, with increased microvessel density and caliber, still a non statistically significant increase in tumour cell-line VM channels was observed.

IGF-I signaling axis has been proposed as a molecular link between obesity and the increased melanoma progression.[80] Our results disclosed significantly decreased circulating levels of IGF-I, with a parallel elevation of free IGFBP-1 in these animals. Antagonistically, in general IGFBP-1 binds to IGF-I, counterbalancing its effects, and most likely contributing to the decreased free IGF-I levels observed in HFD-fed animals serum. HFD animals also exhibited large amounts of circulating FGF-21. FGF-21 is associated with multiple benefits on obesity-related complications.[233] However, serum FGF-21 is elevated in obese individuals and appears to be a superior predictor to other adipokines of metabolic complications.[234] In melanomas, FGF-21 also increases cell proliferation *in vitro* accompanied by an increased tumourigenesis and invasive potential *in vivo*.[178] FGF-21 inhibits hepatic IGF-I production[233] and may also contribute for the down-regulation of plasma IGF-I observed.

HFD-feeding increased the serum levels of IL-10, IL-11, plasminogen activator inhibitor (PAI)-1 and monocyte chemotactic protein (MCP)-1. Emerging roles for IL-11, PAI-1 and MCP-1 signaling in cancer development and metastasis, that correlates with poor disease prognosis, have been unveiled.[235–237] However, IL-10 inhibits the production of a wide range of cytokines in various cell types, suppressing both tumour growth and metastasis of melanoma cells, with a potential inhibition of angiogenesis and tumour-associated inflammation.[238,239]

Development of distant metastases is an early event in melanoma metastatic dissemination from the primary lesion, even from very small tumour masses.[240] As small malignant melanomas may have already acquired vascular blood supply, it is likely that cancer cells have spread throughout the body long before the primary melanoma is diagnosed. Our data corroborates HFD-induced increase of tumour vascularization in melanoma xenografts.[145] In fact, primary tumour microvascular density is associated with melanoma cells lung colonization potential.[99] However, our results disclosed an antagonistic outcome in HFD-modulated melanoma metastasis. Despite the increased microvascular density in tumours from HFD-fed SC animals and the increased circulating serum levels of angiogenic factors present, the number of HFD IV animals with lung-colonizing metastases was significantly lower than SD animals, with a concomitant decrease in the average number of lung metastases found.

Previous studies report that fat-rich diets increase metastasis in several other rodent cancer models via angiogenesis-stimulation mechanisms and factors.[235,236,241,242] However, recently it has been shown that oxidative stress inhibits distant metastasis by human melanoma cells without significantly interfering with the growth of subcutaneous tumours.[243] In fact, visceral adiposity is characterized by a systemic increase in oxidative burden, in part through inflammation but also by increased generation of reactive oxygen species (ROS) and reactive nitrogen species (RNS).[56,70] Furthermore, increased ROS production and oxidative stress precedes the onset of HFD-induced

weight gain and is an initial key event triggering HFD-induced metabolic complications in C57Bl/6J mice.[244,245] This suggests that the systemic circulation of obese animals might become more hostile to circulating melanoma cells, than the subcutaneous environment. In fact, we have found a cutaneous metastasis in an IV overweight animal. Obesity-associated systemic alterations might also be decreasing the lung-specific tropism of B16-F10 cells, deviating circulating melanoma cells to other organ targets. Additionally, excessive oxidative stress can impair the formation of a favourable pre-metastatic microenvironment at distant sites, where circulating metastatic cells may engraft and colonise, limiting the extent of successful metastasising. Nevertheless, histopathologic analysis of lung sections from HFD melanoma-free animals revealed alterations in lung parenchyma, with increased accumulation of lymphocytic infiltrate. Both systemic and local inflammation promotes lung metastasis, so we do not conceive these alterations as a plausible mechanism bestowing the observed B16-F10 hindered metastasising capacity.[246,247]

Melanocytes are cells specialized in melanin pigment production. Although the main function of melanin is to protect against active oxygen species and UV-induced damage, melanoma aberrant melanossomes have been found as an aditional source of ROS.[21] Thus, melanin pigment plays a double role in the etiology of melanoma acting as a two-edged sword: enhancing melanocytes scavenger mechanism against UV and oxidative damages, but simultaneously melanossomes accelerate melanoma progression and resistance to the effects of ROS-generating treatment therapies.[21,22,157] Although no significant alteration in SC tumours pigmentation was observed, lung metastasis from HFD-fed IV animals exhibited higher melanin pigment deposition. In fact, melanogenesis affects melanoma overall and disease-free survival. Hyperpigmented melanomas are associated with significantly shorter disease-free survival[248] and the melanin content in melanoma metastases is a predictor of poor radiotherapy outcome,[23] rendering melanomas ionizing radiation resistant. Accordingly, the more hostile systemic circulation of obese animals might be exerting a selective pressure on circulating tumour cells, allowing only more resistant and aggressive melanoma cells to successfully metastasise, thus enhancing metastasis aggressiveness and treatment resistance.

In summary, our findings disclose a puzzling set of information. Diet-induced obesity enhanced subcutaneous tumour growth with a concomitant increase in vascularization, raising the chances of melanoma cells detaching from the primary tumour, enter the circulation and successfully metastasise. However, obesity-associated changes in redox homeostasis might render the vascular system an inhospitable environment for circulating melanoma cells, decreasing their metastatic potential, thus preventing secondary tumour growth. Nevertheless, this pro-oxidant environment might select a more resistant subset of circulating tumour cells rendering the metastasis formed more aggressive. Although further *in vivo* studies are of paramount importance to identify the molecular pathways involved, the current study already highlights some possible key molecular mediators.

4.5 Acknowledgments

We are immensely grateful to Professor Fátima Gärtner from "Instituto de Ciências Biomédicas Abel Salazar" for her assistance and guidance along the histopathologic interpretation of the slides. We are also in debt to the "Fundação para a Ciência e a Tecnologia" (FCT) and FEDER-COMPETE for financial support through the research unit PEst-OE/SAU/UI0038/2011, UID/BIM/04293/2013 and NORTE2020 - "Programa Operacional Regional do Norte" (NORTE-01-0145-FEDER-000012) as well as the PhD grant attributed to PC (SFRH/BD/80434/2011).

4.6 Supplemental Data

Table 4.s1: Serum Profile by Microarray

Factor	**SD** ±SEM	**HFD**± SEM	Ratio
ADAMTS1	0,0391 ±0,0023	0,0792 ±0,0056	2,02
Adiponectin	0,2296 ±0,0063	0,2511 ±0,0013	1,09
AgRP	0,0236 ±0,0002	0,0496 ±0,0023	2,10
Amphiregulin	0,0413 ±0,0041	0,0654 ±0,0118	1,58
Angiogenin	0,5347 ±0,0155	0,8491 ±0,0132	1,59
Angiopoietin-1	0,5186 ±0,014	0,5293 ±0,012	1,02
Angiopoietin-3	0,0621 ±0,0027	0,0657 ±0,0055	1,06
ANGPT-L3	0,5462 ±0,0005	0,4455 ±0,003	0,82
Coagulation Factor III	0,3202 ±0,0236	0,3514 ±0,0031	1,10
C-Reactive Protein	0,3656 ±0,0012	0,3258 ±0,004	0,89
CXCL16	1,5995 ±0,0237	1,4758 ±0,0081	0,92
Cyr61	0,3549 ±0,0064	0,4386 ±0,0079	1,24
DLL4	0,1043 ±0,0012	0,1025 ±0,0044	0,98
DPPIV	0,9356 ±0,0141	0,8138 ±0,0017	0,87
EGF	0,0349 ±0,0036	0,0281 ±0,0004	0,80
Endocan	0,8068 ±0,0083	0,8747 ±0,0097	1,08
Endoglin	0,5336 ±0,0114	0,4645 ±0,0154	0,87
Endostatin/Collagen XVIII	1,2249 ±0,0262	1,1173 ±0,0124	0,91
Endothelin-1	0,1011 ±0,0036	0,1309 ±0,0104	1,29
Fetuin A	0,2489 ±0,0025	0,197 ±0,0047	0,79
FGF-1	0,0574 ±0,0006	0,1276 ±0,0017	2,22
FGF-2	0,0457 ±0,0019	0,0865 ±0,0016	1,89
FGF-21	0,0874 ±0,0027	0,4135 ±0,0027	4,73
Fractalkine	0,3276 ±0,0027	0,2694 ±0,0069	0,82
GM-CSF	0,0574 ±0,0009	0,0458 ±0,0014	0,80
HB-EGF	0,0813 ±0,0018	0,0988 ±0,0002	1,22
HGF	0,0189 ±0,0012	0,0328 ±0,0012	1,73
ICAM-1	0,5782 ±0,0021	0,4475 ±0,0003	0,77
IGFBP-1	0,6367 ±0,002	0,9494 ±0,0007	1,49
IGFBP-2	2,0987 ±0,0254	2,0658 ±0,0216	0,98
IGFBP-3	2,7338 ±0,0293	2,6859 ±0,0149	0,98

Continued on next page

Table 4.s1: Serum Profile by Microarray

Factor	**SD** ±SEM	**HFD**± SEM	**Ratio**
Continued from the previous page			
IGFBP-5	0,9717 ±0,0094	0,8585 ±0,0171	0,88
IGFBP-6	1,2697 ±0,0011	1,0879 ±0,0135	0,86
IGF-I	0,6118 ±0,0186	0,2992 ±0,0142	0,49
IGF-II	0,0548 ±0,0031	0,0587 ±0,0119	1,07
IL-1α	0,0943 ±0,0074	0,1005 ±0,0036	1,07
IL-1ß	0,0286 ±0,0002	0,0353 ±0,0028	1,24
IL-6	0,0336 ±0,0001	0,0349 ±0,0016	1,04
IL-10	0,0168 ±0,0002	0,0217 ±0,0001	1,30
IL-11	0,021 ±0,0029	0,0372 ±0,0026	1,77
IP-10	0,0876 ±0,0039	0,0586 ±0,0037	0,67
KC	0,1439 ±0,0068	0,1427 ±0,0126	0,99
KGF	0,043 ±0,0075	0,0389 ±0,0029	0,90
Leptin	0,7482 ±0,0117	1,5518 ±0,0005	2,07
LIF	0,0556 ±0,0029	0,0432 ±0,0067	0,78
Lipocalin-2	1,3558 ±0,0062	0,9176 ±0,0174	0,68
MCP-1	0,1451 ±0,0097	0,2179 ±0,0075	1,50
M-CSF	0,5359 ±0,0016	0,5743 ±0,0057	1,07
MIP-1α	0,2071 ±0,0002	0,1769 ±0,0005	0,85
MMP-3 (pro and mature form)	3,7499 ±0,0817	3,6736 ±0,036	0,98
MMP-8 (pro form)	1,4113 ±0,046	1,2953 ±0,037	0,92
MMP-9 (pro and active form)	2,2327 ±0,0424	1,969 ±0,0204	0,88
NOV	2,7234 ±0,0697	2,4931 ±0,0528	0,92
Oncostatin M	0,0489 ±0,0051	0,0273 ±0,0003	0,56
Osteopontin	1,5382 ±0,0043	1,1231 ±0,0004	0,73
PD-ECGF	0,0629 ±0,0067	0,0496 ±0,0071	0,79
PDGF-AA	0,1612 ±0,004	0,1426 ±0,0117	0,88
PDGF-AB/PDGF-BB	1,0405 ±0,0288	0,914 ±0,0309	0,88
Pentraxin 2	0,496 ±0,0011	0,356 ±0,0057	0,72
Pentraxin 3	0,4541 ±0,0014	0,3724 ±0,0052	0,82
Pentraxin-3	1,2756 ±0,0067	1,0924 ±0,0132	0,86
Platelet Factor 4	0,7515 ±0,0069	0,6848 ±0,0102	0,91
PlGF-2	0,8404 ±0,0005	1,0469 ±0,0026	1,25
Continued on next page			

Table 4.s1: Serum Profile by Microarray

Factor	**SD** ±SEM	**HFD**± SEM	**Ratio**
Continued from the previous page			
Pref-1	0,1727 ±0,0092	0,1148 ±0,0024	0,66
Prolactin	0,8047 ±0,0414	0,7208 ±0,0249	0,90
Proliferin	0,133 ±0,0149	0,0762 ±0,0036	0,57
RAGE	0,3759 ±0,001	0,6757 ±0,0002	1,80
RANTES	0,0294 ±0,0034	0,0293 ±0,0052	1,00
RBP4	0,1829 ±0,0115	0,1665 ±0,0194	0,91
Resistin	1,4301 ±0,0311	1,4363 ±0,0413	1,00
SDF-1	0,4251 ±0,007	0,3366 ±0,0008	0,79
Serpin E1	0,8465 ±0,0028	1,2647 ±0,0187	1,49
Serpin F1	1,1474 ±0,0071	1,2118 ±0,0102	1,06
Thrombospondin-2	0,1793 ±0,0107	0,1929 ±0,0117	1,08
TIMP-1	0,5903 ±0,0115	0,5684 ±0,0172	0,96
TIMP-4	1,6214 ±0,0579	2,1735 ±0,0017	1,34
TNF-α	0,0169 ±0,0007	0,0191 ±0,002	1,13
VEGF-A	0,1287 ±0,0006	0,2093 ±0,0035	1,63
VEGF-B	0,0975 ±0,0191	0,1815 ±0,002	1,86

Values are fold-increase relative to positive internal controls. Values are averages of two measurements.

Legend: ADAMTS1: A disintegrin and metalloproteinase with thrombospondin motifs 1; AgRP: Agouti-related peptide; ANGPT-L3: angiopoietin-like 3; CXCL16: CXC chemokine ligand 16; Cyr61: cysteine rich protein 61; DLL4 deltalike protein 4; DPP-IV: dipeptidyl peptidase 4; EGF: epidermal growth factor; FGF: fibroblast growth factor; GM-CSF: granulocyte macrophage colony stimulating factor; HB-EGF: heparin binding EGF-like growth factor; HGF: hepatocyte growth factor; ICAM-1: intercellular adhesion molecule 1; IGF: insulin-like growth factor; IGFBP: insulin-like growth factor-binding protein; IL: interleukin; IP: inducible protein; KC: mouse homolog of human GRO; LIF: leukemia inhibitory factor; MCP-1: monocyte chemotactic protein 1; M-CSF: macrophage colony-stimulating factor; MIP: macrophage inflammatory protein; NOV: nephroblastoma overexpressed; Pref-1: preadipocyte factor 1; PD-ECGF platelet derived endothelial cell growth factor; PDGF: platelet derived growth factor; PlGF-2: placenta growth factor-2; RAGE: receptor for advanced glycation endproducts; RANTES: regulated upon activation normal T cell expressed and presumably secreted; RBP4: retinol binding protein 4; SDF-1: stromal cell-derived factor 1; TIMP-1: tissue inhibitor of metalloproteinase 1; TNF-α: tumour necrosis factor alpha; VEGF: vascular endothelial growth factor.

5

General Discussion

Adipose tissue (AT) releases multiple bioactive molecules and systemic factors, including growth factors and inflammatory, angiogenic or metabolic markers. Deregulated production and/or secretion of these adipokines, an hallmark of excess adiposity and AT dysfunction, contributes to the pathogenesis of obesity and its comorbid conditions and significantly influences tumour behavior.[62,64,70,177]

Moreover, obesity provides a chronic low grade inflammatory condition, further potentiated by the presence of adipose-released hormone cues and pro-inflammatory cytokines, which are strongly associated with cancer progression and tumour-associated macrophage accumulation. Macrophages release factors that paracrinally modulate tumour plasticity and the maintenance of stromal microenvironment.[143] In contrast, our *in vitro* results disclosed a direct effect of adipocytes on melanoma cells, without the influence of neither tumour-associated cell-mediated immunity nor systemic inflammation. Adipocyte-released factors play a role in increasing melanoma cell overall survival, by directly increasing melanoma cell proliferation and simultaneously diminishing programmed cell death. Exposure to *ex vivo* AT organ culture conditioned medium (CM) further resulted in increased motility, enhancing the capacity of melanocytes to migrate and spread. These findings were accompanied by a greater adhesion capacity, in particular to endothelial cells. Moreover, adipose CM minimized melanocytes anoikis, overcoming the apoptotic response to the absence of cell–matrix interactions and potentiated anchorage-independent proliferation, reinforcing the aggressive and metastatic potential of paracrinally adipocyte-stimulated melanocytes.

Visceral adiposity accumulation is accompanied by a systemic increase in oxidative stress, in part through low grade inflammation but also by increased generation of reactive oxygen species (ROS) and reactive nitrogen species (RNS).[56,70] Besides their damaging effects, ROS and pro-oxidants

are key mediators in the regulation and homeostasis of several signal transduction pathways in cancer cells.[150] Obesity-associated impaired antioxidant defences[55] and ROS produced from peritumoural adipose tissue exacerbate oxidative stress within tumour cells and might contribute to the carcinogenic process in obese patients. Nevertheless, our *in vitro* studies revealed that adipocyte CM growth promoting effects overcome the adipocyte-associated pro-oxidant environment, lessening the radiation therapy (RT)-induced damages. Cellular metabolic activity and antioxidant defences of irradiated melanocytes were improved, with enhanced antioxidant capacity and decreased oxidative stress, even with cumulative ionizing radiation doses. Activation of AKT-mediated proproliferative and anti-apoptotic stimuli supplant the adipocyte-derived ROS, enhancing melanoma cells antioxidant defences and endorsing adaptative resistance to the effects of ROS-generating treatment therapies. Thus, an environment rich in adipocyte-released factors protects melanocytes from radiation-induced oxidative stress and viability loss, circumventing the efficacy of RT treatments, contributing to melanomas radioresistance.

To successfully metastasise malignant cells must first escape from the primary cancer, shed into the vascular system where then they are carried around the body in the circulation, triggering a mechanism that is responsible for the majority of cancer-related deaths.[184] Tumour angiogenesis has a pivotal role to provide enough oxygen and nutrients to sustain the exacerbated cancer growth. However, tumour neovascularization also provides malignant cells an entry point to the vasculature to metastasise. Our *in vivo* results demonstrated that adiposity-enhanced melanoma growth is followed by a strong angiogenic response. Tumours develop more capillaries and their caliber expands, providing the growing malignant mass further access to blood flow to sustain its growth. In addition to angiogenesis, melanoma cells are capable of shifting towards an endothelial-like phenotype. Vasculogenic mimicry (VM) is a characteristic microcirculation pattern in melanomas, where tumour cell-lined vascular channels are capable of sustaining a parallel blood supply, with a viable blood flow between VM vascular spaces and endothelium-lined vasculature, not only further nourishing the tumour but also providing an alternative access to systemic circulation, thus enhancing metastasising likeliness.[249] Our results evidenced that upon exposure to adipocyte and AT CM melanoma cells rearranged, on 3D *in vitro* cultures, into characteristic VM vessel-like structures. However, in tumour-bearing high-fat diet (HFD) animals no significant increase in VM density was observed. Nevertheless, in the early stages of melanoma growth VM predominates and as the tumour mass develops these VM-channels are gradually replaced by endothelium-lined vessels.[209] In fact, HFD animals beared significantly larger tumours but, instead of a decreased VM density, a non significant increase in tumour-cell-lined vessels was observed, providing some evidence of *in vivo* obesity-enhanced VM.

The ability to enter circulation is not the only factor that limits distant metastasis. When in circulation malignant cells must properly adapt to survive in a completely different environment until they find a favourable niche where they can engraft and colonise for secondary tumour growth. Our

in vivo lung metastasis results disclosed an intriguing set of information. Despite HFD-induced expansion of tumour vasculature, raising the chances of melanoma cells detaching from the primary tumour and enter into circulation, lung-colonizing metastasis were significantly lower for HFD-fed animals than standard diet (SD) animals. In fact, obesity-associated changes in circulating factors and oxidative stress might render the vascular system an inhospitable environment for circulating melanoma cells, decreasing their metastatic potential, thus preventing secondary tumour growth. The decreased viability of circulating melanoma cells might be exerting a selective pressure on circulating melanoma cells, allowing only more resistant and aggressive melanoma cells to successfully metastasise, thus enhancing melanoma metastasis aggressiveness and treatment resistance.

We focused on growth factors, angiogenic cytokines and adipokines in our search for mechanisms of hight-fat dietary-enhanced melanoma progression. Molecular characterization of adipose-associated serum factors, as well as *in vitro* adipocytes CM, led us to highlight possible mechanisms by which adipose tissue promotes melanoma progression. Increasing levels of fibroblast growth factor (FGF)-2, FGF-21, hepatocyte growth factor (HGF), interleukin (IL)-10 and vascular endothelial growth factor (VEGF) were detected in both adipocytes secretome and obese animals serum. These

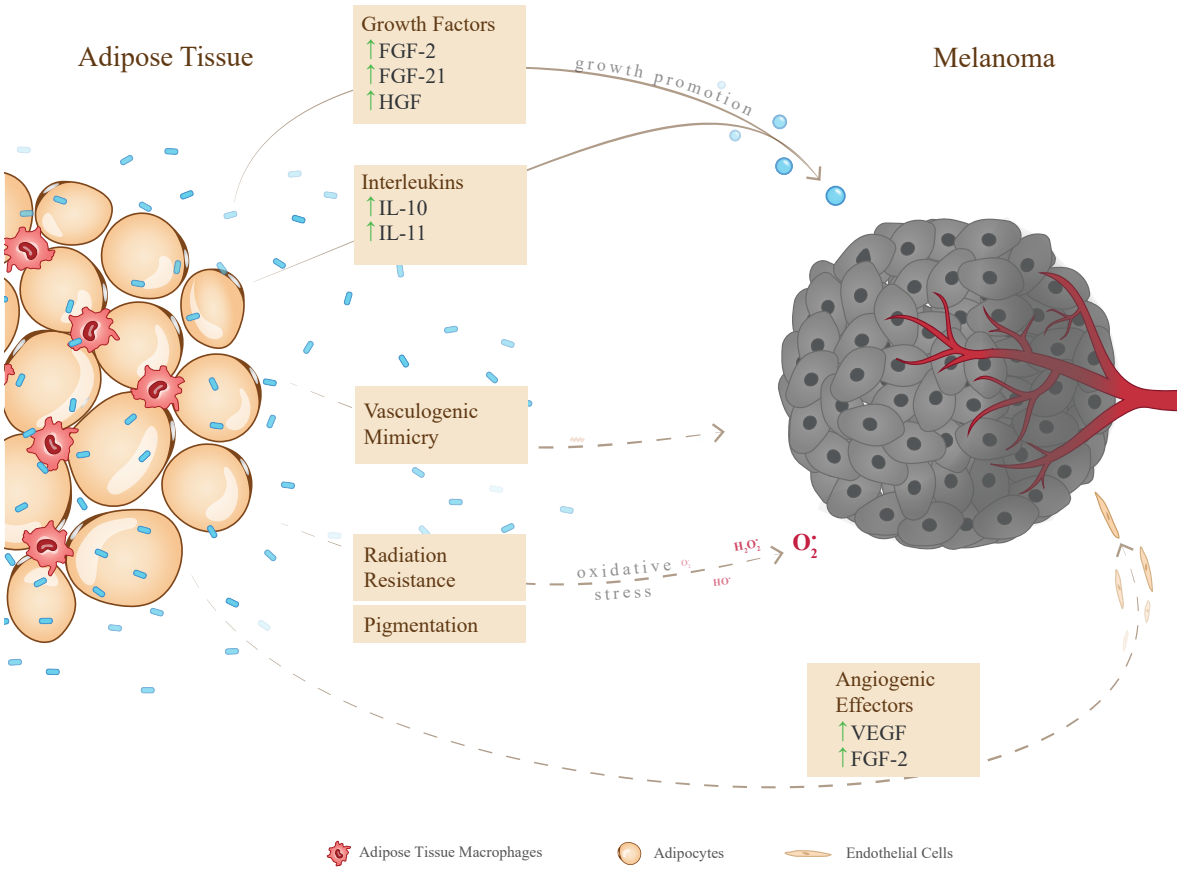

Figure 5.1: Possible new molecular players and mechanisms linking obesity and melanoma.

Legend: FGF: fibroblast growth factor; HGF: hepatocyte growth factor; IL: interleukin; VEGF: vascular endothelial growth factor.

molecular messengers allied to enhanced angiogenesis and VM have putative roles in melanoma etiology, prognosis and treatment resistance, representing novel prospective therapeutical targets in the obesity-melanoma rationale. Moreover, melanogenesis and melanin pigment play a role in melanoma etiology. Despite the relationship between melanin content and metastatic phenotype of melanoma still remains controversial, hyperpigmented melanomas are associated with significantly shorter disease-free survival [248] and the melanin content in melanoma metastases is a predictor of poor radiotherapy outcome, [23] rendering melanomas ionizing radiation resistant. Accordingly, the higher pigmented metastases found in the lungs of overweight animals might be composed of more resistant and aggressive melanoma cells, thus enhancing metastasis aggressiveness and treatment resistance. Figure 5.1 summarizes the main mechanistic links and molecular players tying obesity and melanoma that were disclosed by our findings. However, these mechanisms are not mutually exclusive, nor reject the involvement of other inherent biological systems in this malignant process. Most likely, the relationship between obesity-associated melanoma development is multifactorial and surely complex multi-system mechanisms synergetically co-exist.

According to the International Agency for Research on Cancer, the strength of the evidence of the association between body fatness and melanoma in human available studies is inadequate. [250] It is of uttermost importance that more fundamental and clinical studies are performed to acquire a more clear understanding of the obesity-melanoma relation. Nevertheless, our results add up to accumulating contemporary evidence and epidemiologic data and further strengthen the association between obesity and malignant melanoma progression. [63–65,74,145,160,207] Moreover, high adiposity is associated not only with cancer prevalence, but obesity and its co-morbidities also worsen disease progression, with a negative impact in prognosis and overall survival from the most common forms of cancer in obese patients. [61,62]

Clinical management and control of obesity, either by caloric restriction or with antiobesity pharmacologic treatments, appears an attractive target to arrest obesity-promoted tumour progression and improve the prognosis and survival of obese cancer patients. Our results disclosed a duality in the contribution of adiposity to melanoma progression and metastasis. Adipose-derived factors act as a two-edged sword: promoting subcutaneous primary tumour progression and vascularization, but simultaneously lessening distant metastases formation and secondary cancer growth. Furthermore, weight loss is a common feature among cancer patients and is often one of the first noticeable symptoms of the disease. Weight loss correlates with poorer median survival, emphasizing the prognostic importance of weight loss along cancer treatment. In fact, cancer patients with weight loss share poor prognosis, regardless of their pre-diagnostic body weight. [251] In the absence of solid clinical data, both normoponderal and overweight patients should be advised to maintain their weight and avoid abrupt weight variations along cancer treatment. Our findings also reinforce the need for the clinician to take into account whether the patient is normoponderal or overweight in treatment planning, as adiposity-associated different mechanisms of cancer pathogenesis might lead to

distinct outcomes. Nevertheless, enough evidence exists to endorse recommendations that both children and adults maintain an average weight for their height and ages for multiple health benefits, including decreasing their risk of malignant melanoma.

References

[1] Geller AC, Clapp RW, Sober AJ, Gonsalves L, Mueller L, Christiansen CL, *et al.* Melanoma epidemic: An analysis of six decades of data from the connecticut tumor registry. *J Clin Oncol* 2013; **31**(33):4172–4178.

[2] Tuong W, Cheng LS, Armstrong AW. Melanoma: Epidemiology, Diagnosis, Treatment, and Outcomes. *Dermatol Clin* 2012; **30**(1):113–124.

[3] Marks R. Epidemiology of melanoma. *Clin Exp Dermatol* 2000; **25**(6):459–63.

[4] Garbe C, Leiter U. Melanoma epidemiology and trends. *Clin Dermatol* 2009; **27**:3–9.

[5] Siegel RL, Miller KD, Jemal A. Cancer statistics, 2016. *CA Cancer J Clin* 2016; **66**(1):7–30.

[6] Greinert R, de Vries E, Erdmann F, Espina C, Auvinen A, Kesminiene A, *et al.* European Code against Cancer 4th Edition: Ultraviolet radiation and cancer. *Cancer Epidemiol* 2015; **39**:S75–S83.

[7] Ferlay J, Soerjomataram I, Dikshit R, Eser S, Mathers C, Rebelo M, *et al.* Cancer incidence and mortality worldwide: sources, methods and major patterns in GLOBOCAN 2012. *Int J cancer* 2015; **136**(5):E359–86.

[8] Erdei E, Torres SM. A new understanding in the epidemiology of melanoma. *Expert Rev Anticancer Ther* 2010; **10**(11):1811–23.

[9] Cichorek M, Wachulska M, Stasiewicz A, Tymińska A. Skin melanocytes: Biology and development. *Postep Dermatologii i Alergol* 2013; **30**(1):30–41.

[10] Haass NK, Smalley KSM, Li L, Herlyn M. Adhesion, migration and communication in melanocytes and melanoma. *Pigment Cell Res* 2005; **18**(3):150–9.

[11] Slominski A, Paus R, Schadendorf D. Melanocytes as "Sensory" and Regulatory Cells in the Epidermis. *J Theor Biol* 1993; **164**(1):103–120.

[12] Barnhill RL, Lugassy C, Taylor E, Zussman J. Cutaneous Melanoma. In Pathol. Melanocytic Nevi Melanoma (editors Barnhill RL, Piepkorn MW, Busam KJ), 331–487 (Springer Berlin Heidelberg, Berlin, Heidelberg, 2014).

[13] Bandarchi B, Ma L, Navab R, Seth A, Rasty G. From melanocyte to metastatic malignant melanoma. *Dermatol Res Pract* 2010; **2010**:1–8.

[14] Bittner M, Meltzer P, Chen Y, Jiang Y, Seftor E, Hendrix M, *et al.* Molecular classification of cutaneous malignant melanoma by gene expression profiling. *Nature* 2000; **406**(6795):536–540.

[15] Seftor Ea, Meltzer PS, Kirschmann Da, Pe'er J, Maniotis AJ, Trent JM, *et al.* Molecular determinants of human uveal melanoma invasion and metastasis. *Clin Exp Metastasis* 2002; **19**(3):233–46.

[16] Hendrix MJC, Seftor EA, Hess AR, Seftor REB. Vasculogenic mimicry and tumour-cell plasticity: lessons from melanoma. *Nat Rev Cancer* 2003; **3**(6):411–421.

[17] Caramel J, Papadogeorgakis E, Hill L, Browne G, Richard G, Wierinckx A, *et al.* A Switch in the Expression of Embryonic EMT-Inducers Drives the Development of Malignant Melanoma. *Cancer Cell* 2013; **24**(4):466–480.

[18] Brychtova S, Bezdekova M, Hirnak J, Sedlakova E, Tichy M, Brychta T. Stromal Microenvironment Alterations in Malignant Melanoma. In Res. Melanoma - A Glimpse into Curr. Dir. Futur. Trends (editor Murph M), chapter 16 (InTech, 2011).

[19] Conrad N, Jackson B, Goldberg L. Amelanotic lentigo maligna melanoma: a unique case presentation. *Dermatol Surg* 1999; **25**(5):408–11.

[20] Jimbow K, Lee SK, King MG, Hara H, Chen H, Dakour J, *et al.* Melanin pigments and melanosomal proteins as differentiation markers unique to normal and neoplastic melanocytes. *J Invest Dermatol* 1993; **100**(3):259S–268S.

[21] Jenkins NC, Grossman D. Role of melanin in melanocyte dysregulation of reactive oxygen species. *Biomed Res Int* 2013; **2013**(5):908797.

[22] Slominski RM, Zmijewski MA, Slominski AT. The role of melanin pigment in melanoma. *Exp Dermatol* 2015; **24**(4):258–9.

[23] Brożyna AA, Jóźwicki W, Roszkowski K, Filipiak J, Slominski AT. Melanin content in melanoma metastases affects the outcome of radiotherapy. *Oncotarget* 2016; **7**(14):17844–53.

[24] Ribatti D, Nico B, Floris C, Mangieri D, Piras F, Ennas MG, *et al.* Microvascular density, vascular endothelial growth factor immunoreactivity in tumor cells, vessel diameter and intussusceptive microvascular growth in primary melanoma. *Oncol Rep* 2005; **14**(1):81–4.

[25] Maniotis AJ, Folberg R, Hess A, Seftor EA, Gardner LM, Pe'er J, *et al.* Vascular channel formation by human melanoma cells in vivo and in vitro: vasculogenic mimicry. *Am J Pathol* 1999; **155**(3):739–752.

[26] Ribatti D, Nico B, Cimpean AM, Raica M, Crivellato E, Ruggieri S, *et al.* B16-F10 melanoma cells contribute to the new formation of blood vessels in the chick embryo chorioallantoic membrane through vasculogenic mimicry. *Clin Exp Med* 2013; **13**(2):143–147.

[27] Thies A, Mangold U, Moll I, Schumacher U. PAS-positive loops and networks as a prognostic indicator in cutaneous malignant melanoma. *J Pathol* 2001; **195**(5):537–542.

[28] Cao Z, Bao M, Miele L, Sarkar FH, Wang Z, Zhou Q. Tumour vasculogenic mimicry is associated with poor prognosis of human cancer patients: a systemic review and meta-analysis. *Eur J Cancer* 2013; **49**(18):3914–23.

[29] Ji Z, Flaherty KT, Tsao H. Targeting the RAS pathway in melanoma. *Trends Mol Med* 2012; **18**(1):27–35.

[30] Kim EK, Choi EJ. Pathological roles of MAPK signaling pathways in human diseases. *Biochim Biophys Acta* 2010; **1802**(4):396–405.

[31] Daniotti M, Oggionni M, Ranzani T, Vallacchi V, Campi V, Di Stasi D, *et al.* BRAF alterations are associated with complex mutational profiles in malignant melanoma. *Oncogene* 2004; **23**(35):5968–77.

[32] Flaherty KT, Hodi FS, Fisher DE. From genes to drugs: targeted strategies for melanoma. *Nat Rev Cancer* 2012; **12**(5):349–361.

[33] Vara JÁF, Casado E, de Castro J, Cejas P, Belda-Iniesta C, González-Barón M. PI3K/Akt signalling pathway and cancer. *Cancer Treat Rev* 2004; **30**(2):193–204.

[34] Wu H, Goel V, Haluska FG. PTEN signaling pathways in melanoma. *Oncogene* 2003; **22**(20):3113–22.

[35] Davies Ma. The role of the PI3K-AKT pathway in melanoma. *Cancer J* 2012; **18**(2):142–7.

[36] Shtivelman E, Davies MQa, Hwu P, Yang J, Lotem M, Oren M, *et al.* Pathways and therapeutic targets in melanoma. *Oncotarget* 2014; **5**(7):1701–52.

[37] Davies MA, Stemke-Hale K, Tellez C, Calderone TL, Deng W, Prieto VG, *et al.* A novel AKT3 mutation in melanoma tumours and cell lines. *Br J Cancer* 2008; **99**(8):1265–8.

[38] Stahl JM, Sharma A, Cheung M, Zimmerman M, Cheng JQ, Bosenberg MW, *et al.* Deregulated Akt3 activity promotes development of malignant melanoma. *Cancer Res* 2004; **64**(19):7002–7010.

[39] Mehnert JM, Kluger HM. Driver mutations in melanoma: Lessons learned from bench-to-bedside studies. *Curr Oncol Rep* 2012; **14**(5):449–457.

[40] Johnson DB, Peng C, Puzanov I. Management of 'pan-negative' melanoma: current and emerging strategies. *Melanoma Manag* 2014; **1**(2):87–90.

[41] Testori A, Rutkowski P, Marsden J, Bastholt L, Chiarion-Sileni V, Hauschild A, *et al.* Surgery and radiotherapy in the treatment of cutaneous melanoma. *Ann Oncol* 2009; **20**(suppl 6):vi22–vi29.

[42] Dickson PV, Gershenwald JE. Staging and prognosis of cutaneous melanoma. *Surg Oncol Clin N Am* 2011; **20**(1):1–17.

[43] Middleton MR, Grob JJ, Aaronson N, Fierlbeck G, Tilgen W, Seiter S, *et al.* Randomized phase III study of temozolomide versus dacarbazine in the treatment of patients with advanced metastatic malignant melanoma. *J Clin Oncol* 2000; **18**(1):158–66.

[44] Niezgoda A, Niezgoda P, Czajkowski R. Novel Approaches to Treatment of Advanced Melanoma: A Review on Targeted Therapy and Immunotherapy. *Biomed Res Int* 2015; **2015**:1–16.

[45] Buchbinder EI, Desai A. CTLA-4 and PD-1 Pathways: Similarities, Differences, and Implications of Their Inhibition. *Am J Clin Oncol* 2016; **39**(1):98–106.

[46] Restifo NP, Smyth MJ, Snyder A. Acquired resistance to immunotherapy and future challenges. *Nat Rev Cancer* 2016; **16**(2):121–126.

[47] Forschner A, Heinrich V, Pflugfelder A, Meier F, Garbe C. The role of radiotherapy in the overall treatment of melanoma. *Clin Dermatol* 2013; **31**(3):282–289.

[48] Khan M, Almasan. Future of radiation therapy for malignant melanoma in an era of newer, more effective biological agents. *Onco Targets Ther* 2011; **4**:137.

[49] Diehn M, Clarke MF. Cancer stem cells and radiotherapy: New insights into tumor radioresistance. *J Natl Cancer Inst* 2006; **98**(24):1755–1757.

[50] Olivier KR, Schild SE, Morris CG, Brown PO, Markovic SN. A higher radiotherapy dose is associated with more durable palliation and longer survival in patients with metastatic melanoma. *Cancer* 2007; **110**(August):1791–1795.

[51] Karastergiou K, Mohamed-Ali V. The autocrine and paracrine roles of adipokines. *Mol Cell Endocrinol* 2010; **318**(1-2):69–78.

[52] Monteiro R. Chronic Inflammation in the Metabolic Syndrome: Emphasis on Adipose Tissue. In Oxidative Stress. Inflamm. Angiogenes. Metab. Syndr. (editors Soares R, Costa C) (Springer Netherlands, Dordrecht, 2009).

[53] Haffner S, Taegtmeyer H. Epidemic obesity and the metabolic syndrome. *Circulation* 2003; **108**:1541–1545.

[54] Jung UJ, Choi MS. Obesity and its metabolic complications: the role of adipokines and the relationship between obesity, inflammation, insulin resistance, dyslipidemia and nonalcoholic fatty liver disease. *Int J Mol Sci* 2014; **15**(4):6184–223.

[55] Matsuda M, Shimomura I. Increased oxidative stress in obesity: Implications for metabolic syndrome, diabetes, hypertension, dyslipidemia, atherosclerosis, and cancer. *Obes Res Clin Pract* 2013; **7**(5):1–12.

[56] Furukawa S, Fujita T, Shimabukuro M, Iwaki M, Yamada Y, Nakajima Y, *et al.* Increased oxidative stress in obesity and its impact on metabolic syndrome. *J Clin Invest* 2004; **114**(12):1752–1761.

[57] Xu H, Barnes GT, Yang Q, Tan G, Yang D, Chou CJ, *et al.* Chronic inflammation in fat plays a crucial role in the development of obesity-related insulin resistance. *J Clin Invest* 2003; **112**(12):1821–1830.

[58] Gregor MF, Hotamisligil GS. Inflammatory mechanisms in obesity. *Annu Rev Immunol* 2011; **29**:415–45.

[59] Calle EE, Rodriguez C, Walker-Thurmond K, Thun MJ. Overweight, obesity, and mortality from cancer in a prospectively studied cohort of U.S. adults. *N Engl J Med* 2003; **348**(17):1625–38.

[60] Mendonça FM, de Sousa FR, Barbosa AL, Martins SC, Araújo RL, Soares R, *et al.* Metabolic syndrome and risk of cancer: Which link? *Metabolism* 2015; **64**(2):182–189.

[61] Parekh N, Chandran U, Bandera EV. Obesity in Cancer Survival. *Annu Rev Nutr* 2012; **32**:311–342.

[62] Gallagher EJ, LeRoith D. Obesity and Diabetes: The Increased Risk of Cancer and Cancer-Related Mortality. *Physiol Rev* 2015; **95**(3):727–748.

[63] Renehan AG, Tyson M, Egger M, Heller RF, Zwahlen M. Body-mass index and incidence of cancer: a systematic review and meta-analysis of prospective observational studies. *Lancet* 2008; **371**(9612):569–78.

[64] Roberts DL, Dive C, Renehan AG. Biological mechanisms linking obesity and cancer risk: new perspectives. *Annu Rev Med* 2010; **61**:301–316.

[65] Sergentanis TN, Antoniadis AG, Gogas HJ, Antonopoulos CN, Adami HO, Ekbom A, *et al.* Obesity and risk of malignant melanoma: A meta-analysis of cohort and case-control studies. *Eur J Cancer* 2013; **49**:642–657.

[66] Præstegaard C, Kjær SK, Christensen J, Tjønneland A, Halkjær J, Jensen A. Obesity and risks for malignant melanoma and non-melanoma skin cancer: results from a large Danish prospective cohort study. *J Invest Dermatol* 2015; **135**(3):901–4.

[67] Baranova A, Collantes R, Gowder SJ, Elariny H, Schlauch K, Younoszai A, *et al.* Obesity-related differential gene expression in the visceral adipose tissue. *Obes Surg* 2005; **15**(6):758–65.

[68] van Kruijsdijk RCM, van der Wall E, Visseren FLJ. Obesity and cancer: the role of dysfunctional adipose tissue. *Cancer Epidemiol Biomarkers Prev* 2009; **18**(10):2569–78.

[69] Wang P, Mariman E, Keijer J, Bouwman F, Noben JP, Robben J, *et al.* Profiling of the secreted proteins during 3T3-L1 adipocyte differentiation leads to the identification of novel adipokines. *Cell Mol Life Sci* 2004; **61**(18):2405–2417.

[70] Blüher M. Adipose tissue dysfunction contributes to obesity related metabolic diseases. *Best Pract Res Clin Endocrinol Metab* 2013; **27**(2):163–177.

[71] Antoniadis AG, Petridou ET, Antonopoulos CN, Dessypris N, Panagopoulou P, Chamberland JP, *et al.* Insulin resistance in relation to melanoma risk. *Melanoma Res* 2011; **21**(6):541–6.

[72] Sevim DG, Kiratli H. Serum adiponectin, insulin resistance, and uveal melanoma. *Melanoma Res* 2016; **26**(2):164–172.

[73] Oba J, Wei W, Gershenwald JE, Johnson MM, Wyatt CM, Ellerhorst JA, *et al.* Elevated Serum Leptin Levels are Associated With an Increased Risk of Sentinel Lymph Node Metastasis in Cutaneous Melanoma. *Medicine (Baltimore)* 2016; **95**(11):1–7.

[74] Malvi P, Chaube B, Pandey V, Vijayakumar MV, Boreddy PR, Mohammad N, *et al.* Obesity induced rapid melanoma progression is reversed by orlistat treatment and dietary intervention: role of adipokines. *Mol Oncol* 2015; **9**(3):689–703.

[75] Mantzoros CS, Trakatelli M, Gogas H, Dessypris N, Stratigos A, Chrousos GP, *et al.* Circulating adiponectin levels in relation to melanoma: A case-control study. *Eur J Cancer* 2007; **43**(9):1430–1436.

[76] Rodeck U, Melber K, Kath R, Menssen HD, Varello M, Atkinson B, *et al.* Constitutive expression of multiple growth factor genes by melanoma cells but not normal melanocytes. *J Invest Dermatol* 1991; **97**(1):20–26.

[77] Brandon EL, Gu JW, Cantwell L, He Z, Wallace G, Hall JE. Obesity promotes melanoma tumor growth: Role of leptin. *Cancer Biol Ther* 2009; **8**(19):1871–1879.

[78] Amjadi F, Mehdipoor R, Zarkesh-Esfahani H, Javanmard SH. Leptin serves as angiogenic/mitogenic factor in melanoma tumor growth. *Adv Biomed Res* 2016; **5**:127.

[79] Sun Y, Lodish HF. Adiponectin deficiency promotes tumor growth in mice by reducing macrophage infiltration. *PLoS One* 2010; **5**(8):e11987.

[80] Chen J, Chi M, Chen C, Zhang XD. Obesity and melanoma: exploring molecular links. *J Cell Biochem* 2013; **114**(9):1955–1961.

[81] Garay T, Molnár E, Juhász É, László V, Barbai T, Dobos J, *et al.* Sensitivity of Melanoma Cells to EGFR and FGFR Activation but Not Inhibition is Influenced by Oncogenic BRAF and NRAS Mutations. *Pathol Oncol Res* 2015; **21**(4):957–68.

[82] Li FZ, Dhillon AS, Anderson RL, McArthur G, Ferrao PT. Phenotype switching in melanoma: implications for progression and therapy. *Front Oncol* 2015; **5**:31.

[83] Dutcher JP. Angiogenesis and melanoma. *Curr Oncol Rep* 2001; **3**(4):353–8.

[84] Danielsen T, Rofstad EK. VEGF, bFGF and EGF in the angiogenesis of human melanoma xenografts. *Int J cancer* 1998; **76**(6):836–41.

[85] Pirraco A, Coelho P, Rocha A, Costa R, Vasques L, Soares R. Imatinib targets PDGF signaling in melanoma and host smooth muscle neighboring cells. *J Cell Biochem* 2010; **111**(2):433–41.

[86] Easty DJ, Gray SG, O'Byrne KJ, O'Donnell D, Bennett DC. Receptor tyrosine kinases and their activation in melanoma. *Pigment Cell Melanoma Res* 2011; **24**(3):446–61.

[87] Rosero RA, Villares GJ, Bar-Eli M. Protease-Activated Receptors and other G-Protein-Coupled Receptors: the Melanoma Connection. *Front Genet* 2016; **7**:112.

[88] Chapman PB. Mechanisms of resistance to RAF inhibition in melanomas harboring a BRAF mutation. *Am Soc Clin Oncol Educ Book* 2013;80–82.

[89] Yeh AH, Bohula EA, Macaulay VM. Human melanoma cells expressing V600E B-RAF are susceptible to IGF1R targeting by small interfering RNAs. *Oncogene* 2006; **25**(50):6574–81.

[90] Silverman K, Lund D, Zetter B. Angiogenic activity of adipose tissue. *Biochem ...* 1988; **153**(1):347–352.

[91] Cao Y. Angiogenesis modulates adipogenesis and obesity 2007.

[92] Cao Y. Adipose tissuea angiogenesis as a therapiutic target for obesity and metabolic diseases. *Nat Rev Drug Discov* 2010; **9**(FEBrUAry):107–115.

[93] Han J, Lee JE, Jin J, Lim JS, Oh N, Kim K, *et al.* The spatiotemporal development of adipose tissue. *Development* 2011; **138**(22):5027–5037.

[94] Lemoine AY, Ledoux S, Larger E. Adipose tissue angiogenesis in obesity. *Thromb Haemost* 2013; **110**(4):661–669.

[95] Rubina K, Kalinina N, Efimenko A, Lopatina T, Melikhova V, Tsokolaeva Z, *et al.* Adipose Stromal Cells Stimulate Angiogenesis via Promoting Progenitor Cell Differentiation, Secretion of Angiogenic Factors, and Enhancing Vessel Maturation. *Tissue Eng Part A* 2009; **15**(8):2039–2050.

[96] Bouloumié A, Sengenès C, Portolan G, Galitzky J, Lafontan M. Adipocyte produces matrix metalloproteinases 2 and 9: involvement in adipose differentiation. *Diabetes* 2001; **50**(9):2080–6.

[97] Mantovani A, Sica A. Macrophages, innate immunity and cancer: balance, tolerance, and diversity. *Curr Opin Immunol* 2010; **22**(2):231–7.

[98] Meierjohann S. Hypoxia-Independent Drivers of Melanoma Angiogenesis. *Front Oncol* 2015; **5**:102.

[99] Rofstad EK, Mathiesen B. Metastasis in melanoma xenografts is associated with tumor microvascular density rather than extent of hypoxia. *Neoplasia* 2010; **12**(11):889–98.

[100] Hosogai N, Fukuhara A, Oshima K, Miyata Y, Tanaka S, Segawa K, *et al.* Adipose tissue hypoxia in obesity and its impact on adipocytokine dysregulation. *Diabetes* 2007; **56**(4):901–911.

[101] Rausch ME, Weisberg S, Vardhana P, Tortoriello DV. Obesity in C57BL/6J mice is characterized by adipose tissue hypoxia and cytotoxic T-cell infiltration. *Int J Obes (Lond)* 2008; **32**(3):451–463.

[102] Regazzetti C, Peraldi P, Grémeaux T, Najem-Lendom R, Ben-Sahra I, Cormont M, *et al.* Hypoxia decreases insulin signaling pathways in adipocytes. *Diabetes* 2009; **58**(1):95–103.

[103] Ye J, Gao Z, Yin J, He Q. Hypoxia is a potential risk factor for chronic inflammation and adiponectin reduction in adipose tissue of ob/ob and dietary obese mice. *Am J Physiol Endocrinol Metab* 2007; **293**(4):E1118–E1128.

[104] Yin J, Gao Z, He Q, Zhou D, Guo Z, Ye J. Role of hypoxia in obesity-induced disorders of glucose and lipid metabolism in adipose tissue. *Am J Physiol Endocrinol Metab* 2009; **296**(2):E333–E342.

[105] Loboda A, Jozkowicz A, Dulak J. HIF-1 and HIF-2 transcription factors–similar but not identical. *Mol Cells* 2010; **29**(5):435–442.

[106] Wang B, Wood IS, Trayhurn P. Dysregulation of the expression and secretion of inflammation-related adipokines by hypoxia in human adipocytes. *Pflugers Arch Eur J Physiol* 2007; **455**(3):479–492.

[107] Halberg N, Khan T, Trujillo ME, Wernstedt-Asterholm I, Attie AD, Sherwani S, *et al.* Hypoxia-inducible factor 1alpha induces fibrosis and insulin resistance in white adipose tissue. *Mol Cell Biol* 2009; **29**(16):4467–4483.

[108] Trayhurn P. Hypoxia and adipocyte physiology: implications for adipose tissue dysfunction in obesity. *Annu Rev Nutr* 2014; **34**(April):207–36.

[109] Hashimoto T, Shibasaki F. Hypoxia-Inducible Factor as an Angiogenic Master Switch. *Front Pediatr* 2015; **3**(April):1–15.

[110] He Q, Gao Z, Yin J, Zhang J, Yun Z, Ye J. Regulation of HIF-1{alpha} activity in adipose tissue by obesity-associated factors: adipogenesis, insulin, and hypoxia. *Am J Physiol Endocrinol Metab* 2011; **300**(5):E877–E885.

[111] Zhang X, Lam KSL, Ye H, Chung SK, Zhou M, Wang Y, *et al.* Adipose tissue-specific inhibition of hypoxia-inducible factor 1*α* induces obesity and glucose intolerance by impeding energy expenditure in mice. *J Biol Chem* 2010; **285**(43):32869–32877.

[112] Cullberg KB, Christiansen T, Paulsen SK, Bruun JM, Pedersen SB, Richelsen B. Effect of weight loss and exercise on angiogenic factors in the circulation and in adipose tissue in obese subjects. *Obesity* 2013; **21**(3):454–460.

[113] Silha JV, Krsek M, Sucharda P, Murphy LJ. Angiogenic factors are elevated in overweight and obese individuals. *Int J Obes (Lond)* 2005; **29**(11):1308–1314.

[114] Fusaru AM, Pisoschi CG, Bold A, Taisescu C, St□nescu R, Hîncu M, *et al.* Hypoxia induced VEGF synthesis in visceral adipose depots of obese diabetic patients. *Rom J Morphol Embryol* 2012; **53**(4):903–909.

[115] Bedogni B, Welford SM, Cassarino DS, Nickoloff BJ, Giaccia AJ, Powell MB. The hypoxic microenvironment of the skin contributes to Akt-mediated melanocyte transformation. *Cancer Cell* 2005; **8**(6):443–54.

[116] Bedogni B, Welford SM, Kwan AC, Ranger-Moore J, Saboda K, Powell MB. Inhibition of phosphatidylinositol-3-kinase and mitogen-activated protein kinase kinase 1/2 prevents melanoma development and promotes melanoma regression in the transgenic TPRas mouse model. *Mol Cancer Ther* 2006; **5**(12):3071–7.

[117] Huber R, Meier B, Otsuka A, Fenini G, Satoh T, Gehrke S, *et al.* Tumour hypoxia promotes melanoma growth and metastasis via High Mobility Group Box-1 and M2-like macrophages. *Sci Rep* 2016; **6**(July 2015):29914.

[118] Pucciarelli D, Lengger N, Takáčová M, Csaderova L, Bartosova M, Breiteneder H, *et al.* Hypoxia increases the heterogeneity of melanoma cell populations and affects the response to vemurafenib. *Mol Med Rep* 2016; **13**(4):3281–8.

[119] Sun B, Zhang D, Zhang S, Zhang W, Guo H, Zhao X. Hypoxia influences vasculogenic mimicry channel formation and tumor invasion-related protein expression in melanoma. *Cancer Lett* 2007; **249**(2):188–97.

[120] Chen Z, Zhang T, Wu B, Zhang X. Insights into the therapeutic potential of hypoxia-inducible factor-1*α* small interfering RNA in malignant melanoma delivered via folate-decorated cationic liposomes. *Int J Nanomedicine* 2016; **11**:991–1002.

[121] Pasarica M, Sereda O, Redman L, Albarado D, Hymel D, Roan L, *et al.* Reduced Adipose Tissue Oxygenation in Human Obesity. *Diabetes* 2009; **58**(3):718.

[122] Goossens GH, Bizzarri A, Venteclef N, Essers Y, Cleutjens JP, Konings E, *et al.* Increased adipose tissue oxygen tension in obese compared with lean men is accompanied by insulin resistance, impaired adipose tissue capillarization, and inflammation. *Circulation* 2011; **124**(1):67–76.

[123] Hodson L, Humphreys SM, Karpe F, Frayn KN. Metabolic signatures of human adipose tissue hypoxia in obesity. *Diabetes* 2013; **62**(5):1417–1425.

[124] Kumar SM, Yu H, Edwards R, Chen L, Kazianis S, Brafford P, *et al.* Mutant V600E BRAF Increases Hypoxia Inducible Factor-1 Expression in Melanoma. *Cancer Res* 2007; **67**(7):3177–3184.

[125] Li YM, Zhou BP, Deng J, Pan Y, Hay N, Hung MC. A hypoxia-independent hypoxia-inducible factor-1 activation pathway induced by phosphatidylinositol-3 kinase/Akt in HER2 overexpressing cells. *Cancer Res* 2005; **65**(8):3257–63.

[126] Madonna G, Ullman CD, Gentilcore G, Palmieri G, Ascierto PA. NF-*κ*B as potential target in the treatment of melanoma. *J Transl Med* 2012; **10**:53.

[127] Meierjohann S. Oxidative stress in melanocyte senescence and melanoma transformation. *Eur J Cell Biol* 2014; **93**(1-2):36–41.

[128] Liu YC, Zou XB, Chai YF, Yao YM. Macrophage polarization in inflammatory diseases. *Int J Biol Sci* 2014; **10**(5):520–9.

[129] Weisberg SP, McCann D, Desai M, Rosenbaum M, Leibel RL, Ferrante AW. Obesity is associated with macrophage accumulation in adipose tissue. *J Clin Invest* 2003; **112**(12):1796–1808.

[130] Mills CD. M1 and M2 Macrophages: Oracles of Health and Disease. *Crit Rev Immunol* 2012; **32**(6):463–88.

[131] Lumeng CN, Bodzin JL, Saltiel AR. Obesity induces a phenotypic switch in adipose tissue macrophage polarization. *J Clin Invest* 2007; **117**(1):175–184.

[132] Strissel KJ, DeFuria J, Shaul ME, Bennett G, Greenberg AS, Obin MS. T-cell recruitment and Th1 polarization in adipose tissue during diet-induced obesity in C57BL/6 mice. *Obesity (Silver Spring)* 2010; **18**(10):1918–1925.

[133] Lamagna C, Aurrand-Lions M, Imhof Ba. Dual role of macrophages in tumor growth and angiogenesis. *J Leukoc Biol* 2006; **80**(4):705–713.

[134] Jetten N, Verbruggen S, Gijbels MJ, Post MJ, De Winther MPJ, Donners MMPC. Anti-inflammatory M2, but not pro-inflammatory M1 macrophages promote angiogenesis in vivo. *Angiogenesis* 2014; **17**(1):109–118.

[135] Chanmee T, Ontong P, Konno K, Itano N. Tumor-associated macrophages as major players in the tumor microenvironment. *Cancers (Basel)* 2014; **6**(3):1670–90.

[136] Wu X, Takekoshi T, Sullivan A, Hwang ST. Inflammation and tumor microenvironment in lymph node metastasis. *Cancers (Basel)* 2011; **3**(1):927–44.

[137] Fortes C, Mastroeni S, Mannooranparampil TJ, Passarelli F, Zappalà A, Annessi G, *et al.* Tumor-infiltrating lymphocytes predict cutaneous melanoma survival. *Melanoma Res* 2015; **25**(4):306–11.

[138] Lázár-Molnár E, Hegyesi H, Tóth S, Falus A. Autocrine and Paracrine Regulation By Cytokines and Growth Factors in Melanoma. *Cytokine* 2000; **12**(6):547–554.

[139] Hensley C, Spitzler S, McAlpine BE, Lynn M, Ansel JC, Solomon AR, *et al.* In vivo human melanoma cytokine production: inverse correlation of GM-CSF production with tumor depth. *Exp Dermatol* 1998; **7**(6):335–41.

[140] Hussein MR. Tumour-associated macrophages and melanoma tumourigenesis: integrating the complexity. *Int J Exp Pathol* 2006; **87**(3):163–76.

[141] Tham M, Tan KW, Keeble J, Wang X, Hubert S, Barron L, *et al.* Melanoma-initiating cells exploit M2 macrophage TGFβ and arginase pathway for survival and proliferation. *Oncotarget* 2014; **5**(23):12027–42.

[142] Tjin EPM, Krebbers G, Meijlink KJ, van de Kasteele W, Rosenberg EH, Sanders J, *et al.* Immune-escape markers in relation to clinical outcome of advanced melanoma patients following immunotherapy. *Cancer Immunol Res* 2014; **2**(6):538–46.

[143] Mayi TH, Daoudi M, Derudas B, Gross B, Bories G, Wouters K, *et al.* Human adipose tissue macrophages display activation of cancer-related pathways. *J Biol Chem* 2012; **287**(26):21904–21913.

[144] Wagner M, Bjerkvig R, Wiig H, Melero-Martin JM, Lin RZZ, Klagsbrun M, *et al.* Inflamed tumor-associated adipose tissue is a depot for macrophages that stimulate tumor growth and angiogenesis. *Angiogenesis* 2012; **15**(3):481–495.

[145] Jung JI, Cho HJ, Jung YJ, Kwon SHH, Her S, Choi SS, *et al.* High-fat diet-induced obesity increases lymphangiogenesis and lymph node metastasis in the B16F10 melanoma allograft model: Roles of adipocytes and M2-macrophages. *Int J Cancer* 2015; **136**(2):258–270.

[146] Fried L, Arbiser JL. The reactive oxygen-driven tumor: relevance to melanoma. *Pigment Cell Melanoma Res* 2008; **21**(2):117–22.

[147] Fruehauf JP, Trapp V. Reactive oxygen species: an Achilles' heel of melanoma? *Expert Rev Anticancer Ther* 2008; **8**(11):1751–1757.

[148] Ziech D, Franco R, Pappa A, Panayiotidis MI. Reactive Oxygen Species (ROS)––Induced genetic and epigenetic alterations in human carcinogenesis. *Mutat Res Mol Mech Mutagen* 2011; **711**(1-2):167–173.

[149] Meyskens FL, Buckmeier JA, McNulty SE, Tohidian NB. Activation of nuclear factor-kappa B in human metastatic melanomacells and the effect of oxidative stress. *Clin Cancer Res* 1999; **5**(5):1197–202.

[150] Schieber M, Chandel NS. ROS Function in Redox Signaling and Oxidative Stress. *Curr Biol* 2014; **24**(10):R453–R462.

[151] Hambright HG, Meng P, Kumar AP, Ghosh R. Inhibition of PI3K/AKT/mTOR axis disrupts oxidative stress-mediated survival of melanoma cells. *Oncotarget* 2015; **6**(9):7195–208.

[152] Calvani M, Comito G, Giannoni E, Chiarugi P. Time-dependent stabilization of hypoxia inducible factor-1*a* by different intracellular sources of reactive oxygen species. *PLoS One* 2012; **7**(10):e38388.

[153] Rouaud F, Romero-Perez M, Wang H, Lobysheva I, Ramassamy B, Henry E, *et al.* Regulation of NADPH-dependent Nitric Oxide and reactive oxygen species signalling in endothelial and melanoma cells by a photoactive NADPH analogue. *Oncotarget* 2014; **5**(21):10650–64.

[154] Schaafhausen MK, Yang WJ, Centanin L, Wittbrodt J, Bosserhoff A, Fischer A, *et al.* Tumor angiogenesis is caused by single melanoma cells in a manner dependent on reactive oxygen species and NF-κB. *J Cell Sci* 2013; **126**(Pt 17):3862–72.

[155] Vartanian A, Baryshnikov AY. Crosstalk between apoptosis and antioxidants in melanoma vasculogenic mimicry. *Adv Exp Med Biol* 2007; **601**:145–53.

[156] Bustamante J, Bredeston L, Malanga G, Mordoh J. Role of melanin as a scavenger of active oxygen species. *Pigment Cell Res* 1993; **6**(5):348–53.

[157] Denat L, Kadekaro AL, Marrot L, Leachman SA, Abdel-Malek ZA. Melanocytes as instigators and victims of oxidative stress. *J Invest Dermatol* 2014; **134**(6):1512–8.

[158] Menendez JA, Lupu R. Fatty acid synthase and the lipogenic phenotype in cancer pathogenesis. *Nat Rev Cancer* 2007; **7**(10):763–777.

[159] Kwan HY, Fu X, Liu B, Chao X, Chan CL, Cao H, *et al.* Subcutaneous adipocytes promote melanoma cell growth by activating the Akt signaling pathway: Role of palmitic acid. *J Biol Chem* 2014; **289**(44):30525–30537.

[160] Pandey V, Vijayakumar MV, Ajay AK, Malvi P, Bhat MK. Diet-induced obesity increases melanoma progression: involvement of Cav-1 and FASN. *Int J Cancer* 2012; **130**(3):497–508.

[161] Nomura DK, Long JZ, Niessen S, Hoover HS, Ng SW, Cravatt BF. Monoacylglycerol lipase regulates a fatty acid network that promotes cancer pathogenesis. *Cell* 2010; **140**(1):49–61.

[162] Seguin F, Carvalho MA, Bastos DC, Agostini M, Zecchin KG, Alvarez-Flores MP, *et al.* The fatty acid synthase inhibitor orlistat reduces experimental metastases and angiogenesis in B16-F10 melanomas. *Br J Cancer* 2012; **107**(6):977–87.

[163] Rubenstein AH. Obesity: a modern epidemic. *Trans Am Clin Climatol Assoc* 2005; **116**:103–111.

[164] Berghöfer A, Pischon T, Reinhold T, Apovian CM, Sharma AM, Willich SN. Obesity prevalence from a European perspective: a systematic review. *BMC Public Health* 2008; **8**:200.

[165] Taubes G. Unraveling the Obesity-Cancer Connection. *Science (80-)* 2012; **335**:28–32.

[166] Vucenik I, Stains JP. Obesity and cancer risk: Evidence, mechanisms, and recommendations. *Ann N Y Acad Sci* 2012; **1271**:37–43.

[167] Dennis LK, Lowe JB, Lynch CF, Alavanja MCR. Cutaneous melanoma and obesity in the Agricultural Health Study. *Ann Epidemiol* 2008; **18**(3):214–21.

[168] Morpurgo G, Fioretti B, Catacuzzeno L. The increased incidence of malignant melanoma in obese individuals is due to impaired melanogenesis and melanocyte DNA repair. *Med Hypotheses* 2012; **78**(4):533–5.

[169] Nagel G, Bjørge T, Stocks T, Manjer J, Hallmans G, Edlinger M, *et al.* Metabolic risk factors and skin cancer in the Metabolic Syndrome and Cancer Project (Me-Can). *Br J Dermatol* 2012; **167**(1):59–67.

[170] Friedl P, Alexander S. Cancer invasion and the microenvironment: Plasticity and reciprocity. *Cell* 2011; **147**(5):992–1009.

[171] Humphries M. Cell adhesion assays. *Mol Biotechnol* 2001; **18**:57–61.

[172] Foty R. A simple hanging drop cell culture protocol for generation of 3D spheroids. *J Vis Exp* 2011;(51):2720.

[173] Green H, Kehinde O. An established preadipose cell line and its differentiation in culture. II. Factors affecting the adipose conversion. *Cell* 1975; **5**(1):19–27.

[174] Poulos SP, Dodson MV, Hausman GJ. Cell line models for differentiation: preadipocytes and adipocytes. *Exp Biol Med (Maywood)* 2010; **235**(10):1185–1193.

[175] Chiang AC, Massagué J. Molecular basis of metastasis. *N Engl J Med* 2008; **359**(26):2814–2823.

[176] Chung HJ, Mahalingam M. Angiogenesis, vasculogenic mimicry and vascular invasion in cutaneous malignant melanoma - implications for therapeutic strategies and targeted therapies. *Expert Rev Anticancer Ther* 2014; **14**(5):621–39.

[177] Hanahan D, Weinberg RA. Hallmarks of Cancer: The Next Generation. *Cell* 2011; **144**(5):646–674.

[178] Osawa T, Muramatsu M, Watanabe M, Shibuya M. Hypoxia and low-nutrition double stress induces aggressiveness in a murine model of melanoma. *Cancer Sci* 2009; **100**(5):844–851.

[179] Hoashi T, Kadono T, Kikuchi K, Etoh T, Tamaki K. Differential growth regulation in human melanoma cell lines by TIMP-1 and TIMP-2. *Biochem Biophys Res Commun* 2001; **288**(2):371–379.

[180] Fenouille N, Tichet M, Dufies M, Pottier A, Mogha A, Soo JK, *et al.* The epithelial-mesenchymal transition (EMT) regulatory factor SLUG (SNAI2) is a downstream target of SPARC and AKT in promoting melanoma cell invasion. *PLoS One* 2012; **7**(7):e40378.

[181] Thiery JP. Epithelial-mesenchymal transitions in tumour progression. *Nat Rev Cancer* 2002; **2**(June):442–454.

[182] Kotobuki Y, Tanemura A, Yang L, Itoi S, Wataya-Kaneda M, Murota H, *et al.* Dysregulation of melanocyte function by Th17-related cytokines: Significance of Th17 cell infiltration in autoimmune vitiligo vulgaris. *Pigment Cell Melanoma Res* 2012; **25**:219–230.

[183] Zhao W, Liu H, Xu S, Entschladen F, Niggemann B, Zänker KS, *et al.* Migration and metalloproteinases determine the invasive potential of mouse melanoma cells, but not melanin and telomerase. *Cancer Lett* 2001; **162**:49–55.

[184] Fidler IJ. The pathogenesis of cancer metastasis: the 'seed and soil' hypothesis revisited. *Nat Rev Cancer* 2003; **3**(June):453–458.

[185] Friedl P, Wolf K. Tumour-cell invasion and migration: diversity and escape mechanisms. *Nat Rev Cancer* 2003; **3**(5):362–74.

[186] Ibrahim MM. Subcutaneous and visceral adipose tissue: Structural and functional differences. *Obes Rev* 2010; **11**(1):11–18.

[187] Ali AT, Hochfeld WE, Myburgh R, Pepper MS. Adipocyte and adipogenesis. *Eur J Cell Biol* 2013; **92**(6-7):229–236.

[188] Neudauer CL, McCarthy JB. Insulin-like growth factor I-stimulated melanoma cell migration requires phosphoinositide 3-kinase but not extracellular-regulated kinase activation. *Exp Cell Res* 2003; **286**(1):128–137.

[189] Quax PH, van Muijen GN, Weening-Verhoeff EJ, Lund LR, Dano K, Ruiter DJ, *et al.* Metastatic behavior of human melanoma cell lines in nude mice correlates with urokinase-type plasminogen activator, its type-1 inhibitor, and urokinase-mediated matrix degradation. *J Cell Biol* 1991; **115**(1):191–199.

[190] Naspi A, Panasiti V, Abbate F, Roberti V, Devirgiliis V, Curzio M, *et al.* Insulin-like-growth-factor-binding-protein-3 (IGFBP-3) contrasts melanoma progression in vitro and in vivo. *PLoS One* 2014; **9**(6):e98641.

[191] Meeran SM, Singh T, Nagy TR, Katiyar SK. High-fat diet exacerbates inflammation and cell survival signals in the skin of ultraviolet B-irradiated C57BL/6 mice. *Toxicol Appl Pharmacol* 2009; **241**(3):303–310.

[192] Costa C, Incio J, Soares R. Angiogenesis and chronic inflammation: Cause or consequence? *Angiogenesis* 2007; **10**:149–166.

[193] Fridman WH, Pagès F, Sautès-Fridman C, Galon J. The immune contexture in human tumours: impact on clinical outcome. *Nat Rev Cancer* 2012; **12**(4):298–306.

[194] Hanahan D, Coussens LM. Accessories to the Crime: Functions of Cells Recruited to the Tumor Microenvironment. *Cancer Cell* 2012; **21**(3):309–322.

[195] Loges S, Schmidt T, Carmeliet P. Mechanisms of resistance to anti-angiogenic therapy and development of third-generation anti-angiogenic drug candidates. *Genes Cancer* 2010; **1**(1):12–25.

[196] Kleinman HK, Martin GR. Matrigel: Basement membrane matrix with biological activity. *Semin Cancer Biol* 2005; **15**(5):378–386.

[197] van der Schaft DWJ, Seftor REB, Seftor EA, Hess AR, Gruman LM, Kirschmann DA, *et al.* Effects of angiogenesis inhibitors on vascular network formation by human endothelial and melanoma cells. *J Natl Cancer Inst* 2004; **96**(19):1473–7.

[198] Lirdprapamongkol K, Chiablaem K, Sila-Asna M, Surarit R, Bunyaratvej A, Svasti J. Exploring stemness gene expression and vasculogenic mimicry capacity in well- and poorly-differentiated hepatocellular carcinoma cell lines. *Biochem Biophys Res Commun* 2012; **422**(3):429–35.

[199] Frank NY, Schatton T, Kim S, Zhan Q, Wilson BJ, Ma J, *et al.* VEGFR-1 expressed by malignant melanoma-initiating cells is required for tumor growth. *Cancer Res* 2011; **71**(4):1474–1485.

[200] Matano F, Yoshida D, Ishii Y, Tahara S, Teramoto A, Morita A. Endocan, a new invasion and angiogenesis marker of pituitary adenomas. *J Neurooncol* 2014; **117**(3):485–491.

[201] Hubenak JR, Zhang Q, Branch CD, Kronowitz SJ. Mechanisms of Injury to Normal Tissue after Radiotherapy. *Plast Reconstr Surg* 2014; **133**(1):49e–56e.

[202] Riley PA. Free radicals in biology: oxidative stress and the effects of ionizing radiation. *Int J Radiat Biol* 1994; **65**(1):27–33.

[203] Calle EE, Kaaks R. Overweight, obesity and cancer: epidemiological evidence and proposed mechanisms. *Nat Rev Cancer* 2004; **4**(8):579–591.

[204] Wolin KY, Carson K, Colditz GA. Obesity and Cancer. *Oncologist* 2010; **15**(6):556–565.

[205] Fang P, Tan KS, Troxel AB, Rengan R, Freedman G, Lin LL. High body mass index is associated with worse quality of life in breast cancer patients receiving radiotherapy. *Breast Cancer Res Treat* 2013; **141**(1):125–33.

[206] Strom SS, Kamat AM, Gruschkus SK, Gu Y, Wen S, Cheung MR, *et al.* Influence of obesity on biochemical and clinical failure after external-beam radiotherapy for localized prostate cancer. *Cancer* 2006; **107**(3):631–9.

[207] Coelho P, Almeida J, Prudêncio C, Fernandes R, Soares R. Effect of Adipocyte Secretome in Melanoma Progression and Vasculogenic Mimicry. *J Cell Biochem* 2016; **117**(7):1697–706.

[208] Patwardhan RS, Sharma D, Checker R, Thoh M, Sandur SK. Spatio-temporal changes in glutathione and thioredoxin redox couples during ionizing radiation-induced oxidative stress regulate tumor radio-resistance. *Free Radic Res* 2015; **49**(10):1218–1232.

[209] Zhang S, Guo H, Zhang D, Zhang W, Zhao X, Ren Z, *et al.* Microcirculation patterns in different stages of melanoma growth. *Oncol Rep* 2006; **15**(1):15–20.

[210] Ayala A, Muñoz MF, Argüelles S. Lipid peroxidation: production, metabolism, and signaling mechanisms of malondialdehyde and 4-hydroxy-2-nonenal. *Oxid Med Cell Longev* 2014; **2014**:360438.

[211] Giaid A, Lehnert SM, Chehayeb B, Chehayeb D, Kaplan I, Shenouda G. Inducible nitric oxide synthase and nitrotyrosine in mice with radiation-induced lung damage. *Am J Clin Oncol* 2003; **26**(4):e67–72.

[212] Bussink J, van der Kogel AJ, Kaanders JH. Activation of the PI3-K/AKT pathway and implications for radioresistance mechanisms in head and neck cancer. *Lancet Oncol* 2008; **9**(3):288–296.

[213] Li HF, Kim JS, Waldman T. Radiation-induced Akt activation modulates radioresistance in human glioblastoma cells. *Radiat Oncol* 2009; **4**(1):43.

[214] Gorayski P, Burmeister B, Foote M. Radiotherapy for cutaneous melanoma : current and future applications. 2015; **11**:525–534.

[215] Barker HE, Paget JTE, Khan AA, Harrington KJ. The tumour microenvironment after radiotherapy: mechanisms of resistance and recurrence. *Nat Rev Cancer* 2015; **15**(7):409–425.

[216] Wong JR, Gao Z, Merrick S, Wilson P, Uematsu M, Woo K, *et al.* Potential for higher treatment failure in obese patients: correlation of elevated body mass index and increased daily prostate deviations from the radiation beam isocenters in an analysis of 1,465 computed tomographic images. *Int J Radiat Oncol Biol Phys* 2009; **75**(1):49–55.

[217] Kratchmarova I. A Proteomic Approach for Identification of Secreted Proteins during the Differentiation of 3T3-L1 Preadipocytes to Adipocytes. *Mol Cell Proteomics* 2002; **1**(3):213–222.

[218] Johnson GE, Ivanov VN, Hei TK. Radiosensitization of melanoma cells through combined inhibition of protein regulators of cell survival. *Apoptosis* 2008; **13**(6):790–802.

[219] Eder S, Lamkowski A, Priller M, Port M, Steinestel K. Radiosensitization and downregulation of heterogeneous nuclear ribonucleoprotein K (hnRNP K) upon inhibition of mitogen/extracellular signal-regulated kinase (MEK) in malignant melanoma cells. *Oncotarget* 2015; **6**(19):17178–91.

[220] Macaulay VM, Salisbury aJ, Bohula Ea, Playford MP, Smorodinsky NI, Shiloh Y. Downregulation of the type 1 insulin-like growth factor receptor in mouse melanoma cells is associated with enhanced radiosensitivity and impaired activation of Atm kinase. *Oncogene* 2001; **20**(30):4029–40.

[221] De Bacco F, Luraghi P, Medico E, Reato G, Girolami F, Perera T, *et al.* Induction of MET by ionizing radiation and its role in radioresistance and invasive growth of cancer. *J Natl Cancer Inst* 2011; **103**(8):645–61.

[222] Jung HJ, Suh Y. Regulation of IGF -1 signaling by microRNAs. *Front Genet* 2015; **5**(JAN):1–14.

[223] Rockwell S, Dobrucki IT, Kim EY, Marrison ST, Vu VT. Hypoxia and radiation therapy: past history, ongoing research, and future promise. *Curr Mol Med* 2009; **9**(4):442–458.

[224] Payne AS, Cornelius LA. The role of chemokines in melanoma tumor growth and metastasis. *J Invest Dermatol* 2002; **118**(6):915–22.

[225] Qiao L, Liang N, Zhang J, Xie J, Liu F, Xu D, *et al.* Advanced research on vasculogenic mimicry in cancer. *J Cell Mol Med* 2015; **19**(2):315–26.

[226] Busser B, Sancey L, Brambilla E, Coll JL, Hurbin A. The multiple roles of amphiregulin in human cancer. *Biochim Biophys Acta* 2011; **1816**(2):119–31.

[227] Kishimoto K, Yoshida S, Ibaragi S, Yoshioka N, Hu GF, Sasaki A. Neamine inhibits oral cancer progression by suppressing angiogenin-mediated angiogenesis and cancer cell proliferation. *Anticancer Res* 2014; **34**(5):2113–21.

[228] Miyake M, Goodison S, Lawton A, Gomes-Giacoia E, Rosser CJ. Angiogenin promotes tumoral growth and angiogenesis by regulating matrix metallopeptidase-2 expression via the ERK1/2 pathway. *Oncogene* 2015; **34**(7):890–901.

[229] Fernández-Rodríguez R, Rodríguez-Baena FJ, Martino-Echarri E, Peris-Torres C, Plaza-Calonge MDC, Rodríguez-Manzaneque JC. Stroma-derived but not tumor ADAMTS1 is a main driver of tumor growth and metastasis. *Oncotarget* 2016;.

[230] Casal C, Torres-Collado AX, Plaza-Calonge MDC, Martino-Echarri E, Ramón Y Cajal S, Rojo F, *et al.* ADAMTS1 contributes to the acquisition of an endothelial-like phenotype in plastic tumor cells. *Cancer Res* 2010; **70**(11):4676–86.

[231] Andreucci E, Bianchini F, Biagioni A, Del Rosso M, Papucci L, Schiavone N, *et al.* Roles of different IRES-dependent FGF2 isoforms in the acquisition of the major aggressive features of human metastatic melanoma. *J Mol Med (Berl)* 2016;.

[232] Schnegg CI, Yang MH, Ghosh SK, Hsu MY. Induction of Vasculogenic Mimicry Overrides VEGF-A Silencing and Enriches Stem-like Cancer Cells in Melanoma. *Cancer Res* 2015; **75**(8):1682–90.

[233] Ge X, Wang Y, Lam KS, Xu A. Metabolic actions of FGF21: molecular mechanisms and therapeutic implications. *Acta Pharm Sin B* 2012; **2**(4):350–357.

[234] Woo YC, Lee CH, Fong CH, Xu A, Tso AW, Cheung BM, *et al.* Serum fibroblast growth factor 21 is a superior biomarker to other adipokines in predicting incident diabetes. *Clin Endocrinol (Oxf)* 2016;.

[235] Kimura Y, Sumiyoshi M. High-fat, high-sucrose, and high-cholesterol diets accelerate tumor growth and metastasis in tumor-bearing mice. *Nutr Cancer* 2007; **59**(2):207–16.

[236] Yan L, DeMars LC. Effects of a high-fat diet on spontaneous metastasis of Lewis lung carcinoma in plasminogen activator inhibitor-1 deficient and wild-type mice. *PLoS One* 2014; **9**(10):e110869.

[237] Johnstone CN, Chand A, Putoczki TL, Ernst M. Emerging roles for IL-11 signaling in cancer development and progression: Focus on breast cancer. *Cytokine Growth Factor Rev* 2015; **26**(5):489–98.

[238] Huang S, Xie K, Bucana CD, Ullrich SE, Bar-Eli M. Interleukin 10 suppresses tumor growth and metastasis of human melanoma cells: potential inhibition of angiogenesis. *Clin Cancer Res* 1996; **2**(12):1969–79.

[239] Song S, Wang Y, Wang J, Lian W, Liu S, Zhang Z, *et al.* Tumour-derived IL-10 within tumour microenvironment represses the antitumour immunity of Socs1-silenced and sustained antigen expressing DCs. *Eur J Cancer* 2012; **48**(14):2252–2259.

[240] Meier F, Will S, Ellwanger U, Schlagenhauff B, Schittek B, Rassner G, *et al.* Metastatic pathways and time courses in the orderly progression of cutaneous melanoma. *Br J Dermatol* 2002; **147**(1):62–70.

[241] Park H, Kim M, Kwon GT, Lim DY, Yu R, Sung MK, *et al.* A high-fat diet increases angiogenesis, solid tumor growth, and lung metastasis of CT26 colon cancer cells in obesity-resistant BALB/c mice. *Mol Carcinog* 2012; **51**(11):869–80.

[242] Kim EJ, Choi MR, Park H, Kim M, Hong JE, Lee JY, *et al.* Dietary fat increases solid tumor growth and metastasis of 4T1 murine mammary carcinoma cells and mortality in obesity-resistant BALB/c mice. *Breast Cancer Res* 2011; **13**(4):R78.

[243] Piskounova E, Agathocleous M, Murphy MM, Hu Z, Huddlestun SE, Zhao Z, *et al.* Oxidative stress inhibits distant metastasis by human melanoma cells. *Nature* 2015; **527**(7577):186–91.

[244] Matsuzawa-Nagata N, Takamura T, Ando H, Nakamura S, Kurita S, Misu H, *et al.* Increased oxidative stress precedes the onset of high-fat diet-induced insulin resistance and obesity. *Metabolism* 2008; **57**(8):1071–7.

[245] Vargas-Robles H, Rios A, Arellano-Mendoza M, Escalante BA, Schnoor M. Antioxidative Diet Supplementation Reverses High-Fat Diet-Induced Increases of Cardiovascular Risk Factors in Mice. *Oxid Med Cell Longev* 2015; **2015**:1–9.

[246] Jiang M, Xu X, Bi Y, Xu J, Qin C, Han M. Systemic inflammation promotes lung metastasis via E-selectin upregulation in mouse breast cancer model. *Cancer Biol Ther* 2014; **15**(6):789–96.

[247] El Rayes T, Catena R, Lee S, Stawowczyk M, Joshi N, Fischbach C, *et al.* Lung inflammation promotes metastasis through neutrophil protease-mediated degradation of Tsp-1. *Proc Natl Acad Sci* 2015; **112**(52):16000–16005.

[248] Brożyna AA, Jóźwicki W, Carlson JA, Slominski AT. Melanogenesis affects overall and disease-free survival in patients with stage III and IV melanoma. *Hum Pathol* 2013; **44**(10):2071–4.

[249] Folberg R, Hendrix MJ, Maniotis aJ. Vasculogenic mimicry and tumor angiogenesis. *Am J Pathol* 2000; **156**(2):361–381.

[250] Lauby-Secretan B, Scoccianti C, Loomis D, Grosse Y, Bianchini F, Straif K, *et al.* Body Fatness and Cancer–Viewpoint of the IARC Working Group. *N Engl J Med* 2016; **375**(8):794–8.

[251] Martin L, Birdsell L, Macdonald N, Reiman T, Clandinin MT, McCargar LJ, *et al.* Cancer cachexia in the age of obesity: skeletal muscle depletion is a powerful prognostic factor, independent of body mass index. *J Clin Oncol* 2013; **31**(12):1539–47.

A

Reproduction Licences

JOHN WILEY AND SONS LICENSE TERMS AND CONDITIONS

Sep 09, 2016

This Agreement between Pedro Coelho ("You") and John Wiley and Sons ("John Wiley and Sons") consists of your license details and the terms and conditions provided by John Wiley and Sons and Copyright Clearance Center.

License Number	3944920437787
License date	Sep 09, 2016
Licensed Content Publisher	John Wiley and Sons
Licensed Content Publication	Journal of Cellular Biochemistry
Licensed Content Title	Effect of Adipocyte Secretome in Melanoma Progression and Vasculogenic Mimicry
Licensed Content Author	Pedro Coelho,Joana Almeida,Cristina Prudêncio,Rúben Fernandes,Raquel Soares
Licensed Content Date	Jan 15, 2016
Licensed Content Pages	10
Type of use	Dissertation/Thesis
Requestor type	Author of this Wiley article
Format	Print and electronic
Portion	Full article
Will you be translating?	No
Title of your thesis / dissertation	Obesity and Melanoma: Unravelling the Molecular and Cellular Mechanisms
Expected completion date	Sep 2016
Expected size (number of pages)	120
Requestor Location	Pedro Coelho Rua das Carmelitas, 100 5E Porto, 4050-161 Portugal Attn: Pedro Coelho
Publisher Tax ID	EU826007151
Billing Type	Invoice
Billing Address	Pedro Coelho Rua das Carmelitas, 100 5E Porto, Portugal 4050-161 Attn: Pedro Coelho
Total	0.00 EUR
Terms and Conditions	

TERMS AND CONDITIONS

This copyrighted material is owned by or exclusively licensed to John Wiley & Sons, Inc. or one of its group companies (each a"Wiley Company") or handled on behalf of a society with which a Wiley Company has exclusive publishing rights in relation to a particular work (collectively "WILEY"). By clicking "accept" in connection with completing this licensing transaction, you agree that the following terms and conditions apply to this transaction

(along with the billing and payment terms and conditions established by the Copyright Clearance Center Inc., ("CCC's Billing and Payment terms and conditions"), at the time that you opened your RightsLink account (these are available at any time at http://myaccount.copyright.com).

Terms and Conditions

- The materials you have requested permission to reproduce or reuse (the "Wiley Materials") are protected by copyright.

- You are hereby granted a personal, non-exclusive, non-sub licensable (on a stand-alone basis), non-transferable, worldwide, limited license to reproduce the Wiley Materials for the purpose specified in the licensing process. This license, **and any CONTENT (PDF or image file) purchased as part of your order,** is for a one-time use only and limited to any maximum distribution number specified in the license. The first instance of republication or reuse granted by this license must be completed within two years of the date of the grant of this license (although copies prepared before the end date may be distributed thereafter). The Wiley Materials shall not be used in any other manner or for any other purpose, beyond what is granted in the license. Permission is granted subject to an appropriate acknowledgement given to the author, title of the material/book/journal and the publisher. You shall also duplicate the copyright notice that appears in the Wiley publication in your use of the Wiley Material. Permission is also granted on the understanding that nowhere in the text is a previously published source acknowledged for all or part of this Wiley Material. Any third party content is expressly excluded from this permission.

- With respect to the Wiley Materials, all rights are reserved. Except as expressly granted by the terms of the license, no part of the Wiley Materials may be copied, modified, adapted (except for minor reformatting required by the new Publication), translated, reproduced, transferred or distributed, in any form or by any means, and no derivative works may be made based on the Wiley Materials without the prior permission of the respective copyright owner.**For STM Signatory Publishers clearing permission under the terms of the STM Permissions Guidelines only, the terms of the license are extended to include subsequent editions and for editions in other languages, provided such editions are for the work as a whole in situ and does not involve the separate exploitation of the permitted figures or extracts,** You may not alter, remove or suppress in any manner any copyright, trademark or other notices displayed by the Wiley Materials. You may not license, rent, sell, loan, lease, pledge, offer as security, transfer or assign the Wiley Materials on a stand-alone basis, or any of the rights granted to you hereunder to any other person.

- The Wiley Materials and all of the intellectual property rights therein shall at all times remain the exclusive property of John Wiley & Sons Inc, the Wiley Companies, or their respective licensors, and your interest therein is only that of having possession of and the right to reproduce the Wiley Materials pursuant to Section 2 herein during the continuance of this Agreement. You agree that you own no right, title or interest in or to the Wiley Materials or any of the intellectual property rights therein. You shall have no rights hereunder other than the license as provided for above in Section 2. No right, license or interest to any trademark, trade name, service mark or other branding ("Marks") of WILEY or its licensors is granted hereunder, and you agree that you shall not assert any such right, license or interest with respect thereto

- NEITHER WILEY NOR ITS LICENSORS MAKES ANY WARRANTY OR REPRESENTATION OF ANY KIND TO YOU OR ANY THIRD PARTY, EXPRESS, IMPLIED OR STATUTORY, WITH RESPECT TO THE MATERIALS OR THE ACCURACY OF ANY INFORMATION CONTAINED IN THE MATERIALS, INCLUDING, WITHOUT LIMITATION, ANY IMPLIED WARRANTY OF MERCHANTABILITY, ACCURACY, SATISFACTORY

QUALITY, FITNESS FOR A PARTICULAR PURPOSE, USABILITY, INTEGRATION OR NON-INFRINGEMENT AND ALL SUCH WARRANTIES ARE HEREBY EXCLUDED BY WILEY AND ITS LICENSORS AND WAIVED BY YOU.

- WILEY shall have the right to terminate this Agreement immediately upon breach of this Agreement by you.

- You shall indemnify, defend and hold harmless WILEY, its Licensors and their respective directors, officers, agents and employees, from and against any actual or threatened claims, demands, causes of action or proceedings arising from any breach of this Agreement by you.

- IN NO EVENT SHALL WILEY OR ITS LICENSORS BE LIABLE TO YOU OR ANY OTHER PARTY OR ANY OTHER PERSON OR ENTITY FOR ANY SPECIAL, CONSEQUENTIAL, INCIDENTAL, INDIRECT, EXEMPLARY OR PUNITIVE DAMAGES, HOWEVER CAUSED, ARISING OUT OF OR IN CONNECTION WITH THE DOWNLOADING, PROVISIONING, VIEWING OR USE OF THE MATERIALS REGARDLESS OF THE FORM OF ACTION, WHETHER FOR BREACH OF CONTRACT, BREACH OF WARRANTY, TORT, NEGLIGENCE, INFRINGEMENT OR OTHERWISE (INCLUDING, WITHOUT LIMITATION, DAMAGES BASED ON LOSS OF PROFITS, DATA, FILES, USE, BUSINESS OPPORTUNITY OR CLAIMS OF THIRD PARTIES), AND WHETHER OR NOT THE PARTY HAS BEEN ADVISED OF THE POSSIBILITY OF SUCH DAMAGES. THIS LIMITATION SHALL APPLY NOTWITHSTANDING ANY FAILURE OF ESSENTIAL PURPOSE OF ANY LIMITED REMEDY PROVIDED HEREIN.

- Should any provision of this Agreement be held by a court of competent jurisdiction to be illegal, invalid, or unenforceable, that provision shall be deemed amended to achieve as nearly as possible the same economic effect as the original provision, and the legality, validity and enforceability of the remaining provisions of this Agreement shall not be affected or impaired thereby.

- The failure of either party to enforce any term or condition of this Agreement shall not constitute a waiver of either party's right to enforce each and every term and condition of this Agreement. No breach under this agreement shall be deemed waived or excused by either party unless such waiver or consent is in writing signed by the party granting such waiver or consent. The waiver by or consent of a party to a breach of any provision of this Agreement shall not operate or be construed as a waiver of or consent to any other or subsequent breach by such other party.

- This Agreement may not be assigned (including by operation of law or otherwise) by you without WILEY's prior written consent.

- Any fee required for this permission shall be non-refundable after thirty (30) days from receipt by the CCC.

- These terms and conditions together with CCC's Billing and Payment terms and conditions (which are incorporated herein) form the entire agreement between you and WILEY concerning this licensing transaction and (in the absence of fraud) supersedes all prior agreements and representations of the parties, oral or written. This Agreement may not be amended except in writing signed by both parties. This Agreement shall be binding upon and inure to the benefit of the parties' successors, legal representatives, and authorized assigns.

- In the event of any conflict between your obligations established by these terms and conditions and those established by CCC's Billing and Payment terms and conditions,

these terms and conditions shall prevail.

- WILEY expressly reserves all rights not specifically granted in the combination of (i) the license details provided by you and accepted in the course of this licensing transaction, (ii) these terms and conditions and (iii) CCC's Billing and Payment terms and conditions.

- This Agreement will be void if the Type of Use, Format, Circulation, or Requestor Type was misrepresented during the licensing process.

- This Agreement shall be governed by and construed in accordance with the laws of the State of New York, USA, without regards to such state's conflict of law rules. Any legal action, suit or proceeding arising out of or relating to these Terms and Conditions or the breach thereof shall be instituted in a court of competent jurisdiction in New York County in the State of New York in the United States of America and each party hereby consents and submits to the personal jurisdiction of such court, waives any objection to venue in such court and consents to service of process by registered or certified mail, return receipt requested, at the last known address of such party.

WILEY OPEN ACCESS TERMS AND CONDITIONS

Wiley Publishes Open Access Articles in fully Open Access Journals and in Subscription journals offering Online Open. Although most of the fully Open Access journals publish open access articles under the terms of the Creative Commons Attribution (CC BY) License only, the subscription journals and a few of the Open Access Journals offer a choice of Creative Commons Licenses. The license type is clearly identified on the article.

The Creative Commons Attribution License

The Creative Commons Attribution License (CC-BY) allows users to copy, distribute and transmit an article, adapt the article and make commercial use of the article. The CC-BY license permits commercial and non-

Creative Commons Attribution Non-Commercial License

The Creative Commons Attribution Non-Commercial (CC-BY-NC)License permits use, distribution and reproduction in any medium, provided the original work is properly cited and is not used for commercial purposes.(see below)

Creative Commons Attribution-Non-Commercial-NoDerivs License

The Creative Commons Attribution Non-Commercial-NoDerivs License (CC-BY-NC-ND) permits use, distribution and reproduction in any medium, provided the original work is properly cited, is not used for commercial purposes and no modifications or adaptations are made. (see below)

Use by commercial "for-profit" organizations

Use of Wiley Open Access articles for commercial, promotional, or marketing purposes requires further explicit permission from Wiley and will be subject to a fee.

Further details can be found on Wiley Online Library

http://olabout.wiley.com/WileyCDA/Section/id-410895.html

Other Terms and Conditions:

v1.10 Last updated September 2015

Obesity and Melanoma: Unravelling the Molecular and Cellular Mechanisms

Pedro Miguel Vieira Coelho

FACULDADE DE MEDICINA